STRATHCLYDE INSTITUTE OF PHARMACY & BIOMEDICAL SCIENCES

University of Strathclyde Science

Title A study of the metabolism and metabolomics of polyphenols using isolated rat hepatocytes and liquid chromatography-high resolution mass spectrometry

A thesis presented

By

KHALED M. K. OMAR

A Thesis Submitted in Fulfillment of the Requirements for the Award of Degree of Doctor of Philosophy in Strathclyde Institute of Pharmacy and Biomedical Sciences at the University of Strathclyde

2017

Declaration

‘I declare that, except where specifically indicated, all the work presented in this report is my own and I am the sole author of all parts.’

Signed: _____

Date: _____

Acknowledgments

I wish to express my sincerest gratitude to Allah for providing me with health, commitment and patience to complete my PhD studies. I am deeply grateful to my principal supervisor, Dr David G Watson for allowing me to undertake this exciting research. He has provided invaluable guidance, advice and support throughout the duration of this study with his patience and knowledge for which I will always be truly grateful. I wish also to offer my sincere gratitude to Professor Helen Grant for her immense support, continuous encouragement and motivation throughout my PhD studies. My thanks also extend to Ms Catherine Henderson (Lab assistant) for her efforts and helping me during hepatocyte preparations and incubations.

Particular thanks are owed to all my friends and colleagues in SIPBS for their support during my study.

I am indebted to the Ministry of Higher Education of Libya and Libyan Cultural Bureau in UK for the financial support and their unlimited support, encouragement and help.

I extend my warmest thanks to my parents for their emotional support and prayers, and to my brothers and sisters for their encouragement and love.

Finally, yet importantly, special thanks to my beloved wife and my lovely kids for their patience, support and love.

Table of Contents

List of Figures

List of Tables

List of Abbreviations

µL	Microliter
µm	Micrometre
µM	Micromolar
3D	Three Dimension Ion Trap
ALDH	Aldehyde Dehydrogenases
AO	Aldehyde Oxidases
APCI	Atmospheric Pressure Chemical Ionization
API	Atmospheric Pressure Ionization
APPI	Atmospheric Pressure Photoionization
ATP	Adenosine Triphosphate Coenzyme
BSA	Bovine Serum Albumin
C18	Octadecyl C18
C18-AR	Octadecyl with embedded phenyl functionality
C8	Octyl C8
CAN	Acetonitrile
CI	Chemical Ionization
CID	Collision Induced Decomposition
CYP	Cytochrome P450
DAD	Diode Array Detector
DART	Direct Analysis in Real Time
DB	Database
DC	Direct Current
DESI	Desorption Electrospray Ionization
DMSO	Dimethylsulphoxide
EDIAP	Extraction of Dissolved Ions under Atmospheric Pressure
EDTA	Ethylenediaminetetraacetic Acid
EGTA	Ethylene glycol-bis-(β-amino-ethylether) N'N' tetraacetic acid
EI	Electron Impact
ESI	Electrospray Ionization
eV	Electronvolt
FA	Ferulic Acid
FAB	Fast Atom Bombardment
FK	Formylkynurernine
FMO	Flavin Monooxygenases
FT-MS	Fourier Transform Mass Spectrometry
GC-MS	Gas Chromatography Mass Spectrometer
Gluc	Glucuronic Acid
GSH	Glutathione
GSSG	Oxidised Glutathione

GSTs	Glutathione-S-transferase enzymes
HBA	Hydrobenzoic Acid
HBSS	Hanks' Balanced Salt Solution
HCAs	Hydroxycinnamic Acid Derivatives
HEPES	N-[2-hydroxyethyl] piperazine-N'-[2-ethanesulphonoic acid
HILIC	Hydrophilic Interaction Liquid Chromatography
HPLC	High Performance Liquid Chromatography
HRMS	High-Resolution Mass Spectrometry
IU	International Unit
KA	Krebs-Albumin Buffer
Kg	Kilogram
KH	Krebs Henseleit Buffer
kV	Kilovolts
L	Litre
LC/MS	Liquid Chromatography Mass Spectrometry
LC-PDA-MS	Liquid Chromatography Photodiode Array Mass Spectrometry
LTQ	Hybrid linear ion trap/Orbitrap mass spectrometer
M	Molar
m/z	Mass-to-Charge Ratio
MALDI	Matrix Assisted Laser Desorption Ionisation
MAO	Monoamine Oxidases
mg	Milligram
min	Minute(s)
mL	Millilitre
mm	millimetre
mM	millmolar
mm^3	Cubic millimetre
MRM	Multiple Reaction Monitoring
MS	Mass Spectrometry
MS/MS	Tandem Mass Spectrometric
MW	Molecular Weight
NADH	Nicotinamide Adenine Dinucleotide
NADPH	Nicotinamide Adenine Dinucleotide Phosphate-Oxidase
NESI	Nanoelectrospray Ionization
NL	Neutral Loss
NMR	Nuclear Magnetic Resonance
P-450	Cytochrome P-450 Enzymes
PAPS	Co-factor 3'-phosphoadenosine-5'-phosphosulfate
PBS	Phosphate Buffered Saline
p-CA	*P*-Coumaric Acid
pH	Potential of Hydrogen
PI	Precursor Ion

ppm	Parts Per Million
Q	Quercetin
QIT	Quadrupole Ion Trap
QMS	Quadrupole Mass Analyser
QSRR	Quantitative Structure Retention Relationships
Q-TOF	Quadrupole Time-Of-Flight
Rf	Radio Frequency
RPC	Reversed Phase Chromatography
RPLC	Reverse Phase Liquid Chromatography
rpm	Revolutions Per Minute
RSD	Relative Standard Deviation
SD	Sprague- Dawley rats
SH	Thiol
SIM	Selected Ion Monitoring
SRM	Selected Reaction Monitoring
SULTs	Sulfotransferases Enzymes
TIC	Total Ion Chromatograms
TOF	Time-Of-Flight
t_R	Retention Time
UDPGA	Uridine Diphosphate-Glucuronosyl Transferases Enzymes
UDPGT	Uridine Diphosphate Glucuronyl Transferase
UGTs	UDP-glucuronosyl transferases Enzymes
UV	Ultraviolet
v/v	Volume to Volume
Ver	Version
w/v	Weight to Volume
XAO	Xanthine Oxidase
ZIC-HILIC	Zwitterion Stationary Phase
ZIC-*p*HILIC	Zwitterion Polymer Stationary Phase

Papers published and posters presented

Papers

1. OMAR, K., GRANT, M. H., HENDERSON, C. and WATSON, D. G. (2014). The abundant dietary constituent ferulic acid forms a wide range of metabolites including a glutathione adduct when incubated with rat hepatocytes. *Xenobiotica,* 44**,** 432-437.

2. OMAR, K., GRANT, M. H., HENDERSON, C. and WATSON, D. G. (2014). The complex degradation and metabolism of quercetin in rat hepatocyte incubations. *Xenobiotica,* 44**,** 1074-1082.

Posters

1. OMAR, K., GRANT, M. H., HENDERSON, C. and WATSON, D. G. (2015) LC-MS analysis of the metabolism of the dietary constituent hydroxycinnamates by rat hepatocytes. Scottish Metabolomics Network Inaugural Meeting, Edinburgh, Scotland, UK.

2. OMAR, K., GRANT, M. H., HENDERSON, C. and WATSON, D. G. (2015). LC-MS analysis of the metabolism of the dietary constituent hesperidin by rat hepatocytes. 13th European ISSX meeting, Glasgow, Scotland, UK.

3. OMAR, K., GRANT, M. H., HENDERSON, C. and WATSON, D. G. (2013). High resolution mass spectrometric profiling in a study of the metabolism of ferulic acid in rat hepatocytes. 9th Annual International Conference of the Metabolomics Society, Glasgow, Scotland, UK.

Proposed contributions from this work

1. OMAR, K., GRANT, M. H., HENDERSON, C. and WATSON, D. G. Metabolism of Hesperidin in Rat Hepatocytes.

2. OMAR, K., GRANT, M. H., HENDERSON, C. and WATSON, D. G. Metabolism of *p*-coumaric acid by Isolated Rat Hepatocytes.

3. OMAR, K., GRANT, M. H., HENDERSON, C. and WATSON, D. G. The metabolomic effects of flavonoids and cinnamates on the hepatocyte metabolome.

Abstract

Dietary phenolic compounds have been proposed to have significant benefits for health through their anti-oxidant properties. Their metabolism has been well studied; however, it would be advantageous to have knowledge of the metabolites which can be formed from these compounds in order to monitor their presence in physiological fluids such as plasma and urine. Isolated rat hepatocytes contain a full range of enzymes for carrying out phase I, phase II and phase III metabolism of xenobiotics. In this work, isolated rat hepatocytes were used to transform the phenyl propionates ferulic acid and *p*-coumaric acid and the flavonoids quercetin and hesperidin. The products formed by enzymatic transformation were characterised by liquid chromatography in combination with high resolution mass spectrometry. This was followed by extraction of the data with Sieve software and identification of the metabolites based on their elemental composition. MS^2 and MS^3 experiments were used to further characterise the metabolites. The phenyl propanoid compounds were mainly sulfated but other transformations such as glucuronidation and glycine conjugation occurred. In addition, the two phenyl propanoid compounds also formed conjugates with glutathione which added across the double bond in the side chain. Quercetin underwent both metabolism and complex degradation in the hepatocyte incubation medium leading to a very complex mixture of metabolites from the intact drug and its chemical degradants. Hesperidin, in contrast to quercetin, underwent a rather simple metabolism being mainly converted to its sulfate. In addition, hydrophilic interaction chromatography in combination with high resolution mass spectrometry was used to study the effects of the phenolic compounds on the

hepatocyte metabolome. Quercetin had a strong effect on the metabolome as it depleted the co-factors required for sulfation and glucuronidation. It also had a strong anti-oxidant effect and it appeared to reduce autophagy by the hepatocytes. In conclusion the most interesting compound in the set of compounds studied is quercetin which presents scope for further study.

CHAPTER 1

General Introduction

1. General Introduction

1.1 Introduction to polyphenols and their classification

Simple phenols are aromatic rings with one hydroxyl group attached to the ring while polyphenols contain at least, two phenolic hydroxyl groups. They are sometimes attached with sugars or ester moieties. There are many classes of polyphenols such as flavonoids and non-flavonoids such as hydroxybenzoic and hydroxycinnamic acid derivatives which are widespread in plants. Processed foods and beverages, such as tea, wine, coffee, and cocoa, may contain products of phenolic compound metabolism. Such compounds are best described as derived polyphenols. A more appropriate description of a polyphenolic compound is a compound that has more than one phenolic moiety in its structure. A convention often used for describing phenols is to define the number of carbons present in the 'aromatic ring' structures and fragments present in the molecule. For example, a C6-C3 compound implies a six membered aromatic ring attached to a three carbon chain fragment (Knight, 2003, Del Rio *et al*., 2013).

The major classes of polyphenols are flavonoids and non-flavonoids. The scheme, **Figure 1.1**, shows the major subgroups of flavonoids and non-flavonoids with their sources and general health benefits (Del Rio *et al*., 2013).

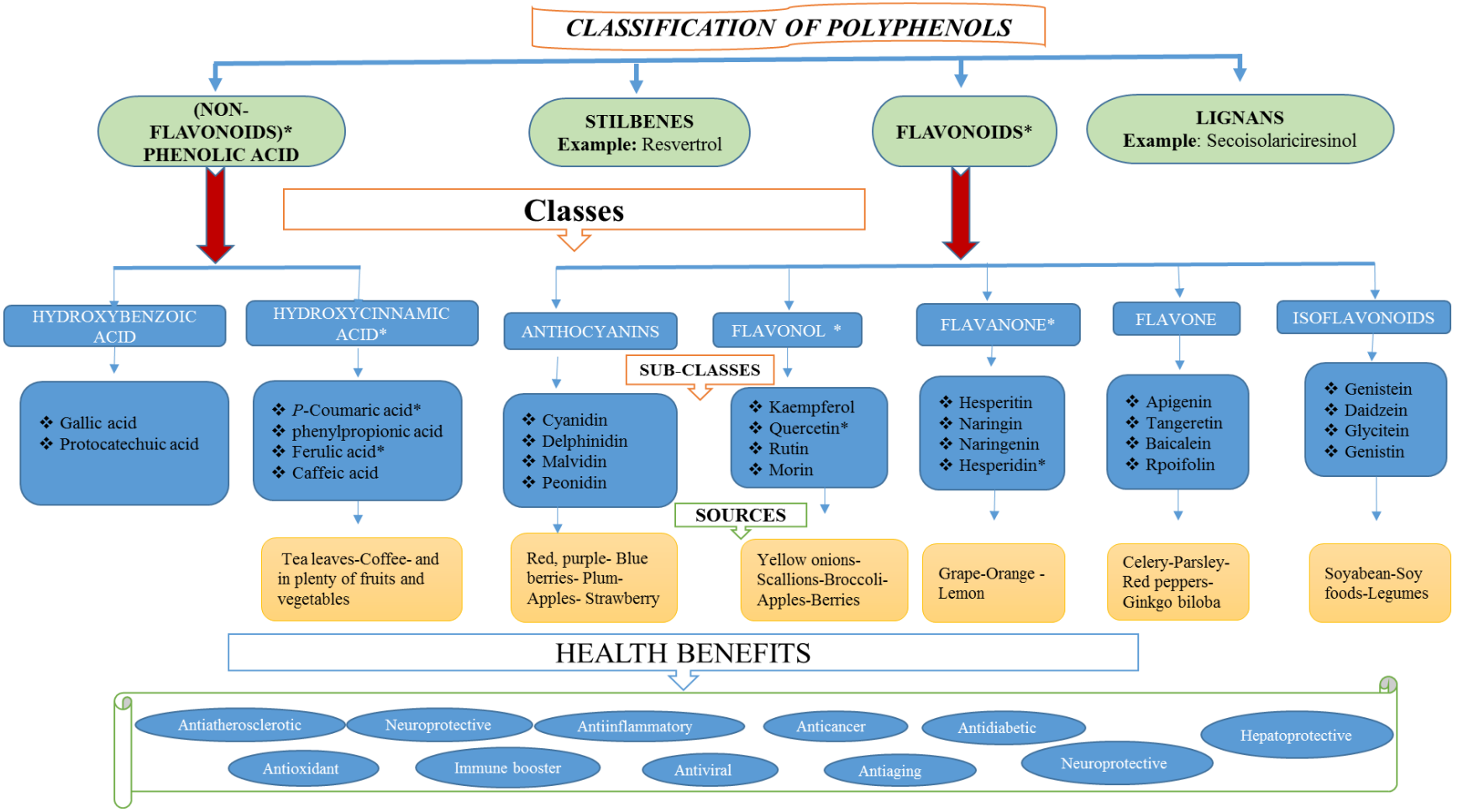

Figure 1.1 Scheme of major classes of polyphenols along with their sources and general health benefits.

* Samples of polyphenols studied.

1.1.1 Flavonoids

In the last decade, studies of flavonoids have increased. They are the largest class of polyphenolic compounds containing 15 carbons with two aromatic rings (A and B) linked by an oxygenated heterocyclic ring (C) moiety (C6-C3-C6) (**Figure 1.2**).

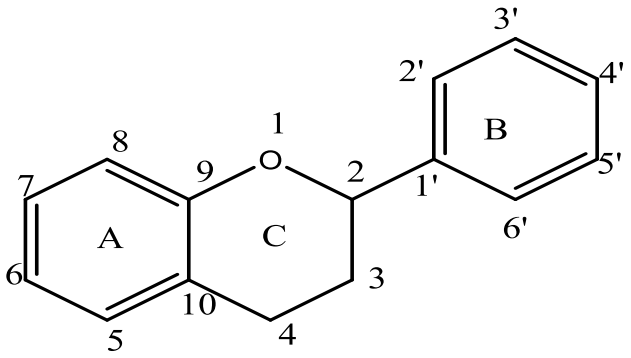

Figure 1.2 Basic flavonoid skeleton.

Their structures depend on variations in the substitution and oxidation of the heterocyclic ring, the hydroxylation pattern of the ring structure and the substitution in the 3-position. Flavonoids are classified into major classes such as flavonols, flavanones, isoflavonoids, flavones, anthocyanins. The basic chemical structures of these subclasses of flavonoids are given in **Figure 1.3**. Flavonoids usually form glycosides with sugar residues replacing the proton of any the OH groups in the compound (Del Rio *et al*., 2013, Crozier *et al*., 2009, Kohlmeier, 2003, Jeremy *et al*., 2003b, Omar, 2013). Flavonoids are widely distributed as secondary metabolites in plants and perform various metabolic functions. Flavonoids are responsible for the

purple, blue and red colours in flowers, fruits, and seeds (Crozier *et al*., 2008, Omar, 2013).

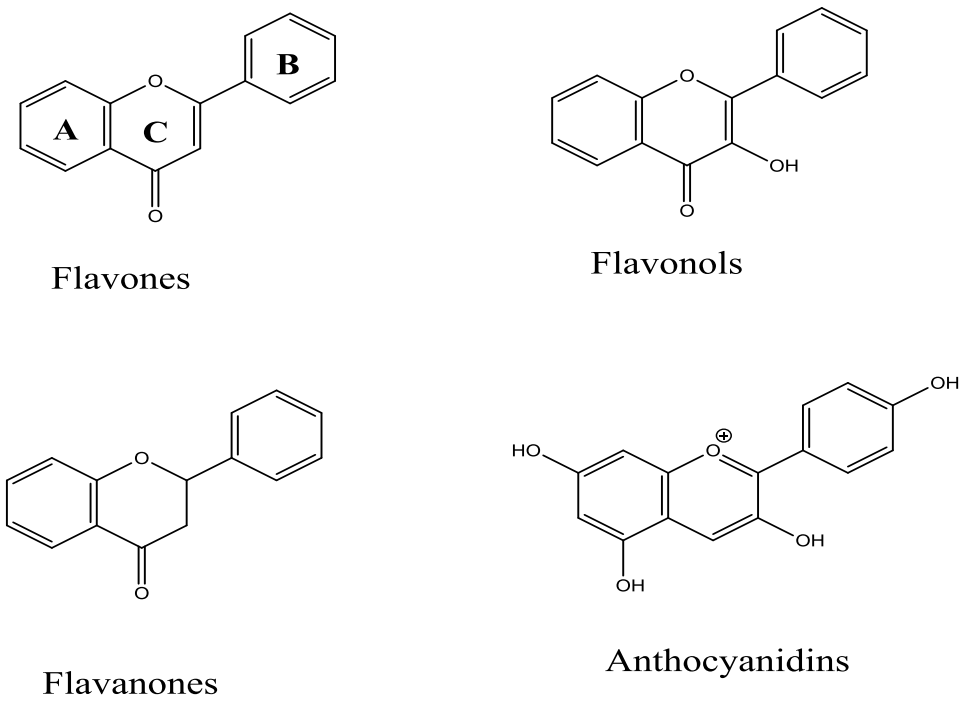

Figure 1.3 Subclasses of flavonoids.
Classification is based on variations in the heterocyclic C-ring.

1.1.1.1 Health benefits of flavonoids

In recent years, there have been an increasing number of reports on the physiological functions or biological effects of flavonoids as nutrition products in human health. About 3000 different types of flavonoids have been reported. The majority of flavonoids have low toxicity in humans and some of them are widely used in medical treatments due to their antioxidant abilities and hold promise for preventing age-related diseases including heart disease by maintenance of capillary microcirculation

through reducing the fragility of blood capillaries. Furthermore, flavonoids have several biological effects such as anti- inflammatory, anti- hepatotoxic and anti-ulcer actions (Narayana *et al*., 2001). The chemical structure of flavonols plays a very important role for antioxidant activity due to the existence of a hydroxyl group at C-3 and a C-2 and C-3 double bond (Srivastava and Bezwada, 2015). Their health benefits must be considerate as they are obtained from diets rich in vegetables, fruits, herbs and beverages such as teas and wines. Flavonoids are associated with a broad spectrum of health promoting effects and are indispensable components in a variety of nutraceutical, pharmaceutical, medicinal and cosmetic preparations. They are known to possess antioxidant, anti-inflammatory and anti-carcinogenic properties coupled with a capacity to modulate key cellular and enzyme functions (Kohlmeier, 2003).

1.1.1.2 Major classes of flavonoids

1.1.1.2.1 Flavonols

Flavonols contain a carbonyl group at C-4 and a hydroxyl group at position C-3 **(Figure 1.3)**. They are present in various fruits and vegetables such as grape, apple, berries, onions, lettuce, tomato, and kale as well as beverages (tea and wine). The major flavonols are quercetin, kaempferol, myricetin and rutin (Srivastava and Bezwada, 2015, Omar, 2013). In plants these compounds are usually conjugated with sugars to form glycosides. The common sugar moieties found as conjugates are glucose and galactose (Omar, 2013, Chanet *et al*., 2012). The consumption of flavonols provides a wide range of health benefits to humans which include

antioxidant activity and reducing the risk of vascular diseases (Srivastava and Bezwada, 2015). **Figure 1.4** shows the structures of some flavonols.

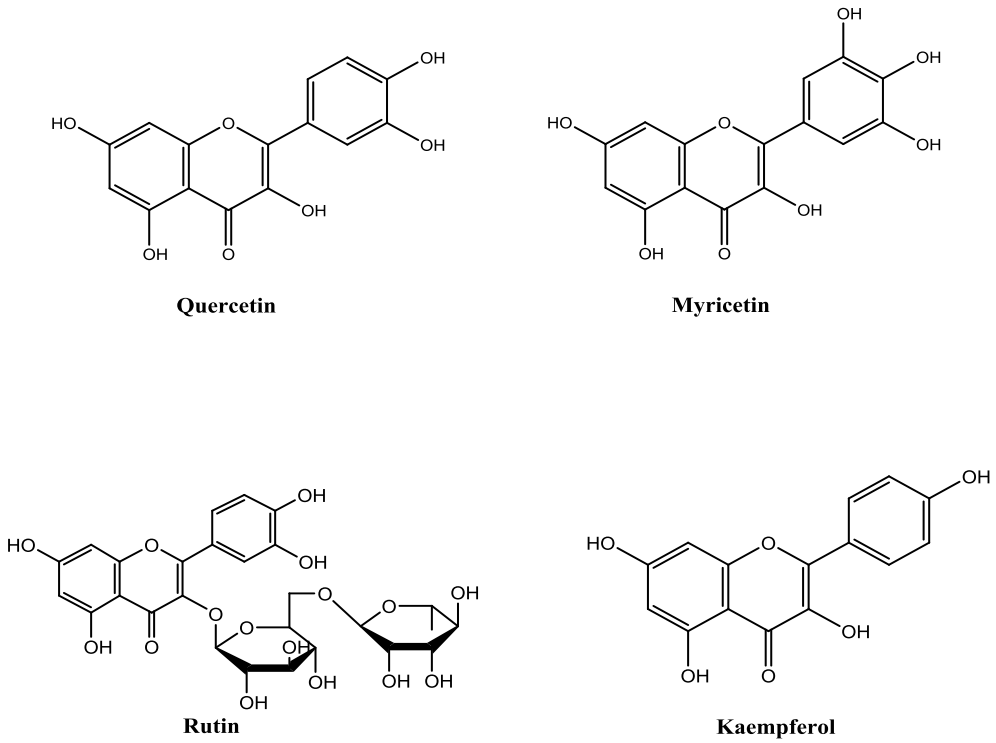

Figure 1.4 Common flavonols.

1.1.1.2.2 Flavones

Flavones are one of the flavonoid class of compounds and are widely distributed in plant leaves, flowers and fruits as glycosides. Flavones have a double bond between position 2 and 3 in the C-ring of their structures with usually a lack of oxygenation or substituent at C-3 **(Figure 1.3)** (Omar, 2013, Del Rio *et al*., 2013). The possible substitutions with flavones are hydroxylation, methylation, O- and C-glycosylation, and alkylation (Del Rio *et al*., 2013).The major flavones are apigenin, luteolin and tangeritin which are substantially found in celery, parsley, red and green peppers,

chamomile, mint and *Ginkgo biloba*. Other flavones such as tageretin, nobiletin and sinensetin which are polymethoxylated flavones are extensively found in peels of citrus fruits (Manach *et al*., 2004). They display various biological functions. **Figure 1.5** shows the structures of some flavones.

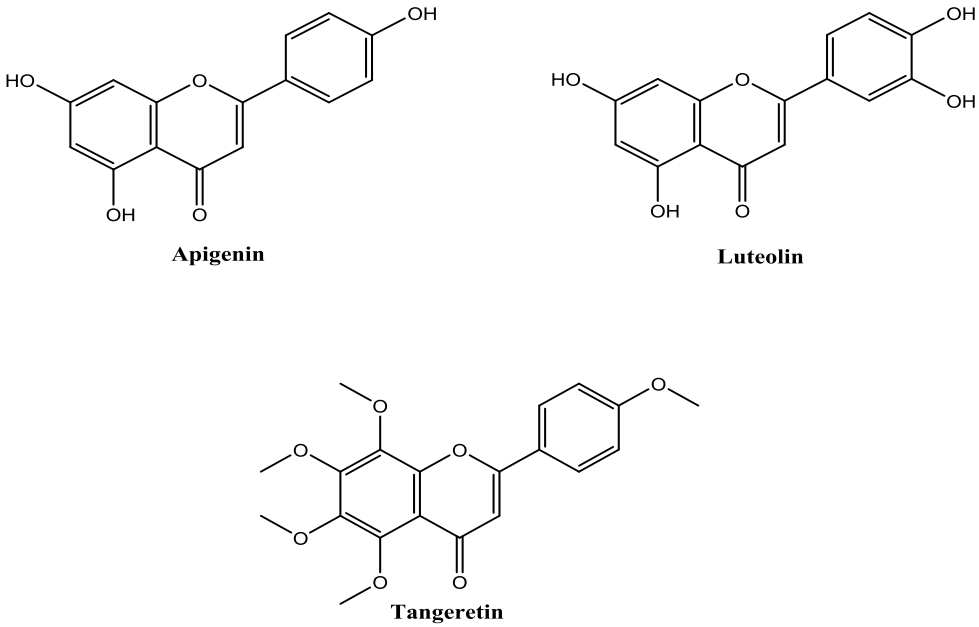

Figure 1.5 Common flavones.

1.1.1.2.3 Flavanones

Flavanones are a class of flavonoids generally present in citrus fruits such as oranges, lemons, grapes etc. Hesperidin, hesperitin, naringenin, naringin and eriodictoyl are examples of flavanones. Since they have free radical scavenging properties, flavanones play important roles in many beneficial health effects in human as antioxidants, anti-inflammatory, reducing lipid and cholesterol levels in blood. Hesperidin, eriocitrin, and naringin are glycosides (disaccharide substitution) at

position C-7 of hesperetin, eriodictyol, and naringenin. These glycosides give the bitter taste of the juice and peel of citrus fruits (Srivastava and Bezwada, 2015, Chanet *et al*., 2012). **Figure 1.6** shows the structures of some flavanones.

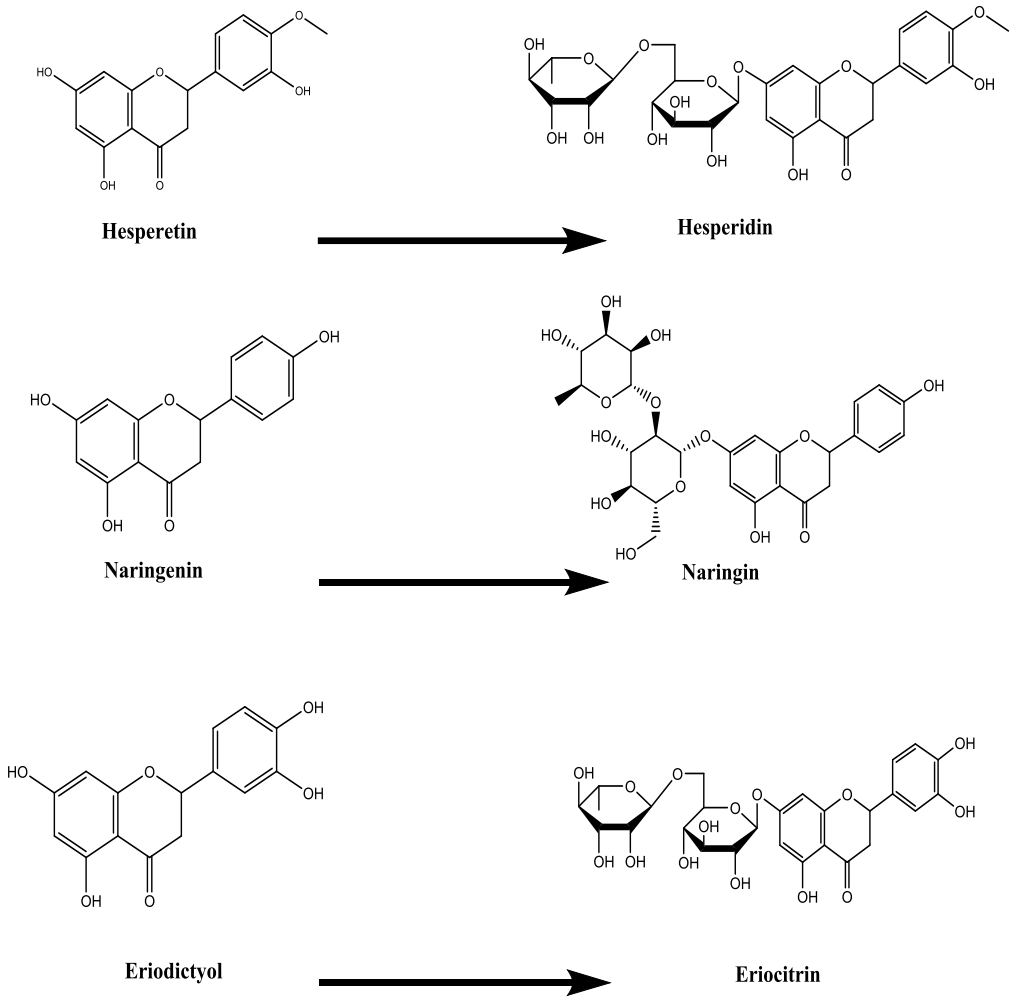

Figure 1.6 Some common flavanones.

1.1.1.2.4 Anthocyanins

Anthocyanins are the glycoside form of anthocyanidins. They are responsible for the colouring of flowers, seeds and fruits in plants. They are present in the outer cell layers of fruits such as cranberry, blackcurrant, red grape, merlot, raspberry, strawberry, blueberry, bilberry and blackberry. The most widely distributed anthocyanidins in flowers are cyanidin, delphinidin, malvidin, pelargonidin and peonidin. Anthocyanins display health benefits such as anti-oxidant, anti-inflammatory, anti-microbial and anti-carcinogenic activities in humans. In addition, they play a role for reducing the risk of coronary heart disease by exhibiting significant effects on blood vessels and blood platelets. Anthocyanins have colouring properties and they are used in the food industry as additives and food colorants due to their chemical stability and health benefits (Charron *et al*., 2009, Srivastava and Bezwada, 2015). **Figure 1.7** shows the structures of some anthocyanidins.

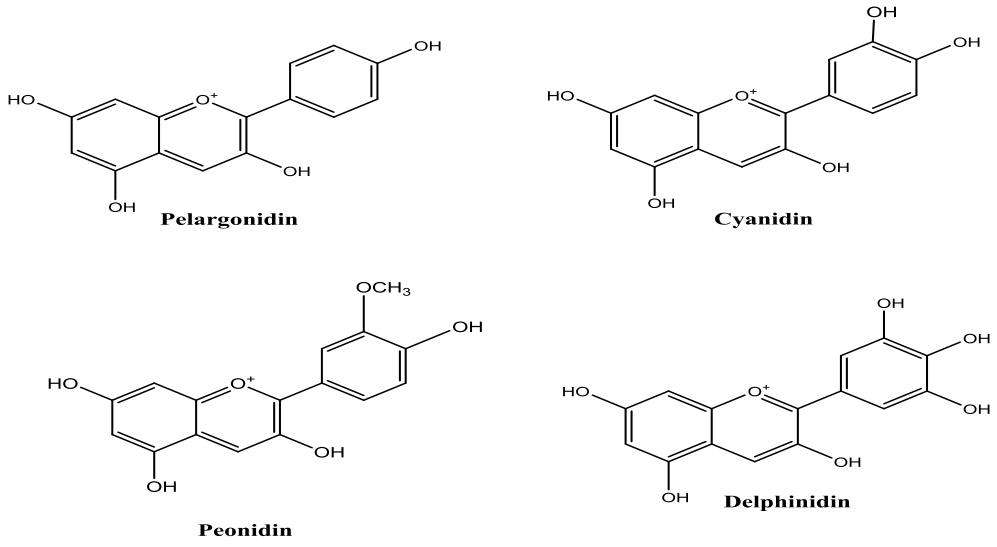

Figure 1.7 Common anthocyanidins.

1.1.1.2.5 Isoflavonoids

Isoflavonoids or isoflavones have the usual C-2-phenyl ring substituted at the C-3 position. They have a limited distribution in plants and are predominantly found in soybeans and other leguminous plants. Some isoflavonoids occur in microbial organisms. The common types of isoflavonoids are genistein and daidzein. Isoflavonoids have biological properties and health benefits in humans; playing roles in promoting strong and healthy bones by improving bone mass and reducing bone resorption. Isoflavonoids also have anti-oxidant properties and display great prospect in combating a number of diseases such as cancer including breast cancer and prostate cancer (Srivastava and Bezwada, 2015, Del Rio *et al*., 2013, Peterson and Dwyer, 1998, Omar, 2013). **Figure 1.8** shows the structures of some isoflavonoids.

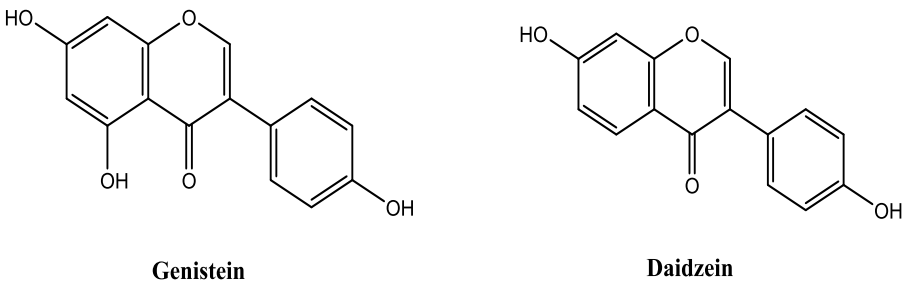

Figure 1.8 Common isoflavonoids.

1.1.2 Non-flavonoid phenolic compounds

Non-flavonoid phenolic compounds are derivatives of benzoic acid and phenyl propanoic acid (hydroxycinnamic acid). Their main classes are hydroxycinnamic acid and hydroxybenzoic acid.

1.1.2.1 Hydroxybenzoic acids (HBA)

Hydroxybenzoic acid is one of the non-flavonoid class of compounds having a C6-C1 skeleton and the most common derivatives are gallic acid and protocatechuic acid **(Figure 1.9)**. Gallic acid is present in wine and in variety of fruits such as raspberries, strawberries, and blackberries and play major roles in stabilizing and enhancing the colour of red wine and also add to the flavour of the wine (Moreno-Arribas and Polo, 2009, Del Rio *et al*., 2013).

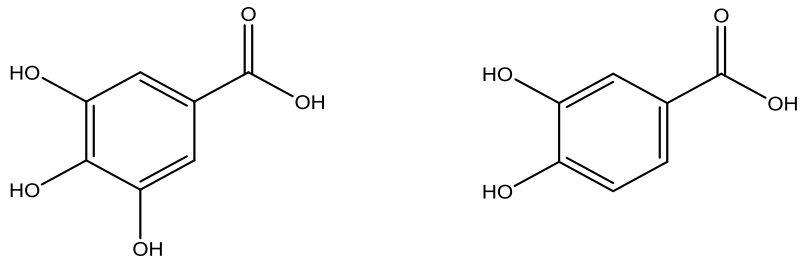

Figure 1.9 Common hydroxybenzoic Acids.

1.1.2.2 Hydroxycinnamic acids (HCA)

Hydroxycinnamic acids are non-flavonoid compounds having a C6-C3 skeleton. The C3 part is almost always unsaturated with a double bond. They are widely distributed in plants, foodstuffs and beverages such as coffee, wine and fruit juices (Clifford,

2000). They have one or more hydroxyl groups or methoxy groups attached to the benzene ring. Caffeic, *p*-coumaric, ferulic, and sinapic acids are some hydroxycinnamates found in foods **(Figure 1.10)** (Clifford, 2000, Manach *et al*., 2004). Hydroxycinnamic acids occur both as free acids and as esters of quinic acid, glucose or carboxylic acids such as shikimic or tartaric acids (Herrmann and Nagel, 1989). Esters of caffeic, ferulic and *p*-coumaric acids with quinic acid are commonly known as a family of compounds referred to as chlorogenic acids. They are found in coffee beverages, artichoke, cherries, blueberries, aubergine and apples (Herrmann and Nagel, 1989, Clifford, 2000, Manach et al., 2004). Dietary hydroxycinnamic acids have been reported to have strong antioxidant activities and ability to inhibit cardiovascular diseases, diabetes and Alzheimer. They also have antibacterial and anti-inflammatory activities (Omar, 2013).

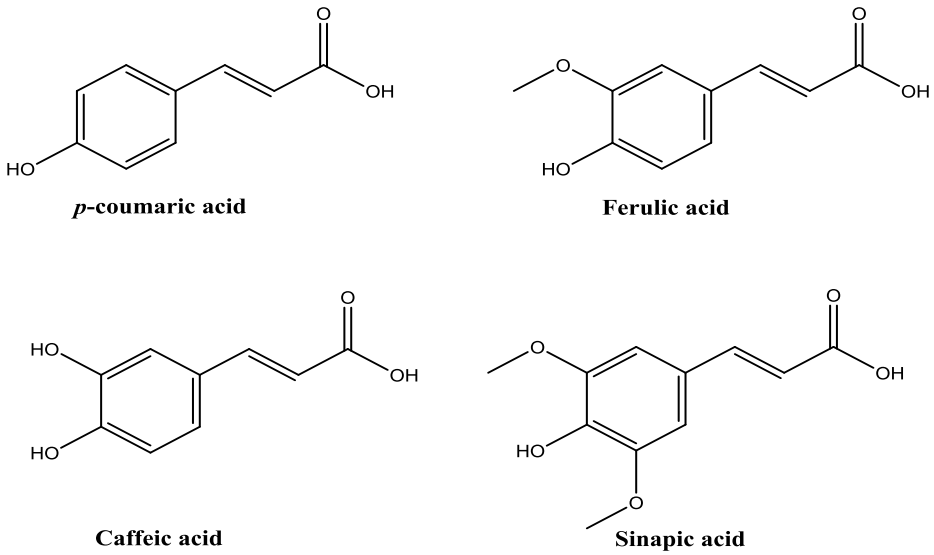

Figure 1.10 Common hydroxycinnamic acids.

1.2 Physiological sites of xenobiotic metabolism

There are numerous sites responsible for xenobiotic metabolism in the body. Xenobiotic metabolism is catalysed by enzymes present in the walls of the gut, lungs, kidney, plasma, placenta and skin but the most active site of xenobiotic metabolism is the liver. Generally, the metabolic processes are divided into hepatic metabolism in the smooth endoplasmic reticulum (which has a variety of enzymes) of the liver cells and extra-hepatic metabolism which occurs in other organs which have a limited extent in the metabolism processes.

In this study, the biotransformation of nutritional substances such as polyphenols under hepatic metabolism by rat hepatocytes isolated from the liver was studied. The liver was chosen because it is the fundamental organ and the key processor or site of metabolism of xenobiotics and detoxification of drugs by human and animals via phase I oxidative and phase II conjugative pathways in the body. The liver due to its location and function has a substantial amount of cells with high blood supply and metabolic enzymes (Li, 2000, Vagbjiani, 2008, Vickers, 1996).

1.2.1 The liver

1.2.1.1 Anatomy of the liver

The liver is the largest organ in the body. It is located under the diaphragm in the right upper quadrant of the abdomen and protected by the ribs. The surface of the liver is divided into a right and left lobes on the front face and four lobes on the underside. All nutritional substances such as drinks and xenobiotics consumed are absorbed by the gut and perfused by the blood stream to pass through the hepatic

portal circulation in the liver and are then excreted either in the bile or in urine (Holt and Smith, 2008).

1.2.1.2 Functions of the liver

The liver is the key organ providing an immune barrier to pathogens in the body and it carries out the biotransformation of xenobiotics and excretion of undesirable substances and toxins from the body (Holt and Smith, 2008). It is the main vascular organ in the visceral and receives around 1.3 L of blood per minute. This blood is rich in nutrients and oxygen from the intestinal tract and ready for the metabolic processes in the liver. This metabolic process is termed as the *first-pass* metabolism and it produces water-soluble metabolites that are excreted from the body either in the urine or the bile. The blood passes through the liver in two ways; 75% of the blood is passed through the portal vein and drained by the gut while the remainder flows through the hepatic artery (Li, 2000, Holt and Smith, 2008, Coleman, 2010b). In addition, the liver is considered central as it provides energy, carbohydrates, and amino acids to peripheral tissues of the body **(Figure 1.11)** (Vickers, 1996).

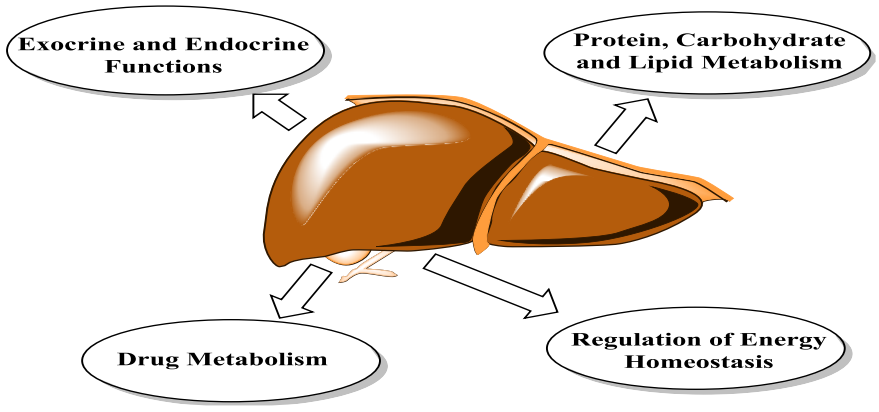

Figure 1.11 Summarised scheme of liver functions.

1.2.1.3 Cells of the liver

The liver tissue consists of parenchymal and non-parenchymal cells. The parenchymal cells or hepatocytes are the predominant cells in the liver and occupy about 80-88% of the total volume of the liver in humans. The remaining part of the liver is occupied by the non-parenchymal or liver sinusoidal cells which consist of Kupffer cells and endothelial cells, fat storage cells and bile duct epithelial cells (Holt and Smith, 2008, Vickers, 1996).

1.2.1.3.1 Hepatocytes

The principal site for xenobiotic metabolism in the liver is in the hepatocytes (Coleman, 2010b). Hepatocytes originate from the dissociation of liver tissues by enzymes and are an abundant source of cytochrome P450 enzymes (McQueen and Williams, 1987). Morphologically, hepatocytes are large cells with polyhedral shapes which have up to six surfaces and measure between 20-30 μm in diameter. They are arranged in plates around the liver sinusoids by one or two thick layers (Holt and Smith, 2008). Hepatocytes play roles in the preservation of body health via the regulation of energy homoeostasis, protein synthesis and drug detoxification (Holt and Smith, 2008), as they have the ability to resist toxic substances in the body (Coleman, 2010b).

1.2.1.3.1.1 Biotransformation of xenobiotics by hepatocytes

Identification of a substance or drug pathway is usually carried out *in vivo* using animal models such as rats, dogs and monkeys. This is useful in the preliminary stages of substance or drug discovery and development in order to determine their

toxicity or health benefits when consumed. This may seem uneconomical and morally unacceptable thus in recent studies. The use of isolated hepatocytes *in vitro* has become more popular for simulating the metabolic pathways of substances in the body. The isolated hepatocytes contain whole enzymes and cofactors for metabolising substances (Guillouzo, 1996) under the influence of a variety of easily controlled conditions to mimic the body environment such as temperature and atmosphere. Studies of the biotransformation of substances by isolated hepatocytes bridges the important gap between *in vitro* and *in vivo* study systems. One advantage of using isolated hepatocytes in biotransformation studies is to avoid the effect of extra hepatic factors that could make the investigation of the metabolic pathway more complicated and could lead to health problems in animal models. Moreover, *in vitro* experiments can be maintained in terms of the relationship between the cytochrome P-450 based systems and other drug metabolizing pathways which exist *in vivo* (Renton, 1987) as well as, the isolated cell systems used in pharmacokinetics and pharmacodynamics studies of candidate drugs and the isolated hepatocytes. This is beneficial and an easy experiment for determining the relationships between dose–response and the effect of inhibitors of biotransformation pathways of the drugs (Renton, 1987, Thomson, 2008).

1.2.1.3.1.2 Isolation of hepatocytes

Hepatocytes are produced by the dissociation of liver tissues. A number of the early methods for the production of hepatocytes from liver tissues using hyaluronidase and collagenase enzymes on slices of the liver seem to produce impoverished cell viability. Nowadays, to improve cell viability, hyaluronidase and collagenase

enzymes are perfused into the liver in a circulating system through cannulation of the hepatic portal vein (McQueen and Williams, 1987). In recent years, the number of protocols for the isolation of hepatocytes with high cell viability and functionality in suspension or in monolayer cultures has increased.

Generally, in order to study xenobiotic metabolism *in vitro*, a two-step perfusion method using hyaluronidase and collagenase enzymes is becoming a popular protocol for the isolation of hepatocytes from the liver of humans and laboratory animals such as rats, mice, hamsters, guinea pigs and rabbits (McQueen and Williams, 1987). Numerous early methods employed for the isolation of hepatocytes were mechanical, chemical and enzymatic as well as a combination of these methods. However, the separation method for liver cells by ancient techniques such mechanical force maybe lead to cell membrane damage and change of morphological structure of cells. In 1967 Howard, *et al* illustrated an enzymatic protocol for disintegrating intact cell membranes by shaking liver slices in enzymatic buffered medium containing hyaluronidase and collagenase **(Figure 1.12)**. However, this protocol produces very low isolated cell viability about 5% of the original liver tissue. Metabolism studies require sufficient amounts of intact cells. A modified enzymatic method was used to improve the quantity of disintegrated parenchymal cells with rapid isolation of intact cells from rat liver. A collagenase enzyme was perfused at 37°C into the liver tissue by cannulising the hepatic portal vein instead of using liver slices (Berry and Friend, 1969, Doo-Hoon Lee and Lee, 2014). Several minor modifications of the preparation of hepatocytes have been made such as changes of perfusion medium, duration of the liver perfusion and transport of the

liver from rodents prior to perfusion or alteration of the washing cells (Berry *et al*., 1991).

Generally, in all perfusion methods involving the isolation of hepatocytes, the exposure of the cells in the absence of Ca^{2+} ions allows the cleavage of hepatic desmosomes (*Macula adherens*) and the activation of the collagenase medium in presence of Ca^{2+}. These requirements for the isolation of hepatocytes have been resolved by the 'two-step' procedure (Berry *et al*., 1991) which was initially introduced by Seglen in 1976 and was the first to pre-perfuse the liver with a Ca^{2+} free enzyme buffer for at least 10 minutes and accomplished the perfusion with a Ca^{2+} enriched collagenase-containing buffer solution. This technique has become popular for isolating intact hepatocytes with improved cell viability. Recently, some researchers perfuse the liver by a 'five-step' procedure as a modification of the 'two-step' procedure using EDTA, Ca^{2+} free, low Ca^{2+} collagenase and cold washing buffers in sequence (Doo-Hoon Lee and Lee, 2014).

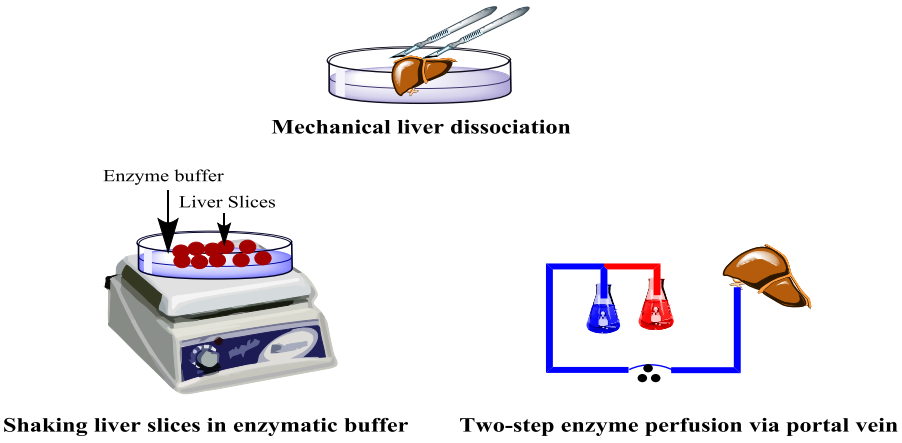

Figure 1.12 History of hepatocyte isolation techniques.

1.3 Hepatic metabolism

Hepatic metabolism also regarded as metabolic detoxification is a series of conjugation processes to make relatively insoluble unwanted substances more water soluble for easy elimination in the urine or bile. There are several pathways responsible for purifying the body of xenobiotic toxicants (Bronk, 1999).

The hepatic metabolism of substances and drugs is accomplished by enzymes termed as the cytochrome P450 system in the smooth endoplasmic reticulum of the hepatocytes in the microsomes (Williams, 1972, Vaghjiani, 2008). Xenobiotics can undergo oxidation (phase I metabolism) involving the cytochrome P450 enzymes and then by conjugation (phase II metabolism) by compounds such as glucose, sulfates, cysteine or glutathione to produce high polar metabolites with higher molecular weights (>200 Da) which lead to secretion by hepatocytes into the bile as phase III metabolism while lower molecular weight metabolites are released back into blood stream and excreted in urine through the kidneys (Li, 2000, Vaghjiani, 2008).

The main purpose of metabolism of substances in the body is to produce active or inactive metabolites, but toxic intermediates or active metabolites may also be generated and this must be considered when studying drugs or substances which show hepatotoxic activity compared to the parent compound. This is known as metabolic activation (Vaghjiani, 2008).

1.3.1 Metabolism of xenobiotics

Metabolism is an enzymatic process aimed at converting molecules of substances that can pass through biological membranes into one that can be removed generally in the urine hence each progressive metabolic step usually reduces the lipophilicity of the compound. Xenobiotic metabolism reactions occur in three different phases termed phase I, phase II and phase III biotransformations. Phase I transformations are preparative processes to phase II metabolism and it occurs by the introduction or unmasking of a functional group in the parent compounds such as oxygenation or hydrolysis and are usually accomplished by the cytochrome P450 family (CYP) of enzymes. Thereafter or independently, in case the parent substances have hydroxyl, carboxyl, amino, heterocyclic nitrogen and thiol groups they (the acceptor function groups) are conjugated with polar molecules such as glucuronides, glutathione, amino acids and sulfate to increase the polarity of metabolites known as the conjugative processes (phase II) **(Figure 1.13)**. This is catalysed by six enzyme families for elimination in the urine or bile On the other hand, many xenobiotics and drugs are excreted unchanged in faeces or urine without any transformation (Silverman, 2004, Ma and Zhu, 2009, Coleman, 2010a, Hoffmann *et al*., 2014). Although metabolism is considered as a detoxification process of xenobiotics and drugs this is not always the case since some reactive metabolites or intermediates are not excreted from the body and may have terminated biological activity or toxicity properties (Ma and Zhu, 2009). Recently, the 'Phase III' pathway has been found to play an important mechanism in detoxification by allowing the hydrophilic molecules and the metabolites to migrate out of the cells to interstitial fluids, blood and finally the kidneys (Coleman, 2010a, Hoffmann *et al*., 2014). The rate of drug

metabolism can be affected by various factors such as species, strain, sex, age, hormones, pregnancy and liver diseases (Hargreaves, 1968, Silverman, 2004).

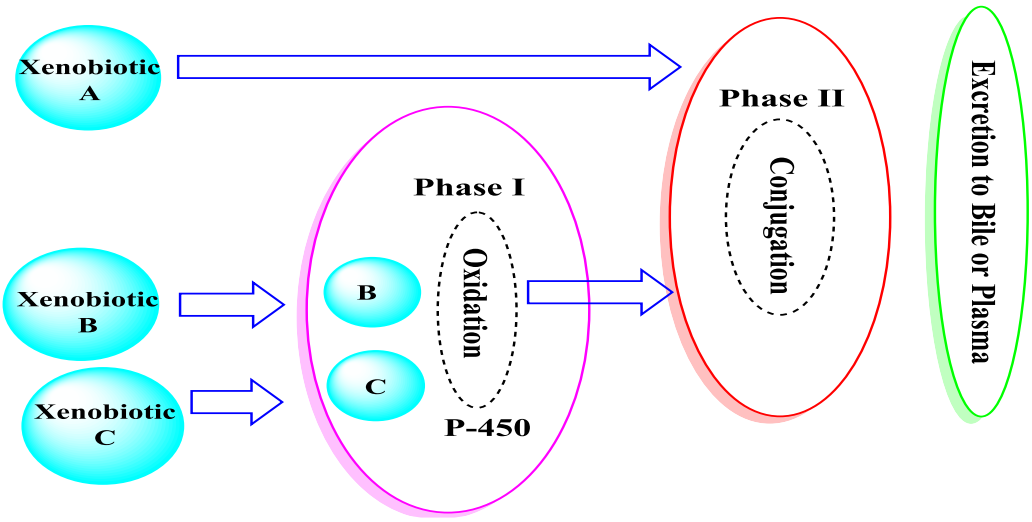

Figure 1.13 Summarised scheme of sequential metabolism.

1.3.1.1 Common metabolism pathways

Biotransformation have been classified to modification (phase I), conjugation (phase II) and transport (phase III). The common classifications of the metabolic reactions are given in **Table 1-1**.

Table 1-1 Common chemical reactions of phase I and phase II metabolism (Silverman, 2004, Silverman and Holladay, 2014)

Phase I Reactions	Phase II Reactions
Oxidation	Glucuronidation / Glucosidation
Reduction	Sulfation
Hydrolysis	Methylation
Hydration	Acetylation
Dethioacetylation	Amino acid conjugation
Isomerisation	Glutathione conjugation

1.3.1.1.1 Phase I biotransformation

Phase I reactions are basically divided to the most common reactions such as oxidation, redaction and hydrolysis.

1.3.1.1.1.1 Oxidation reactions

Oxidation reactions are the most common phase I biotransformation processes aimed at increasing the hydrophilicity of the xenobiotic via loss of electrons and insertion of a single oxygen atom or removal of hydrogen atoms from substrates. There are numerous classes of enzymes that catalyse these reactions by either microsomal mixed – function oxidases system cytochrome P450s (CYP 450) which consist of hydroxylation, deamination and epoxidation or non-microsomal enzymes such as flavin monooxygenases (FMO), monoamine oxidases (MAO), xanthine oxidase (XAO), aldehyde oxidases (AO), aldehyde dehydrogenases (ALDH) and peroxidases (Wen and Nelson, 2011, Schonborn and Gwinnutt, 2010, Taxak and Bharatam, 2014).

1.3.1.1.1.2 Reduction reactions

Reduction reactions are the second type of phase I biotransformation and aimed at producing polar function groups in substances such as amino and hydroxyl by the gain of electrons and removal of oxygen atoms or addition of hydrogen atoms for further metabolic processes. These reactions are catalysed by some enzymes found in the liver and other body tissues under anaerobic conditions such as cytochrome P450 enzymes, molybdenum reductases, alcohol dehydrogenases, carbonyl reductases, NADPH-cytochrome P450 reductase, NAD(P)H-quinone oxidoreductases and intestinal microflora enzymes (Wen and Nelson, 2011, Schonborn and Gwinnutt, 2010, Taxak and Bharatam, 2014).

1.3.1.1.1.3 Hydrolysis reactions

Hydrolysis is the final type of phase I biotransformation and is aimed at splitting the substrate molecule or breaking a bond by the addition of water. This reaction occurs in substrate molecules containing amide and esters functional groups by esterase and amidase enzymes which are found in many body tissues but specifically in the small intestines (Wen and Nelson, 2011, Schonborn and Gwinnutt, 2010, Taxak and Bharatam, 2014).

1.3.1.1.2 Phase II biotransformation

Phase II metabolism is aimed at conjugating the xenobiotic or drug substrate to reactive groups of compounds to increase water solubility and the elimination of the substance through the urine or bile. The conjugation is usually to glucuronic acid, sulfate, glutathione, acetyl and methyl groups. The common phase II reactions are summarised in **Table 1-2**.

Table 1-2 Common phase II reactions
(Silverman, 2004, Silverman and Holladay, 2014).

Reaction	Enzyme	Functional group
Glucuronidation	UDP-Glucuronosyltransferase	-OH, -COOH, -NH_2, SH
Glycosidation	UDP-Glycosyltransferase	-OH, -COOH, -SH
Sulfation	Sulfotransferase	-NH_2, -SO_2NH_2, -OH
Methylation	Methyltransferase	-OH, NH_2
Acetylation	Acetyltransferase	-NH_2, -SO_2NH_2, -OH
Amino acid conjugation		-COOH
Glutathione conjugation	Glutathione-S-transferase	Epoxide, Organic halides

1.3.1.1.2.1 Glucuronidation reactions

Glucuronidation is the most common pathway in phase II metabolism reactions. It involves the sugar acid, glucuronic acid conjugating with active substrates in the xenobiotics. This reaction is catalysed by uridine diphosphate-glucuronosyl transferases (UDPGA) or UDP-glucuronosyl transferases (UGTs) enzymes in microsomal and nuclear membranes bound to liver cells or as extra-hepatic cells in other tissues such as the lungs, small intestines, kidneys and skin. Glucuronidation reactions are hydrophilic and it involves the anomeric carbon of glucuronic acid

being attached to nucleophilic groups in substances such as O-, N-, S- and active carbon atoms. Sometimes glucuronidation is combined with phase I metabolism with limited oxidation of the substrate by cytochromes P450 enzyme if the substances do not have nucleophilic groups to conjugate with glucuronic acid.

Since glucuronides are water soluble conjugates, they are useful for the detoxification of most xenobiotics by excretion of the conjugated metabolites in urine, if the molecular weight of the conjugate is less than 300 Da, or in bile if the molecular weight of the conjugate is greater than 300 Da. On the other hand, apart from the detoxification of drugs, glucuronidation is also capable of causing cellular injury or hepatotoxicity and carcinogenesis as it tends to produce reactive intermediates which could also be transported into target tissues (Conway *et al*., 1987, Wen and Nelson, 2011, Silverman, 2004, Ionescu, 2006, Coleman, 2010c). For example the glucuronide conjugate of valproic acid yielded toxic compounds and shows glucuronidation could produce hepatotoxic substances (Lee *et al*., 2009). Glucuronidation of xenobiotics is an important phase II reaction in mammals. There are four general classes of glucuronides (O-, N-, S- and C- bonded). The sites of glucuronidation reaction for most substrates having one or more functional groups are shown in **Figure 1.14**. Oxygen containing substrates that from glucuronides are alcohols, carboxylic acids and phenols. Nitrogen containing substrates that from glucuronides include all types of amines and some amides while sulfur substrates that form glucuronides are thiols and thiocarbonyl groups and carbon substrates that form glucuronides are usually amide carbons with acidic hydrogen atoms (Wen and Nelson, 2011).

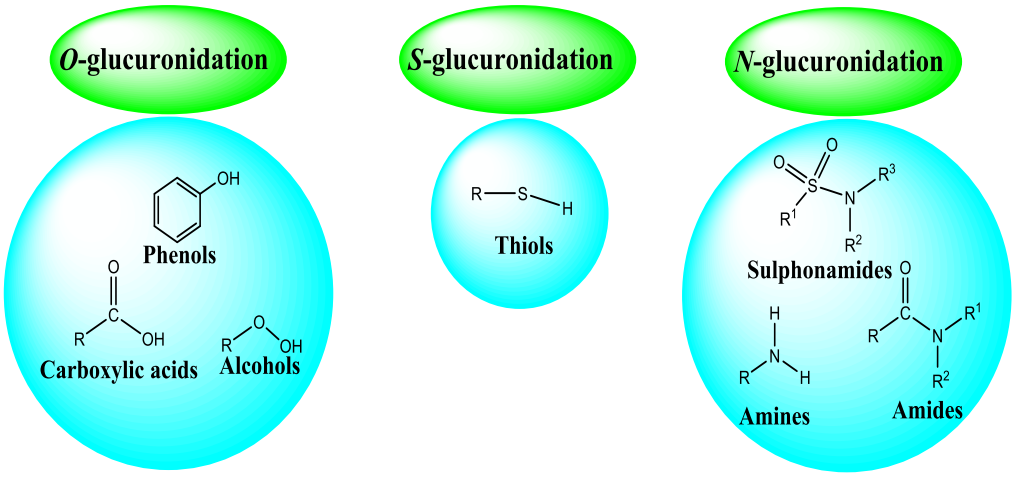

Figure1.14 Scheme of substrates of xenobiotics that form conjugates via glucuronidation in presence of UDP-Glucuronosyl transferase enzymes.

1.3.1.1.2.2 Sulfation reactions

Sulfation is the second reaction of phase II metabolism but less common than glucuronation conjugation processes in humans. Sulfation reaction requires the presence of sulfates in body cells and due to poor availability of the activated sulfates in cells; this process is not a very common metabolic process. In fact the substrates that are known to undergo sulfation reactions are phenols, alcohols and *N*-hydroxy compounds. Others are hydroxyl groups on alcohols and on hydroxylamines and hydroxyamides, and nitrogens of amines and some amides (Silverman, 2004, Ionescu, 2006, Bo Wen 2011).

Sulfation is achieved by a set of enzymes known as sulfotransferases (SULTs) and it involves the transmission of a charged sulfonate group from the co-factor 3'-phosphoadenosine-5'-phosphosulfate (PAPS) by electrophilic interactions and can react with -C-OH, -N-OH and -NH groups. The liver, small intestine, main intestine

and colon are the major sites of sulfation, although they are also found in the brain and the placenta.

Generally, sulfation reactions are aimed at making xenobiotics more water soluble and less active pharmacologically and thereafter eliminated in urine and bile (Maurice *et al*., 2004, Coleman, 2010c, Bo Wen 2011). Indeed, several xenobiotics can undergo glucuronidation and sulfation reactions and thus competition for substrates can occur between these two pathways. However, glucuronidation dominates at high substrate concentrations whereas sulfation predominates at low substrate concentrations. This is due to the relatively high abundance of uridine diphosphoglucuronic acid (UDPGA) compared with PAPS, the activated conjugating agent for sulfation reactions (Skett, 1986).

1.3.1.1.2.3 Glutathione reactions

Conjugation of xenobiotic substrates to glutathione is another pathway involved in phase II metabolism. Glutathione (GSH) is a tripeptide containing a γ-glutamyl-cysteinyl-glycine that is not hydrolysed by normal peptidases because of its γ-glutamyl linkage (Wen and Nelson, 2011) **(Figure 1.15)**.

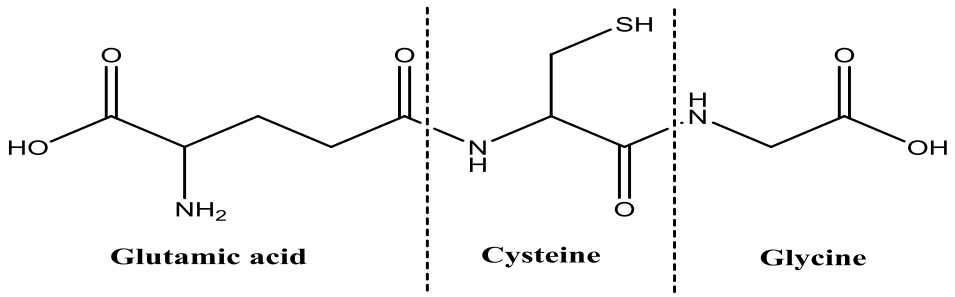

Figure 1.15 Scheme of the glutathione composition.

The tripeptide glutathione is present in all mammalian tissues particularly in the liver and it contains a cysteinyl moiety where the reactive group is the thiol –SH which acts as a nucleophile reacts with electrophilic heteroatoms or groups (O, N and S) in the xenobiotic substance (Bo Wen 2011, Maurice *et al*., 2004). Drug substrates usually involved in these conjugation reactions with glutathione include epoxides, enones and enals as well as similarly conjugated systems; at saturated and unsaturated carbon atoms that have strong electron withdrawing groups and at heteroatoms that have good leaving groups attached (Bo Wen 2011). This pathway is more involved in the detoxification of radical or highly reactive substances for the protection of cells against oxidative damage by forming a thio-ether link with the electrophilic centre of the compound although the GSH diminution could lead to toxicity (Tyson and Green, 1987, Maurice *et al*., 2004, Ma and Zhu, 2009). Since some substances are not transformed by glucuronidation and sulfation enzyme processes and these metabolites escape into the cytosol and nucleus they may conceivably cause carcinogenic effects but these compounds are conjugated by GSH (Coleman, 2010b). The conjugation reaction occurs in the cytoplasm of cells and it is catalysed by glutathione-S-transferase enzymes (GSTs) which family of cytosolic enzymes present in most body organs with high abundance in liver, intestine, kidney adrenal and lung (Maurice *et al*., 2004, Silverman, 2004). On the other hand, in high reactive electrophilic compounds, the glutathione reaction occurs non-enzymatically. Glutathione conjugates are seldom eliminated in urine because of their high molecular weights and amphiphilic characteristics; therefore, usually eliminated in the bile and faecal in addition some glutathione conjugates metabolised further in

phase III metabolism which forms water - soluble products that will be easily excreted through the kidney (Silverman, 2004, Bo Wen 2011).

1.3.2 Metabolism of polyphenol compounds

The determination of the biological activity, distribution and clearance of polyphenols depend on the type of pathway and position of the conjugate *in vivo*. The bioavailability and intestinal metabolism varies for polyphenols. The common pathways of polyphenol metabolism are glucuronidation, sulfation and methylation.

Figure 1.16 illustrates the possible routes for consumed dietary polyphenols in human. Flavonoids are metabolised in the intestine before absorption is complete or in the liver and other metabolically active organs. Most of these reactions are not well characterized (Kohlmeier, 2003). The study and investigation of flavonoid conjugates and metabolites are essential for the determination of their bioactivity. The metabolism of flavonoids occurs in the small intestine, liver and by enzymes of the colonic microflora. The aglycones are conjugated with sulfate, glucuronide and methyl groups in the enterocytes before passing to the blood stream and target organs. Flavonoid metabolites in the bloodstream can be subjected to further metabolism in the liver and transported in the bile and recycled to the small intestines (Gunter, 2003, Crozier *et al*., 2009).

Unabsorbed flavonoids from small intestines pass into the colon, where the sugar elements are fragmented by microflora enzymes (Olthof *et al*., 2003). Moreover, the enzymes cleave the ring structures of numerous polyphenols and produce small molecular weight phenolic acids. Unconjugated flavonoids may escape into cytosol and the cell nucleus and any potential cytotoxic flavonoid is conjugated via

intercellular interaction with thio –SH of glutathione. For instance, quercetin can be conjugated with GSH to produce mono-and diglutathionyl adducts in its A-ring. Interestingly, the conjugation of flavonoids with GSH may cause depletion in cellular thiols (Jeremy *et al*., 2003a).

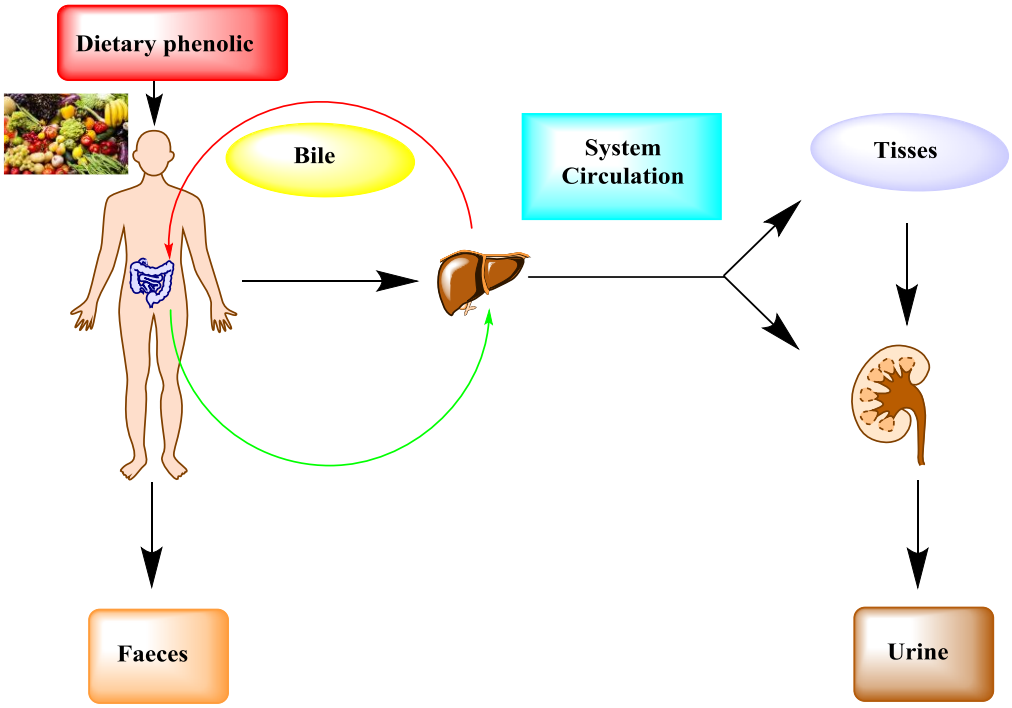

Figure 1.16 Possible routes for consumed dietary phenolic in humans.

1.4 Identification of metabolites using liquid chromatography-mass spectrometry

Metabolite profiling and identification by liquid chromatography and mass spectrometric (LC-MS) techniques is highly useful in pharmaceutical research. Xenobiotic metabolites identification by LC-MS involves the detection of ions of metabolites in a biological matrix and the acquisition of their product ion spectra for structural description. Based on LC-MS data analysis for the candidate sample, metabolites obtained from it can be classified to common (expected) and uncommon (unexpected) metabolites. The expected or common biotransformation of samples is known as phase I, phase II and phase III biotransformation. Uncommon metabolites can be produced via unconventional or multiple steps of biotransformation reactions. Mass shifts of uncommon metabolites in complex biological matrixes are difficult to determine and expected from the parent compounds because the uncommon metabolites are present at small quantities and also are often masked by background noise and endogenous components in their mass spectrum.

Electrospray ionisation mass spectrometry (ESI-MS) has been used as a major analytical tool for the detection and profiling of metabolites of xenobiotic candidates *in vitro* due to its sensitivity and selectivity. These metabolites were detected and screened by the predicted molecular mass or by fragmentation patterns of metabolites. For multiple reactions, detection has been considered to depend on the combination of predicted molecular masses and fragmentation patterns such as *N*-acetyl cysteine conjugates, glutathione (GSH) adducts, and oxidative metabolites. Common metabolites are determined using full MS scan via product ion spectra in a single LC-MS run followed by extracted ion chromatographic analysis or by

employing list-dependent tandem mass spectrometric (MS^n) methods with ion trap instruments including 3D ion traps, linear ion traps, hybrid quadrupole ion traps and time-of-flight (TOF) instruments. Uncommon metabolites are determined by predicted fragmentation patterns via ether precursor ion (PI) or neutral loss (NL). Scanning techniques are usually with triple-quadrupole or hybrid triple-quadrupole-linear ion trap, Orbitrap, and quadrupole time-of-flight (Q-TOF) mass spectrometers. Conventionally, high-resolution mass spectrometry (HRMS) is used for identification of molecular formulae and their accurate mass fragments and characterization of the chemical structure of common metabolites based on their predicted mass shifts. However, HRMS instruments have not been the main LC-MS platform for regular metabolite profiling due to the lack of ability for some high-resolution mass spectrometers to perform true PI scan or NL scan analysis for identification of uncommon metabolites (Zhang *et al*., 2009). The identification of metabolites by LC-MS has depended on the retaining the essential structure of the parent substrate moiety hence the parent compound the corresponding metabolites would be expected to undergo similar fragmentations and yield mass spectra that show major or common substructures (Klohr, 2010).

1.4.1 Separation techniques for metabolite identification

Xenobiotics and their metabolites have appropriate chemical and physical characteristics for separation via reverse phase liquid chromatography (RPLC) and this is accomplished by using a nonpolar stationary phase such as octadecyl (C18) and octyl (C8). The separation of the metabolites is achieved by optimizing the column composition, column particle size, column temperature, and polar mobile phase composition that must be compatible with MS process containing a high

volatile buffer at low concentration. On the other hand, HILIC separation such as ZIC-HILIC and ZIC-pHILIC columns can be used as an alternative to conventional reverse phase HPLC. In HILIC separation highly polar analytes are retained longer in hydrophilic stationary phase such as bare silica gel or polar-bonded phase and can be eluted away from the early eluting matrix components such as phospholipids. Hydrophilic interaction requires a mobile phase that has less polarity than stationary phase since the retention of polar analytes is decreased with increasing water content in the mobile phase (Ragu Ramanathan, 2010).

1.4.2 Identification of polyphenols by mass spectrometry

There are numerous reports on LC-MS determination of natural substances such as polyphenols and their metabolites in blood, plasma, serum, urine, bile or faeces. The study of the absorption and metabolism of polyphenols is important to determine the potential effects of consuming polyphenols. A series of evaluations on the absorption, metabolism, and bioactivity of flavonoids have been published and many metabolic investigations of flavonoids in biological samples have been reported using methods such as LC-MS, LC-ion trap and Quadrupole Time-Of-Flight (Q-TOF) instruments (Xing *et al*., 2007).

In recent years, the use of mass spectrometry for identification of the flavonoids and their fragmentation reactions using electron impact (EI) and chemical ionization (CI) techniques has increased. Since flavonoids and their glycosides are polar and non-volatile, it is possible to produce signals of aglycone molecular ions. The use of soft ionization techniques such as electrospray ionization (ESI) and atmospheric pressure chemical ionization (APCI) allows the generation of large molecule ions without

fragmentation. APCI has advantages over the ESI source for increasing the flow rates and the potential to gain ions from aqueous solutions even at flow rates well above 1mL/min. These techniques are used to obtain strong signals for the quasi-molecular ions, $[M+H]^+$ and $[M-H]^-$ even for the glycosides. Both techniques utilize energy collision induced decomposition (CID MS/MS). With instruments equipped with a quadrupole ion trap (QIT) mass analyser, several consecutive tandem MS experiments on sequential product ions can be performed (MS^n), permitting structural information from one single analysis. Characteristic fragmentation patterns can also be used for the identification of certain compounds in LC-MS. Several mass spectrometry techniques have been used to investigate the flavonoids and their metabolites *in vivo* (Gunter, 2003). Flavonoids can be identified in both positive and negative ion modes, even under acidic conditions. Positive ion mode usually generates higher noise levels while the negative mode produces lower noise levels thus improving the quality of the signals. The fragmentation of flavonoids can be affected by the ion polarity (Cuyckens *et al*., 2001), and phenolic substances undergo less fragmentation in negative mode than in positive ion mode so the negative mode can be used for structure elucidation of flavonoids and their metabolites. In general, negative ESI has proved to be the best ionization method for flavonoids and their metabolites for identification. Flavonoids and their metabolites have been reported to be unstable at high temperatures, however the high temperatures in the APCI source do not seem to cause any damage to these compounds (Gunter, 2003).

The majority of the metabolic pathways of flavonoids were glucuronidation, sulfation and methylation. O'Leary *et al*. (2003) reported that quercetin-3-glucuronide pathway can be extra metabolized to methylation of the catechol

function group and hydrolysis of the glucuronide by endogenous *β*-glucuronidase followed by sulfation to quercetin-3-sulfate (O'Leary *et al*., 2003). Mullen *et al*. (2004) identified 23 metabolites of quercetin *in vivo* (from the consumption of red onions) by LC-ion trap mass spectrometer that included methylation of aglycone and the formation of mono-, diglucuronides, and sulfate conjugates. The position of conjugation by glucorinidation cannot be confirmed by MS techniques only, usually NMR spectra of a reference or standard are required (Mullen *et al*., 2004). In some cases, time-of-flight (TOF) has been used to determine the flavonoids metabolism (Ichiyanagi *et al*., 2005). Moreover, the flavonoid metabolites were identified by liquid chromatography photodiode array mass spectrometry (LC-PDA-MS) assay. HPLC linked with ESI and APCI interfaces in positive and negative ion mode has been used in the quantitative analysis of flavonoids and their metabolites in biofluids. The data was collected in selected ion monitoring (SIM), selected reaction monitoring (SRM) or multiple reactions monitoring (MRM) mode (Xing *et al*., 2007).

1.5 Fundamentals of mass spectrometry

1.5.1 Mass spectrometer components

All mass spectrometry instruments are composed of four key components made up of a sample inlet, an ion source, a mass analyser and a detector. A schematic diagram of the key components of a mass spectrometer are illustrated in **(Figure 1.17)** (Ramanathan and Lelacheur, 2008).

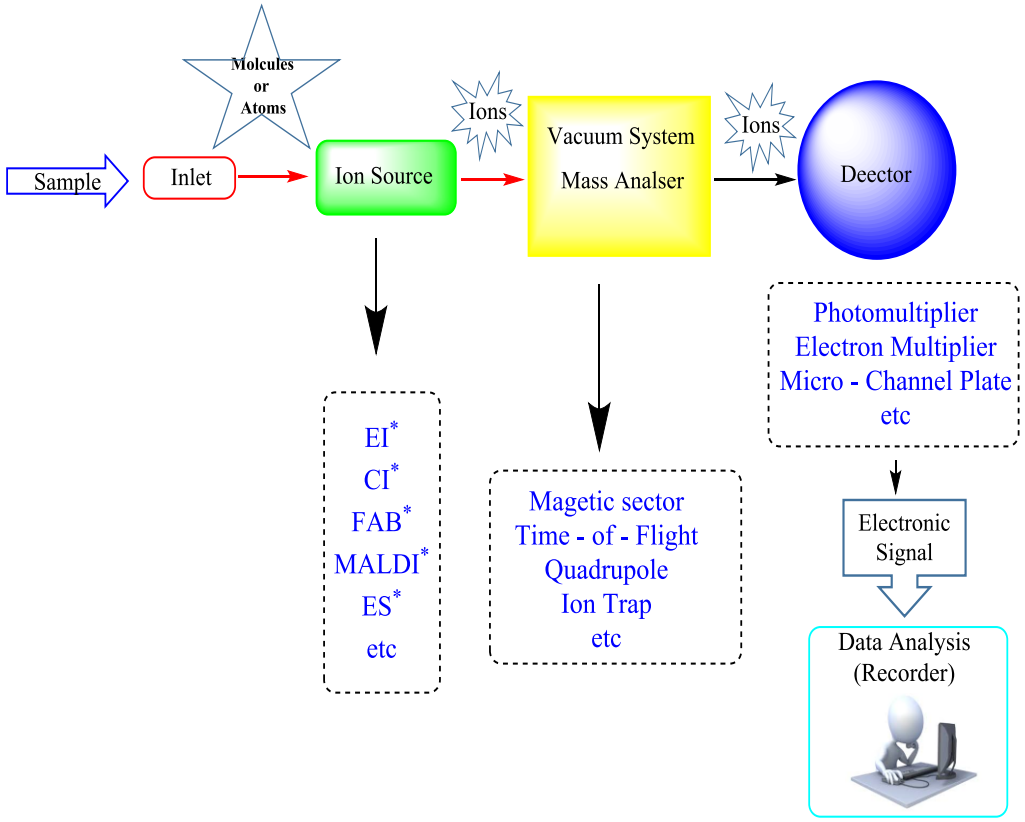

Figure 1.17 Schematic diagram of the key components of a mass spectrometer.

Electron Impact (EI), Chemical Ionisation (CI), Fast Atom Bombardment (FAB), Matrix Assisted Laser Desorption Ionisation (MALDI) and Electro Spray (ES).

1.5.1.1 Sample inlet and source

The sample inlet is the main component of any mass spectrometer device and it is the route of introducing the sample into the instrument in liquid or gaseous state. It delivers the sample to the mass spectrometer ion source. There are different types of ion sources some of which are used with gas chromatography such as Electron Impact Ionization (EI) and Chemical Ionization (CI). However, these ion sources are not described here due to the significant decline of the use of gas chromatography mass spectrometer (GC-MS) in metabolism studies compared with improvements in LC-MS. In LC-MS, there are several common sources including, Electrospray Ionization (ESI), Atmospheric Pressure Ionization (API), Atmospheric Pressure Chemical Ionization (APCI), Atmospheric Pressure Photoionization (APPI), Matrix Assisted Laser Desorption Ionisation (MALDI), Desorption Electrospray Ionization (DESI), Direct Analysis in Real Time (DART), and Nanoelectrospray Ionization (NESI). A general concept for all ions sources is that the sample must be ionized and transformed from a liquid or solid phase to the gas phase prior to entering the mass analyser for successful analysis. Electrospray is currently one of the most commonly used ionization techniques and it can be interfaced with liquid chromatography and a mass spectrometer as described below.

1.5.1.1.1 Electrospray ionisation (ESI) mass spectrometry

ESI for mass spectrometry was established by John Fenn and co-workers in an attempt to analyse large biomolecules by mass spectrometry by extraction of dissolved ions under atmospheric pressure (Hopfgartner, 2013), and in 2003, John Fenn received the Noble prize for this invention. ESI is a soft ionisation method

which converts ions basically pre-formed in solution into ions in the gas phase, where only slight fragmentation of the analyte occurs. This ionisation procedure is useful for the analysis of polar compounds, including metabolites by producing ions in multiple charged states. The general concept of the ESI mechanism is illustrated in **Figure 1.18**. The sample is sprayed in solution into the source via a needle which is held at a high electric potential typically between 3.0-4.5 kV to generate ions at atmospheric pressure to form an aerosol which is assisted by a flow of heated nitrogen gas in a direction co-axial with the needle towards mass spectrometer. A positively charged needle is used to analyse positive ions such as $[M + H]^+$, $[M + Na]^+$ and $[M + NH_4]^+$ while a negatively charged needle is used to analyse negative ions $[M + H]^-$ and $[M + Cl]^-$. The sample passes through a narrow orifice in a metal cone to a chamber or region under intermediate vacuum and then passes through a second orifice into a high vacuum region (Watson, 2012).

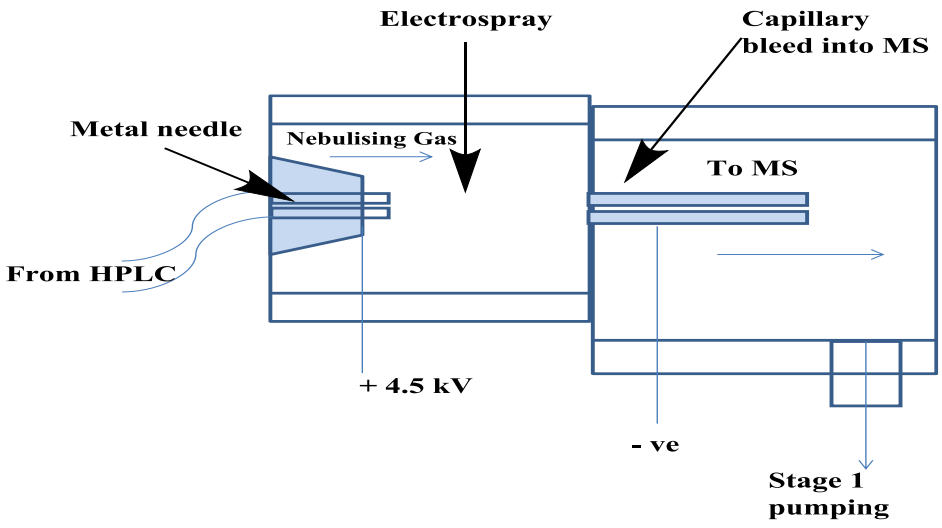

Figure 1.18 The ESI source.

At the tip of the capillary, positive ions are detached from the negative ions which are dragged towards the capillary while the isolated positive ions are repelled by the capillary and this force breaks up the surface tension of the liquid in which the sample is dissolved generating a conical shape termed the Taylor cone and this breaks up into charged droplets **(Figure 1.19)**. When the analytes have formed into charged droplets the surplus of positive charges in the droplets produces repulsion, which causes the droplets to break up further. This is assisted by evaporation of solvent from the droplets which increases their charge thus further promoting their break up. At the final stage the analyte is believed to abstract one or more protons from the solvent (or donate a proton if a negative ion is being formed) to form a positively charged gas phase ion (Watson, 2012).

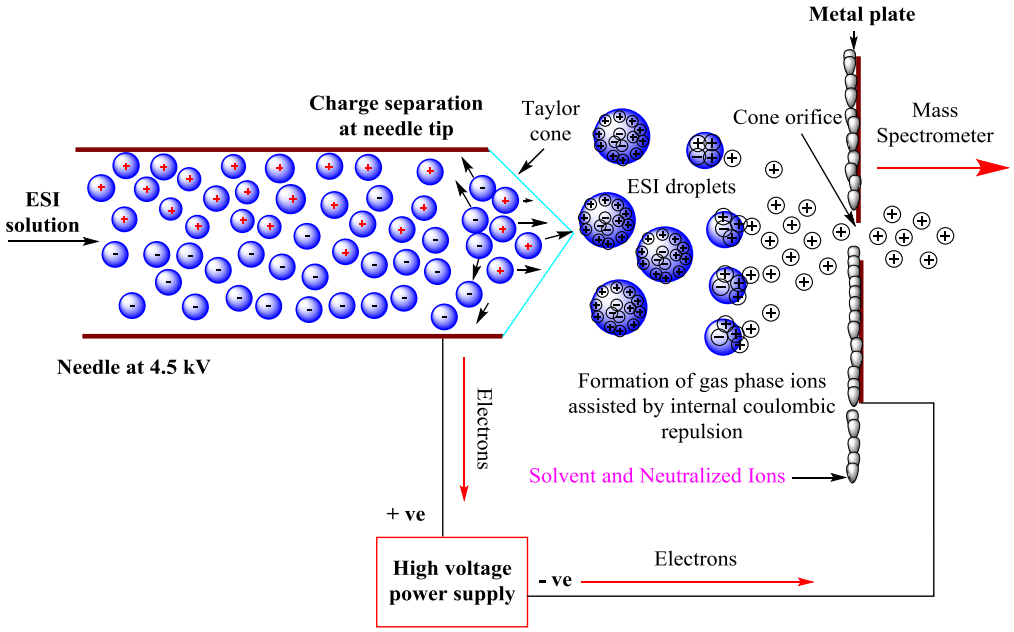

Figure 1.19 The electrospray process.

1.5.1.1.2 Atmospheric pressure chemical ionisation (APCI)

The ion source for Atmospheric pressure chemical ionisation (APCI) are considered to be very similar to that of ESI and a common ion source can be used for the two methods and on the same instrument. As in ESI the eluent passes through a charged needle before eluting to the mass spectrometer as described above but in APCI an aerosol is formed via a heated tube. The aerosol generated by electric field and heated tube will then be reacted with H_3O^+ and Na^+ adducts which leads to the ionisation of the target substances. Overall, the ESI is sufficient technique for polar compounds such as drug molecules but the APCI is compatible for the ionisation of low polar compounds (Watson, 2012).

1.5.1.2 Mass analysers

Generally, the mass analyser is used as a basis for distinguishing and discussing various types of mass spectrometers. Analysis of the analyte depends on the charge to mass ratio (m/z) which occurs in the mass analyser of the instrument. There are various types of mass analysers. Those considered to operate at a high resolving power are denoted by high resolution mass spectrometers (HRMS) such as Quadrupole mass analyser (QMS) Time of Flight (TOF), Orbitrap, Tandem Mass Spectrometer and Hybrid Mass Spectrometers. The most common mass analysers are described below.

1.5.1.2.1 General concepts of the trap mass spectrometers and the orbitrap mass analyser

In a low-resolution trap, the ionised analyte is introduced into the trap which is trapped by application of a radio frequency (Rf) voltage to the circular electrode **(Figure 1.20)**. The energy of the ions in the trap is quenched by helium which is passed into the trap. The ions can be selectively ejected by accelerating the Rf potential with the help of a direct current (DC) thus producing ion masses which are detected by an electron or photomultiplier tube. The fragmentation of ions of interest can be achieved by adjusting the Rf voltage for exciting ions before colliding with helium atoms. The generated fragments are ejected and detected by the mass detector (Watson, 2012).

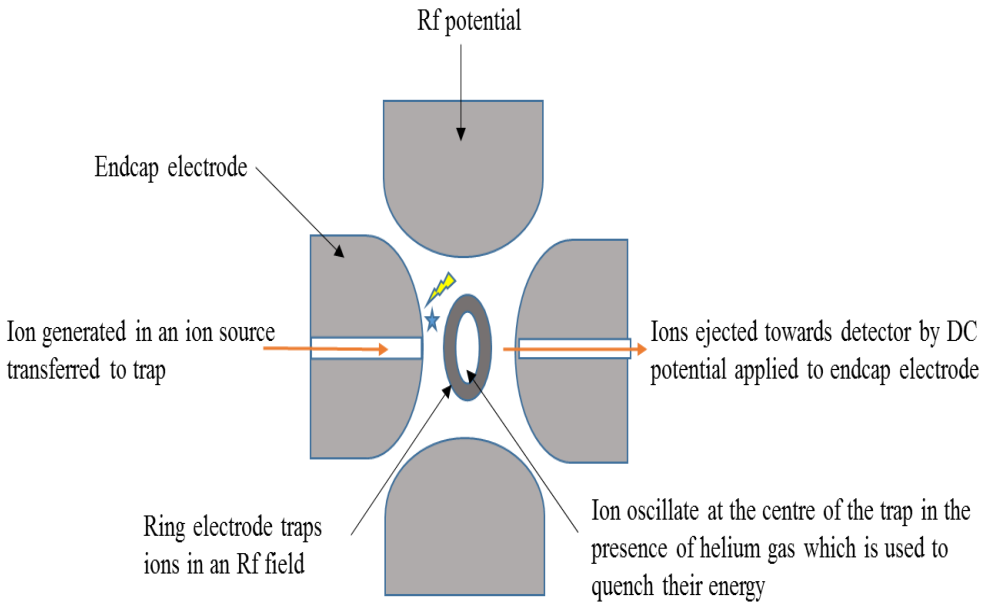

Figure 1.20 Schematic diagram of an ion trap.

1.5.1.2.2 The Orbitrap mass spectrometer

In 2005 Thermo Finnigan introduced the Orbitrap, originally invented by Makarov in 1999. The Orbitrap depends on electrostatically trapped ions circulating between two oval electrodes. The mass/charge ratio of ions is determined as an image current generated by the axial oscillation which can be converted into highly accurate masses and the Orbitrap can measure masses to five decimal places (Watson, 2012). Orbitraps have a high mass accuracy (1-2 ppm), a high resolving power (up to 200,000) and a high dynamic range (around 5000) (Kang, 2012). The Orbitrap Fourier transform mass spectrometer was first produced in 2005 as Orbitrap analyser which utilises an electrostatic field to trap ions so that they orbit around a central spindle electrode rather than the magnetic field which is employed in cyclotron resonance instruments. The cyclotron resonance instruments are very expensive instruments compared with Orbitraps. The Orbitrap analyser is employed in hybrid linear ion trap/Orbitrap mass spectrometer (LTQ Orbitrap) (Watson, 2012). **Figure 1.21** illustrates parts of the LTQ including ionisation source, linear ion trap which produces MS and MS^n spectra that pass to the quadrupole called C-trap and finally the ions are injected into the Orbitrap. In the Obitrap, specific masses are selected for fragmentation during a selected time event. The product ions are obtained by a sequence of operations in the scan function and are formed by collision induced dissociation (CID) of the selected ion using helium buffer gas (Al-Asmari, 2009).

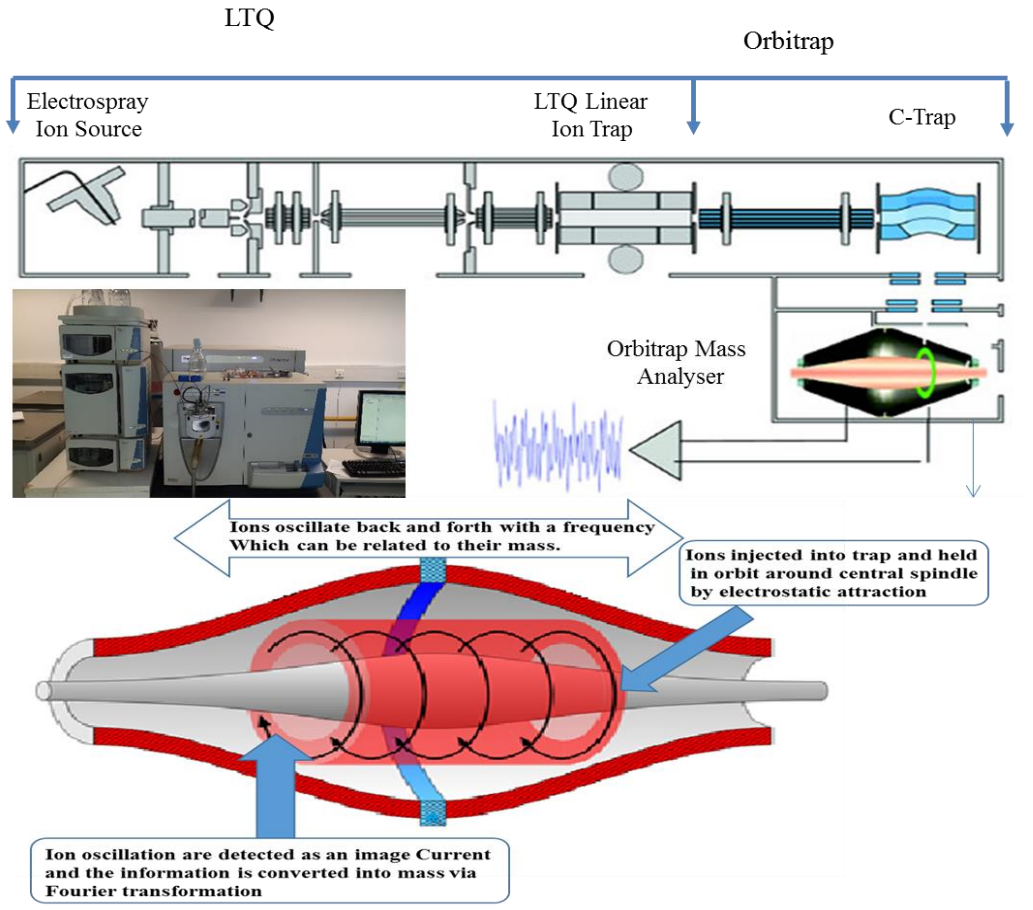

Figure 1.21 The schematic diagram of LTQ instrument portions including ESI source, LIT, C- trap and Orbitrap.

Moreover, The Orbitrap analyser is employed in high resolution mass spectrometry (Exactive™) as benchtop LC/MS system that can measure wide mass range of spectra at high resolution but has no fragmentation capability because it does not have CID which able to selected ion fragmentation which LTQ Orbitrap has (Watson, 2010).

1.5.1.2.3 Quadrupole instruments

Quadrupole mass spectrometers are cheap and sensitive instruments which have been used for many years for the separation of ions according to their m/z ratio by electrostatic fields DC and other oscillates at radiofrequency Rf applied at right angles to each other via four parallel rods **(Figure 1.22)**. Quadrupole mass spectrometer is based on the quadrupole mass analyser (QMS) which creates a resonance frequency for each m/z value and the ions that resonate in the range of the quadrupole are able to pass through it and are detected. However, the lower or higher m/z will collide with the rods and will not reach the detector. In industry-standard, quadrupole analysers are incorporated with triple quadrupole mass spectrometers for determination of drugs in biological fluids (Watson, 2012).

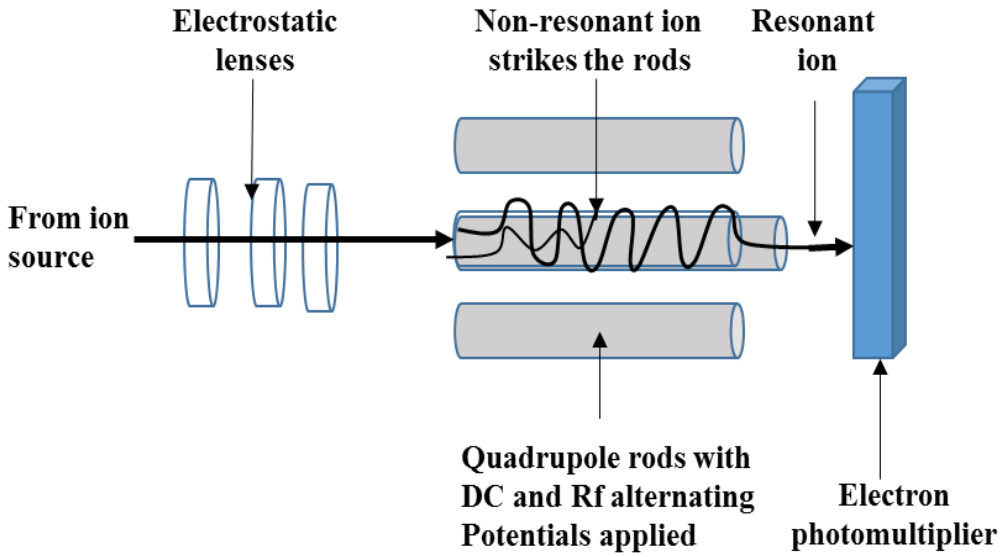

Figure 1.22 Schematic diagram of ions separation using a quadrupole mass spectrometer.

1.5.1.2.4 Time of flight (TOF) ion separation

Commercially, the Time of flight was first introduced in 1990 and is used for the separation of high molecular weight compounds such as proteins. The general concept of TOF technique is that small ions are detected before the large ions since they move quicker after accelerating them through an electric field. The TOF separation was first used with matrix assisted laser desorption ionization (MALDI) which use short pulses of laser energy focused on the sample dissolved in a UV light absorbing matrix or electrospray ionisation may be used in combination with a gating mechanism which allows the introduction of the ions in electric field for separation. Generally, the energy kinetics of the ions formed by the ion source vary and leads to poor mass resolution. However, for the production of accurate mass measurements by TOF a reflectron device is applied in the TOF to focus the kinetic energies of the ions so the greater kinetics ions (fast ions) will penetrate further into the reflectron to allow the slower moving ions to catch up and the faster ions are retained **(Figure 1.23)** (Watson, 2012).

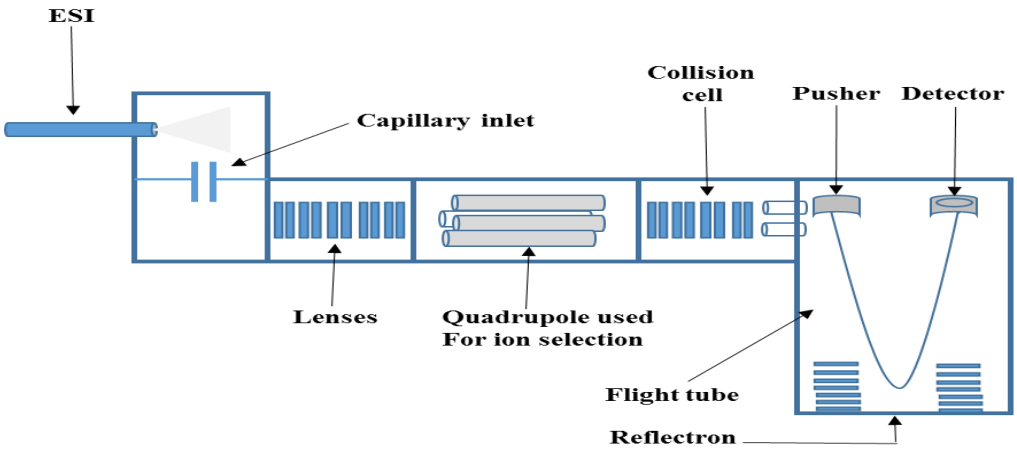

Figure 1.23 Schematic diagram of a quadrupole time of flight (QTOF) mass spectrometer.

The last part of the mass spectrometer is the detector which detects the generated ions by the mass analyser. The detectors include the electron multiplier which is used in quadrupole instruments and the microchannel plate (any array of electron multipliers), which have been used in TOF instruments. The detector is a relatively "invisible" part of a mass spectrometer needing little or no regular attention or maintenance as it is an enclosed part of the instrument (Ramanathan and Lelacheur, 2008).

1.6 Aims and objectives

1. To determine the metabolites of ferulic acid, quercetin, hesperidin and *p*-coumaric acid on incubation with isolated rat hepatocytes followed by analysis by liquid chromatography in combination with high resolution mass spectrometry.
2. To develop data extraction methods to determine the full range of the metabolites formed from the phenolic compounds.
3. To characterise the metabolites formed from the phenolic compounds using high resolution MS^2 and MS^3.
4. To examine the impact of the phenolic compounds on the metabolome of hepatocytes using hydrophilic interaction chromatography in combination with high resolution mass spectrometry.
5. To provide more information to support the health benefits of these dietary xenobiotics.

CHAPTER 2

General Methodology

2. General Methodology

2.1 Introduction

In recent years a number of investigations of xenobiotic metabolism *in vitro* using isolated parenchymal cells (hepatocytes) from rodent liver have become one of the most practical studies of xenobiotic biotransformation and metabolism. In the present study, hepatocytes were isolated from adult Sprague-Dawley (SD) rats under Licence PPL/60/3685 (UK Home Office Guidelines) by a two-step collagenase perfusion process at the Bioengineering laboratory, University of Strathclyde Glasgow (Oliveira *et al*., 2002, Berry *et al*., 1991).The collagenase solution (at 37°C) was diffused through the liver and the digested liver parenchyma (hepatocyte) suspended in ice-cold Hanks solution. Subsequently, the hepatocyte suspension was washed with 50 mL of Krebs Henseleit buffer (KH) (Liu *et al*., 2002). Some of the polyphenols were incubated with the isolated hepatocytes suspension (2×10^6 viable cells mL^{-1}) in Krebs Henseleit (KH) buffer containing 12.5 mM HEPES (pH 7.4) at 37°C under an atmosphere of 95% O_2, 5% CO_2 in rotary evaporator system for 120 min. Three incubation solutions as (control, treated and blank) for each polyphenol compound was prepared in 50 mL round bottomed flasks. To ascertain cell viability the Trypan blue exclusion test was used before and during the incubation procedures.

2.2 Methods and protocols for isolation rat hepatocytes

2.2.1 Perfusion apparatus

1. Carbogen cylinder: (95% O_2 / 5% CO_2).
2. Surgical tools: (such as small and large scissors, small and large forceps, stainless steel cannula with an internal diameter of 1.75 mm and exterior diameter of 2.5 mm and artery slip to hold the cannula in place).
3. Rotary evaporator system and 50 mL round bottomed flasks.
4. Thermostated shaking water bath.
5. Light microscope and counting chamber (haemocytometer).
6. Perfusion device: including perfusion pump and water bath with three reservoirs.
7. Laminar flow cabinet.

2.2.2 Perfusion reagents

1. Sodium pentobarbital (60 mg/mL) (preserved at 4°C in the dark) for deep rat anaesthesia.
2. Sodium Heparin (5000 IU/mL) (stored at 4°C) to avoid blood coagulation in the liver.
3. Trypan blue for ascertaining the cell viability.
4. Perfusion solution buffers: [Hank's Buffer (10X), Krebs-Henseleit Buffer (2X), Hank's I buffer, Hank's II buffer, Krebs-Albumin Buffer (KA), and Krebs-HEPES Buffer (KH)] (Berry *et al*., 1991, Shen *et al*., 2012).

2.3 Preparation of perfusion solutions

2.3.1 Preparation of stock solution buffers

1. Hanks' buffer (ten-fold concentration, 10X)

Hanks' buffer (balanced salt solution) was prepared by dissolving accurate weights of the following salts in 1 litre distilled water using a volumetric flask and then preserved at 4°C until used.

NaCl	80.0 g	KCl	4.0 g
$MgSO_4.7H_2O$	2.0 g	$Na_2HPO_4.2H_2O$	0.60 g
KH_2PO_4	0.60 g		

2. Krebs-Henseleit buffer (two-fold concentration, 2X)

Krebs-Henseleit buffer composed of two solutions (A) and (B) below was prepared as follows:

(A)

Distilled H_2O	785 mL	16.09 % (w/v) NaCl	200 mL
1.10 % (w/v) KCl	150 mL	0.22 M KH_2PO_4	25 mL
2.74 % (w/v) $MgSO_4.7H_2O$	50 mL		

(B)

$NaHCO_3$	9.71g in 1L

Solution (A) was prepared by adding the solutions in amber coloured 2 litre glass bottle and 5% CO_2 and 95% O_2 was bubbled through the final solution for 10 min. Simultaneously a stream of 5% CO_2 and 95% O_2 was passed through solution (B) and then added to solution (A) under the same gas flow rate for 10 min and stored at 4°C before until required.

2.3.1.1 Preparation of perfusion buffer

A Perfusion buffer consisting of four solutions (Hanks' I buffer, Hanks' II buffer, Krebs-Albumin buffer and Krebs-HEPES buffer) was prepared as follows:

1. **Hanks' I buffer**

Hank's buffer was prepared by dissolving 1.50 g N-[2-hydroxyethyl] piperazine-N'-[2-ethanesulphonoic acid] (HEPES), 3.33 g of Bovine Serum Albumin BSA (fraction V), 114 mg of Ethylene glycol-bis-(β-amino-ethylether) N'N' tetraacetic acid (EGTA) in 50 mL of Hanks' (10X) buffer stock solution and made up to a 500 mL by distilled water and the pH adjusted to 7.4 by adding 5 M sodium hydroxide (NaOH).

2. **Hanks' II buffer**

Hanks' II buffer was prepared by dissolving 1.05 g sodium bicarbonate ($NaHCO_3$), 1.50 g N-[2-hydroxyethyl] piperazine-N'-[2-ethanesulphonoic acid] (HEPES), and 147 mg of calcium chloride dehydrate ($CaCl_2.2H_2O$) in 50 mL of Hanks' (10X) buffer stock solution and making up to a 500 mL with distilled water and the pH adjusted to 7.4 by adding 5 M NaOH. This solution was also used as a Hanks'

Balanced Salt Solution (HBSS) for incubating the hepatocytes with the drug substrates.

3. **Krebs-Albumin buffer (KA)**

Krebs-Albumin buffer was prepared by dissolving 1.50 g N-[2-hydroxyethyl] piperazine-N'-[2-ethanesulphonoic acid] (HEPES) and 5.0 g of Bovine Serum Albumin (BSA) in 250 mL of 2X Krebs-Henseleit Buffer stock solution and made up to a 500 mL with distilled water and the pH adjusted to 7.4 by adding 5 M sodium hydroxide.

4. **Krebs-HEPES buffer (KH)**

Krebs-HEPES buffer was prepared by dissolving 1.50 g of HEPES in 250 mL of 2X Krebs-Henseleit buffer stock solution and made up to a 500 mL by distilled water and the pH adjusted to 7.4 by the addition of 5 M sodium hydroxide. The four solutions were filtered and sterilized using vacuum filter/storage bottle systems through a 0.22 µm membrane filter and kept at 4°C.

2.3.2 Perfusion of the rat liver for hepatocytes isolation

The perfusion system consists of the pump silastic tubing, a water bath and three reservoir plastic beakers with caps. The first beaker was filled with Hanks' I buffer, the second beaker with Hanks' II buffer and third beaker with Krebs Albumin buffer. 5% CO_2 and 95% O_2 were bubbled through the solutions at 37°C during the incubation procedure. The perfusion apparatus is illustrated in **Figure 2.1**.

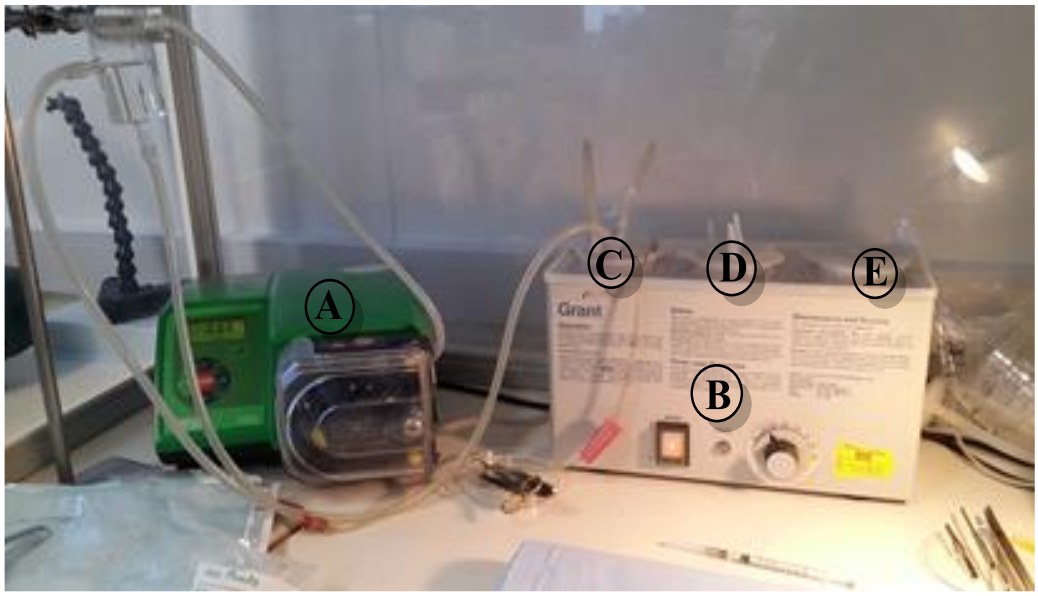

Figure 2.1 Perfusion instrument.
(A) pump; (B) water bath; (C) Hanks' I buffer; (D) Hanks' II buffer; (E) Krebs Albumin.

The rat hepatocytes were prepared by perfusion of the liver of adult Male Sprague-Dawley rats (200-250 g body weight) after being anaesthetised by an intraperitoneal injection of sodium pentobarbital at a dose of 60 mg per kg of body weight, and the deepness of anaesthesia was checked by the toe pinch test. The unconscious rat was placed in a laminar flow cabinet with abdomen in the upwards position and its legs secured by adhesive tape to the platform. The abdominal hair was shaved and the surgical area cleaned with 70% (v/v) alcohol and the peritoneal cavity opened by a mid-transversal incision (midline incision) from the tip of the sternum to the pubis. A 0.1 mL of heparin [0.1 mL, 1000 IU/mL in sterile Phosphate Buffered Saline (PBS), pH 7.4] was injected into liver tissue through the hepatic portal vein. The liver being exposed by carefully moving it away from the abdominal cavity. Thereafter, a steel cannula was inserted into the liver to diffuse the Hanks' I buffer through the hepatic vein in the liver and then dissected from the body and placed into

a 250 mL beaker containing Hanks' I buffer using a surgical bull dog clip for 10 min. The liver was relocated into a second beaker containing 150 mL of Hanks' II buffer and 78.0 mg collagenase for 10-20 min until liver becomes pale in color (digested liver parenchyma) or the cells in the liver were dissociated. The perfusion solutions were bubbled with carbogen gas and kept at 37°C during the perfusion procedure.

2.3.2.1 Isolation of hepatocytes

At the end of the digestion period and complete cells dissociation, the cells were gently dispersed by using forceps into a sterile petri dish with approximately 100 mL of Krebs Albumin buffer (warmed to 37°C). In order to remove the connective tissues and undigested tissue fragments the resulting cell suspension was filtered using a sterile cotton (gauze mesh 50 µm) into a 100 mL bottle. The suspension of hepatocytes was placed in ice and the cells allowed settling under gravity and the supernatant of Krebs Albumin buffer was removed and the precipitated cells were re-suspended by adding 50 mL Krebs HEPES buffer (KH) and again cells were allowed to settle and the supernatant of Krebs HEPES buffer was finally removed.

2.3.2.2 Determination of cell viability

For ascertaining cell viability, the live cells were counted under a Nikon Diaphot-TMD (Nippon Kogaku KK, Japan) light microscope by using Trypan blue exclusion test before and during the incubation procedures. The cell viability was determined by adding a 10 µL aliquot of the cell suspension to 990 µL of Trypan Blue (0.1% w/v in PBS, pH 7.4) and loaded onto the counting chambers of a haemocytometer on both sides. The viable cells were counted using nine square

areas on each side totalling eighteen sections (volume per square area = 0.1 mm^3). The viability of the cells was expressed by percentage and calculated using the following equations:

Equation 2.1

$$\%\ viability\ of cells\ = \frac{№\ of\ live\ cells}{Total\ №\ of\ cells} X\ 100$$

And the total number of viable cells/mL (viable cell concentration) of hepatocyte suspension was calculated by the below equation.

Equation 2.2

$$Total\ of\ viable\ cells = \frac{№\ of\ live\ cells}{18}\ X\ 10^4\ X\ 100$$

Where 100 is the initial dilution factor, 10^4 is the conversion factor to allow for the volume of the haemocytometer and 18 is the number of sections in the haemocytometer. The viability of the cells was determined during the incubation of polyphenols with hepatocytes at various time intervals of 0 min, 30 and then 120 min by adding 50 µL of Trypan blue (0.1% w/v in water) to 50 µL of withdrawn samples. After treatment with Trypan blue, the percentage of total viable cells was calculated using equation 2.1.

2.4 Incubation of the polyphenols

2.4.1 Chemicals and reagents

Polyphenol compounds such as flavonoids [Quercetin (99%), Hesperidin (99%)], phenolic acids [Ferulic acid (99%), *p*- coumaric acid (99%)] and dimethylsulphoxide (DMSO) were obtained from Sigma Aldrich, Dorset UK. HPLC grade acetonitrile (CAN) and formic acid HCOOH 99-100% were obtained from Fisher Scientific (Loughborough, UK). Distilled Water was obtained from a Milli-Q water-purification system (Millipore, Watford UK) in laboratory.

2.4.2 Preparation of polyphenol compounds for incubation with rat hepatocytes

Stock solutions of Quercetin (Q), Hesperidin, Ferulic acid (FA), *p*- coumaric acid (*p*-CA), [MW of quercetin: 302.24; MW of hesperidin: 610.56; MW of ferulic acid: 194.18; MW of *p*-coumaric acid: 164.16] were prepared by dissolving 100 millimolar (mM) of each sample in 1 mL of DMSO. A 100 mM of quercetin was prepared by dissolving 30.2 mg of quercetin in 1 mL of DMSO, a 100 mM of hesperidin was prepared by dissolving 61.06 mg of hesperidin in 1 mL of DMSO, a 100 mM of ferulic acid was prepared by dissolving 19.9 mg in 1 mL of DMSO, a 100 mM of *p*-coumaric acid was prepared by dissolving 16.4 mg in 1 mL of DMSO. Separately, these solutions were incubated at 100 µM by adding 0.01 mL to 10 mL of 2 x 10^6 isolated hepatocytes per ml at 37°C under an atmosphere of 95% O_2, 5% CO_2 in a rotating 50 mL round bottomed flask for 120 min **(Figure 2.2)**. Blank incubations were carried out without cells. Control incubation was concurrently run

with hepatocytes but without the polyphenols. Four aliquots (0.5 mL) were taken from the incubation solutions at 0, 30 and 120 min. The reaction terminated by the addition of 1 mL of acetonitrile and the samples were preserved at -80°C. **Figure 2.3** illustrates incubation of polyphenol compounds incubated with rat hepatocytes.

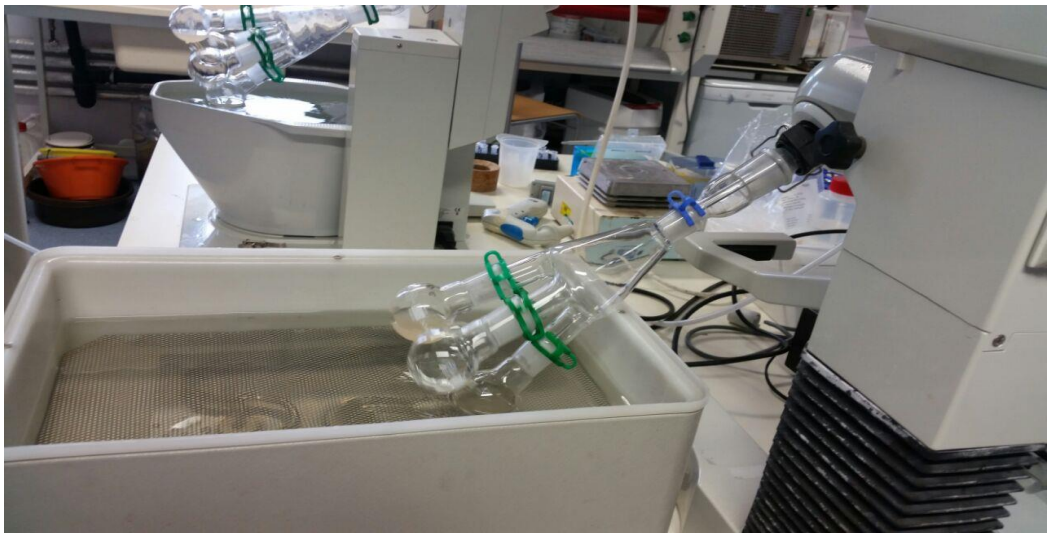

Figure 2.2 Rotor incubator system used for incubation of the polyphenols with hepatocytes.

2.4.3 Extraction of incubation solutions

Prior to analysis samples were thawed at room temperature, sonicated and centrifuged at (5000 rpm for 5 min) using a mini centrifuge to remove proteins and the supernatants were collected for analysis of metabolites by LC-MS and LC-MS^2.

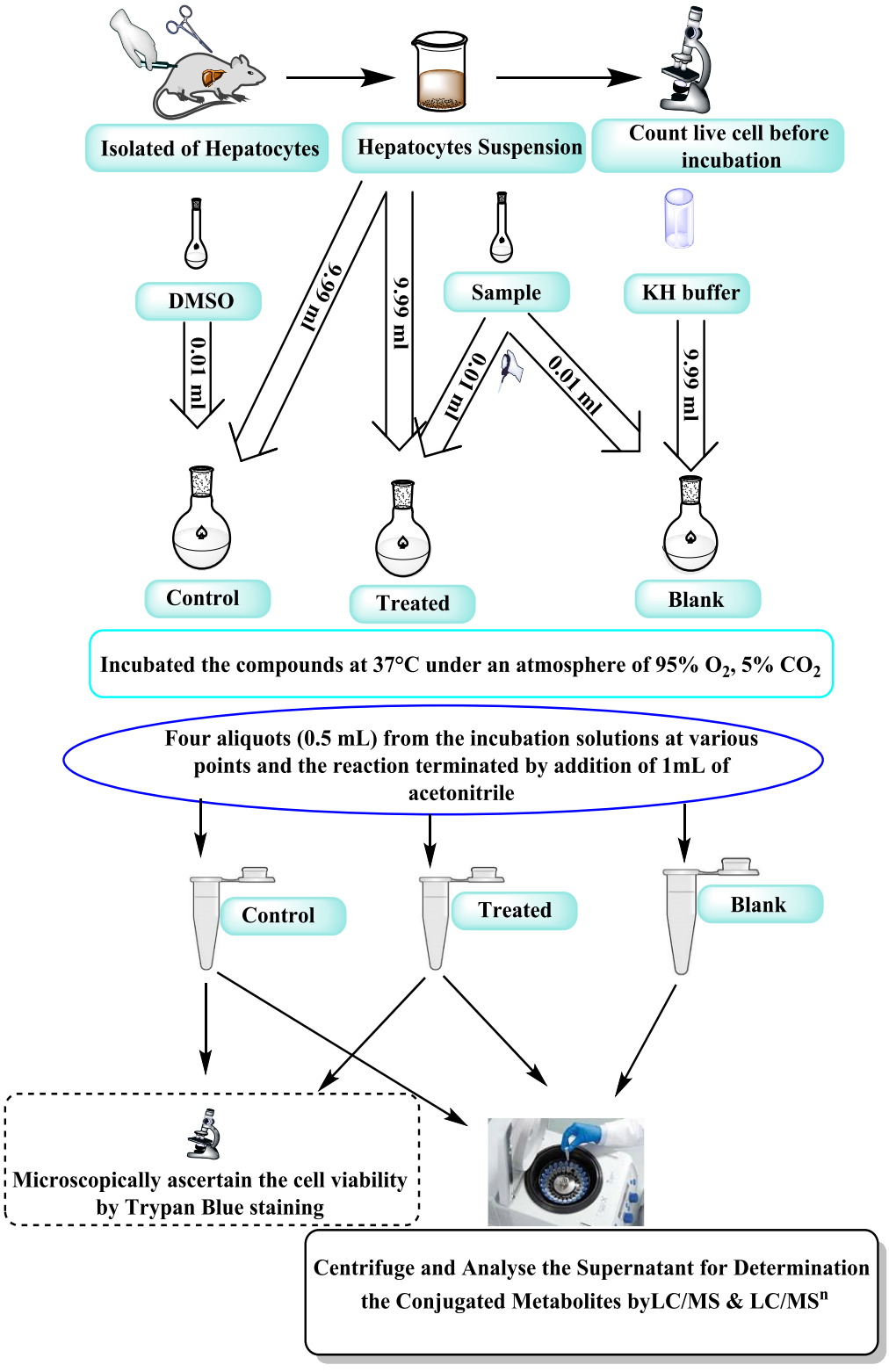

Figure 2.3 Schematic diagram illustrating incubation and extraction process of polyphenols compounds incubated with rat hepatocytes.

2.5 Preparation of mobile phase for LC-MS and LC-MS^n

The mobile phase was composed of two mobile phases (A) 0.1% formic acid in water prepared by adding 1 mL of formic acid to1 litre distilled water and (B) 0.1% formic acid in acetonitrile prepared by adding 1 mL of formic acid to 1 litre of acetonitrile.

2.5.1 Instrumentation and data processing

Preliminary identification of the chemical structure of polyphenols metabolites ware performed using a Dionex HPLC (Dionex Corporation, USA) connected to an Exactive Orbitrap (Thermo Fisher Scientific, UK). The HPLC was fitted with an ACE® 5 C18-AR column (5 µm, 150 mm x 4.6 mm, HiChrom, Reading UK). C18-AR is octadecyl (C18) with embedded phenyl functionality which has unique selectivity to improve separations that are proving problematic on C18 columns and it is compatible with highly aqueous mobile phase to enable the retention and separation of polar compounds. Moreover, C18-AR is recommended for separation that involve compounds containing aromatic rings such polyphenols. The mobile phases consisted of 0.1% formic acid in water (A) and 0.1% formic acid in acetonitrile (B). The gradient system was 10% B, (0 min); 80% B, (30-32 min); 10% B, (32-40 min). The flow rate of the mobile phase was 0.3 mL/min. Mass spectra were recorded using electrospray ionization (ESI) in negative mode using a needle voltage of 4.0 kV and source temperature 320°C. Optimum nebulization was achieved using nitrogen at sheath gas flow rate 50 and auxiliary gas flow rate 17 (units not specified by the manufacturer). Scanning of total ion chromatograms (TIC) range was between *m/z* 75-1000. For confirmation of the structure of the metabolites

MS^2 was carried out by using an LTQ Orbitrap (Thermo Fisher Scientific, UK) with the same chromatographic conditions as were used with the Exactive and the selected predecessor ions were fragmented through collision induced dissociation (CID) with neutral gas (Helium) molecules in the ion trap. Finally, the data were collected and processed using Xcalibur software Ver. 2.0, Thermo- Fisher Corporation, UK, SIEVE Software Ver. 1.2.1, Thermo- Fisher Corporation, UK, Metworks Software Ver. 1.3, Thermo- Fisher Corporation, UK and mzMatch software.

SIEVE Software is one of the commercial software programmes. It is used for metabolite identification. It is an automated software package which carries out comparative analyses of samples by comparing the raw data from LC/MS of control and treatment samples in order to identify the changes in two sample sets. In addition, Metworks software is metabolite identification and it can be used for small molecules and their metabolites. It can combine with Xcalibur data features and can be used with a high degree of accuracy and assurance to find and detect a variety of xenobiotic candidate metabolites. mzMatch is metabolomics data analysis software and it was designed to provide small tools for common processing tasks for LC/MS. In details mzMatch has been used to study the effect of quercetin, *p*-coumaric acid and ferulic acid on the hepatocyte metabolome (Chapter 7).

CHAPTER 3

The Complex Degradation and Metabolism of Quercetin in Rat Hepatocytes

3. The Complex Degradation and Metabolism of Quercetin in Rat Hepatocytes

3.1 Abstract

The current study demonstrates that there is still new information to be obtained on the chemical and biological transformation of the widely studied flavonoid quercetin. In rat hepatocytes, 35 metabolites of quercetin were observed using high-resolution mass spectrometry. The metabolites included glucuronides, sulfates, mixed sulfate/glucuronide metabolites and methylated versions of these metabolites. Several metabolites were formed from chemical degradation products of quercetin which were formed in Krebs–Henseleit (KH) buffer, degradants of quercetin were also formed in the buffer under the conditions used for hepatocyte incubation. The degradants and metabolites of quercetin were characterized by high-resolution MS^2. It was observed that the glutathione (GSH) conjugates of quercetin formed in large amounts in ammonium bicarbonate solution although the pattern of conjugates formed was different from that observed in hepatocytes suggesting some degree of enzymatic control on GSH conjugate formation in the hepatocyte incubations. GSH conjugates were not formed when GSH was included in incubations of quercetin in KH buffer alone and only small amounts of quercetin degradation occurred. Instead, GSH was extensively converted into GSSG, thus presumably reducing the levels of oxygen in the incubation thus preventing quercetin degradation.

3.2 Introduction

There is strong evidence to suggest that dietary phenolic compounds can confer health benefits including protection against cardiovascular disease, neurodegenerative disease and cancer (Del Rio *et al*., 2013). Phenolic compounds comprise a wide range of structural types including flavones, flavonols, isoflavones, flavanones, anthocyanins, chalcones and phenolic acids. One of the most studied phenolic compounds is the flavonol quercetin. Quercetin is abundant in the diet where it occurs both as the aglycone and in conjugated form with, most commonly, glucose or the disaccharide rutinose. Quercetin aglycone only occurs at low levels in foodstuffs. Quercetin itself can be directly absorbed from the intestine but the more abundant glycosides have to be converted to the aglycone via the action of a hydrolytic enzyme such as lactase phlorizidin hydrolase which occurs in the brush border membrane cells of the small intestine (Del Rio *et al*., 2013). Thus, feeding of fried onions to subjects results in rapid appearance of quercetin sulfate and glucuronide metabolites in the blood stream following cleavage of the glucoside conjugates of quercetin which are abundant in onions (Mullen *et al*., 2006). The other abundant conjugate of quercetin in the diet is quercetin rutinoside which is not absorbed in the small intestine but passes into the large intestine where it is converted into the aglycone via the action of colonic microbiota. When tomato juice, which contains large amounts of quercetin 3-*O*-rutinoside was given to human volunteers the appearance of quercetin metabolites in plasma was much delayed in comparison with the absorption from onions and the levels absorbed were much lower (Jaganath *et al*., 2006). Part of the reason for the lower absorption of quercetin from the large intestine is due to the fact that the microbiota produce a range of

degradation products from quercetin formed via cleavage of the C- ring producing a range of phenolic acids (Serra *et al.*, 2012). Mullen *et al*. (2006) observed a range of quercetin metabolites in human plasma and urine following consumption of onions using LC-MS^2. Two sulfates, three glucuronides, two glucuronide sulfates, three diglucuronides, two methylquercetin diglucuronides plus a number of glucoside conjugates were observed. A recent study identified 15 metabolites of quercetin in human plasma following consumption of apple sauce with added apple peel or onion (Lee *et al.*, 2012) using high - resolution LC-MS/MS. The metabolites included one sulfate, three glucuronides, one diglucuronide sulfate, four diglucuronides, two methyl glucuronides, three methyldiglucuronides and a glutathione (GSH) adduct. The levels of four major quercetin conjugates were determined in human plasma after three months of supplementation with quercetin. The most abundant conjugates detected were isorhamnetin-3-glucuronide, quercetin 3-glucuronide, quercetin 3-sulfate and quercetin diglucuronide (Cialdella-Kam *et al*., 2013). In addition, this study examined the effects of quercetin supplementation on global metabolite profiles of the subjects in the study. The metabolites of a number of polyphenols including quercetin were analysed in humans following consumption of cranberry syrup. Quercetin aglcyone and methylated and glucuronide metabolites of quercetin were detected (Iswaldi *et al*., 2013).

There have also been numerous *in vitro* studies of quercetin metabolism. Incubation of quercetin with rat and human hepatocytes led to identification of 14 metabolites of quercetin including methylated, glucuronidated and sulfated metabolites. In this study, the identity of the metabolites and thus positions of methylation, glucuronidation and sulfation were confirmed by using NMR for full structure

elucidation (van der Woude *et al*., 2004). Quercetin was incubated with murine hepatocytes and 18 metabolites of quercetin were identified in the incubations including methylated, glucuronidated and sulfated metabolites but in addition a range of glutathione adducts were observed. These included the glutathione adducts of methyl quercetin, quercetin quinone and glucuronides of glutathione quercetin and methyl quercetin. In addition, the observations in hepatocytes led to the observation of the presence of several mercapturic acid conjugates of phenolic acids derived from quercetin in human urine following onion consumption (Hong and Mitchell, 2006). An aspect of quercetin behaviour which has not been clearly integrated with its biological behaviour is the relative ease with which it undergoes chemical degradation. It was observed that 18 degradation products of quercetin were formed upon its electrochemical degradation. The products included phenolic acids formed via ring scission, oxidised forms of quercetin and dimers of quercetin. It was proposed that the degradation occurred via quinone formation and via a carbocation which led to the scission of ring C (Zhou *et al*., 2007). Another study used peroxidase from onions to oxidise quercetin and found similar degradation products (Osman and Makris, 2010). In this case, it was proposed that the ring scission of the C- ring took place via formation of a free radical at position 2 in ring C followed by addition of oxygen to form an oxygen bridge across ring C. The degradation of quercetin in aqueous solutions at 75°C and 85°C in aqueous solution at pH 5.9 and pH 7.4 was studied using continuous infusion into a high- resolution mass spectrometer (Barnes *et al.*, 2013). Again degradation took place under these relatively mild pH conditions to a range of ring scission products and dimers.

Thus it would seem that although quercetin has been intensively studied it still remains an active subject of study and each new study seems to reveal further aspects of its chemistry and biochemistry. In the current study the metabolism of quercetin was carried out in rat hepatocytes using liquid chromatography- high resolution mass spectrometry to elucidate the metabolites formed. A metabolomics approach was taken in order to see if the range of metabolites and degradation products could be extended beyond what is currently known.

3.3 Experimental

3.3.1 Incubation of quercetin with rat hepatocytes protocol

The incubation of quercetin with rat hepatocytes and extraction of incubation solutions are described in detail in (General Methodology Chapter 2 pages 58:60).

3.3.2 Instrumentation and data processing

These details have been reported in (General Methodology Chapter 2 pages 61, 62).

3.3.3 Preparation of GSH conjugate of quercetin

A 10 µL of quercetin solution (30.2 mg/1 mL of DMSO) was added to GSH solution (1 mg/1 mL in 0.2% ammonium bicarbonate). The sample was left at room temperature for 24 hours before analysis. For analysis the sample was diluted 10:1 with 0.1% formic acid and then analysed by LC-MS.

In order to test the degradation of quercetin in blank solution under the above condition (95% O_2, 5% CO_2) in a rotating 50 mL round bottomed flask. 10 µL of quercetin solution (30.2 mg/1 mL of DMSO) with 10 µL of GSH at different

concentrations (60 mg, 120 mg/1 mL 0.2% ammonium bicarbonate) were incubated with 10 mL of KH buffer. Four aliquots (0.5 mL) were taken from the incubation solutions at 0, 30 and 120 min and the reaction terminated by addition of 1 mL of acetonitrile. The samples were stored at -80°C until analysis of the samples by LC-MS. Some samples were also shaken at room temperature for three hours by using a thermomixer in order to study the role of increasing the level of O_2 in the chemical reaction between the quercetin and GSH.

3.4 Results and discussion

Table 3-1 shows hepatocyte viability following incubation indicating that there was no significant loss of viability over 120 min of incubation either in the controls (KH buffer) or in the presence of quercetin.

Table 3-1 Viability of suspension hepatocytes during two hours of treatment period with 100 µM quercetin

Incubation time (min)	Viability of control	Viability with Quercetin
0	64%	68%
30	72%	82%
120	82%	72%

Quercetin was metabolised very rapidly by hepatocytes and on a peak area percentage basis, only 1.80% remained at 120 min **(Table 3-2)**. Upon inspection of the data, the range of metabolites obtained for quercetin appeared to be more complex than described previously and included ring scission products and their metabolites which have been described as products of microbial degradation (Serra *et al*., 2012).

Table 3-2 Metabolites of quercetin and its degradants putatively identified according to accurate mass in incubations with rat hepatocytes

Metabolite/Degradant	$[M-H]^-$	Elemental Composition	t_R min.	Area %30 min	Area %120 min
D3	153.01	$C_7H_5O_4$	11.2	2.85	2.02
Quercetin	301.03	$C_{15}H_9O_7$	21.5	0.58	1.80
Quercetin GSH Conjugate M1	606.10	$C_{25}H_{24}O_{13}N_3S$	14.0	0.18	0.213
Quercetin GSH Conjugate M2	606.10	$C_{25}H_{24}O_{13}N_3S$	14.5	6.93	3.95
Quercetin GSH Conjugate M3	606.10	$C_{25}H_{24}O_{13}N_3S$	15.45	Nil	0.0580
Quercetin GSH Conjugate M4	604.08	$C_{25}H_{22}O_{13}N_3S$	15.7	0.475	0.0500
Quercetin GSH Conjugate M5	604.08	$C_{25}H_{22}O_{13}N_3S$	16.2	2.69	0.540
M6	458.08	$C_{17}H_{20}O_{10}N_3S$	6.7	0.60	1.083
M7	458.08	$C_{17}H_{20}O_{10}N_3S$	9.4	Nil	0.167
M8	232.97	$C_7H_5O_7S$	6.1	1.067	0.587
M9	246.99	$C_8H_7O_7S$	10.0	Nil	0.605
M10	246.99	$C_8H_7O_7S$	10.5	Nil	0.280
M11	304.01	$C_{10}H_{10}O_8NS$	6.7	Nil	1.84
M12	304.01	$C_{10}H_{10}O_8NS$	9.3	Nil	0.470
Quercetin sulfate M13	380.99	$C_{15}H_9O_{10}S$	17.5	Nil	0.138
Quercetin sulfate M14	380.99	$C_{15}H_9O_{10}S$	19.3	2.43	0.47
Quercetin glucuronide M15	477.06	$C_{21}H_{17}O_{13}$	15.3	12.8	4.54
Quercetin 3-glucuronide M16	477.06	$C_{21}H_{17}O_{13}$	17.5	10.20	1.86
M17	343.06	$C_{14}H_{15}O_{10}$	6.7	0.0277	0.346
Methylated quercetin M18	315.05	$C_{16}H_{11}O_7$	23.9	0.074	0.068
Methylated quercetin glucuronide M19	491.08	$C_{22}H_{19}O_{13}$	16.6	Nil	5.60
Methylated quercetin glucuronide M20	491.08	$C_{22}H_{19}O_{13}$	17.4	5.75	0.81
Methylated quercetin glucuronide M21	491.08	$C_{22}H_{19}O_{13}$	17.7	3.22	0.79
Methylated quercetin glucuronide M22	491.08	$C_{22}H_{19}O_{13}$	18.1	2.48	0.56
Quercetin monglucuronide sulfate M23	557.02	$C_{21}H_{17}O_{16}S$	13.9	16.55	4.40
Quercetin monglucuronide sulfate M24	557.02	$C_{21}H_{17}O_{16}S$	14.5	3.56	18.4
Quercetin monglucuronide sulfate M25	557.02	$C_{21}H_{17}O_{16}S$	15.0	2.17	11.4

Methylated quercetin monglucuronide sulfate M26	571.04	$C_{22}H_{19}O_{16}S$	13.8	0.707	4.40
Methylated quercetin monglucuronide sulfate M27	571.04	$C_{22}H_{19}O_{16}S$	14.2	0.867	5.72
Methylated quercetin monglucuronide sulfate M28	571.04	$C_{22}H_{19}O_{16}S$	14.9	0.692	5.92
Methylated quercetin monglucuronide sulfate M29	571.04	$C_{22}H_{19}O_{16}S$	15.6	0.203	2.30
Quercetin-3,7-diglucuronide M30	653.1	$C_{27}H_{25}O_{19}$	13.5	13.25	14.15
Quercetin-3,7-diglucuronide M31	653.1	$C_{27}H_{25}O_{19}$	14.3	1.53	1.63
Quercetin-3,7-diglucuronide M32	653.1	$C_{27}H_{25}O_{19}$	14.7	2.13	1.89
Methylated quercetin sulfate M33	395.008	$C_{16}H_{11}O_{10}S$	14.2	Nil	0.045
Methylated quercetin sulfate M34	395.008	$C_{16}H_{11}O_{10}S$	19.05	0.053	0.243
Methylated quercetin sulfate M35	395.008	$C_{16}H_{11}O_{10}S$	19.5	0.055	0.11

It was observed that most of these "metabolites" also occurred in the blank incubations of quercetin in KH buffer alone. Thus it was thought perhaps that the KH incubation buffer might somehow be contaminated with microbes. However, a fresh batch of sterile buffer was prepared, tested for sterility and the same range of degradants was observed. These degradants, which are rapidly formed *in vitro* at physiological pH under an atmosphere containing 95% oxygen, contribute to the overall metabolism of quercetin since they form in the incubation medium and are then metabolised by the hepatocytes. In order to simplify consideration of the hepatic metabolites of quercetin, the degradants formed are considered first. The observed degradants in KH buffer are summarised in **Table 3-3** and **Figure 3.1** shows the proposed structures for the major chemical degradants of quercetin. Most of these

degradants form almost immediately when quercetin is dissolved in the incubation buffer and only *ca.* 25% of the quercetin remains after a few minutes.

Table 3-3 Formation of quercetin degradants in KH buffer at 0, 30 and 120 minutes

Degradant	$[M-H]^-$	Elemental Composition	t_R min.	Area % 0 min	Area % 30 min	Area % 120 min
$C_7H_5O_4$ D3	153.0195	$C_7H_5O_4$	11.9	9.7	15.3	37
$C_7H_5O_5$ D4	169.0145	$C_7H_5O_5$	11.2	2.5	4.1	9.1
$C_8H_5O_5$ D5	181.0146	$C_8H_5O_5$	6.8	0.62	1.15	3.3
$C_8H_5O_6$ D6	197.0095	$C_8H_5O_6$	10.2	6.6	7.9	13.5
$C_8H_7O_6$	199.0252	$C_8H_7O_6$	6.3	0.68	1.2	1.2
Quercetin –CO	273.041	$C_{14}H_9O_6$	15.8	0.16	0.13	0.09
Quercetin quinone D7	299.0203	$C_{15}H_7O_7$	22.7	3.5	3.0	2.7
Quercetin	301.0358	$C_{15}H_9O_7$	22.2	25.8	27.4	6.20
Chalcone quinone D8	315.0155	$C_{15}H_7O_8$	18.3	1.40	0.92	0.50
D1 “chalcone”	317.0308	$C_{15}H_9O_8$	15.8	44.5	33.9	20.3
Oxidised chalcone oxygen bridge	331.0104	$C_{15}H_7O_9$	14.7	0.75	0.77	1.6
Quercetin oxygen bridge D2	333.0261	$C_{15}H_9O_9$	19.8	1.0	0.71	0.43
Adduct 169/273	425.0525	$C_{21}H_{13}O_{10}$	18.4	0.05	0.22	1.3
197 + quercetin adduct	497.0372	$C_{23}H_{13}O_{13}$	16.6	0.68	0.99	1.3
Quercetin dimer	601.0635	$C_{30}H_{17}O_{14}$	23.9	0.16	0.52	0.41
Quercetin + 317	617.0581	$C_{30}H_{17}O_{15}$	19.8	0.82	0.75	0.51

Putative identification of degradants according to accurate mass with 2 ppm deviation from theoretical mass.

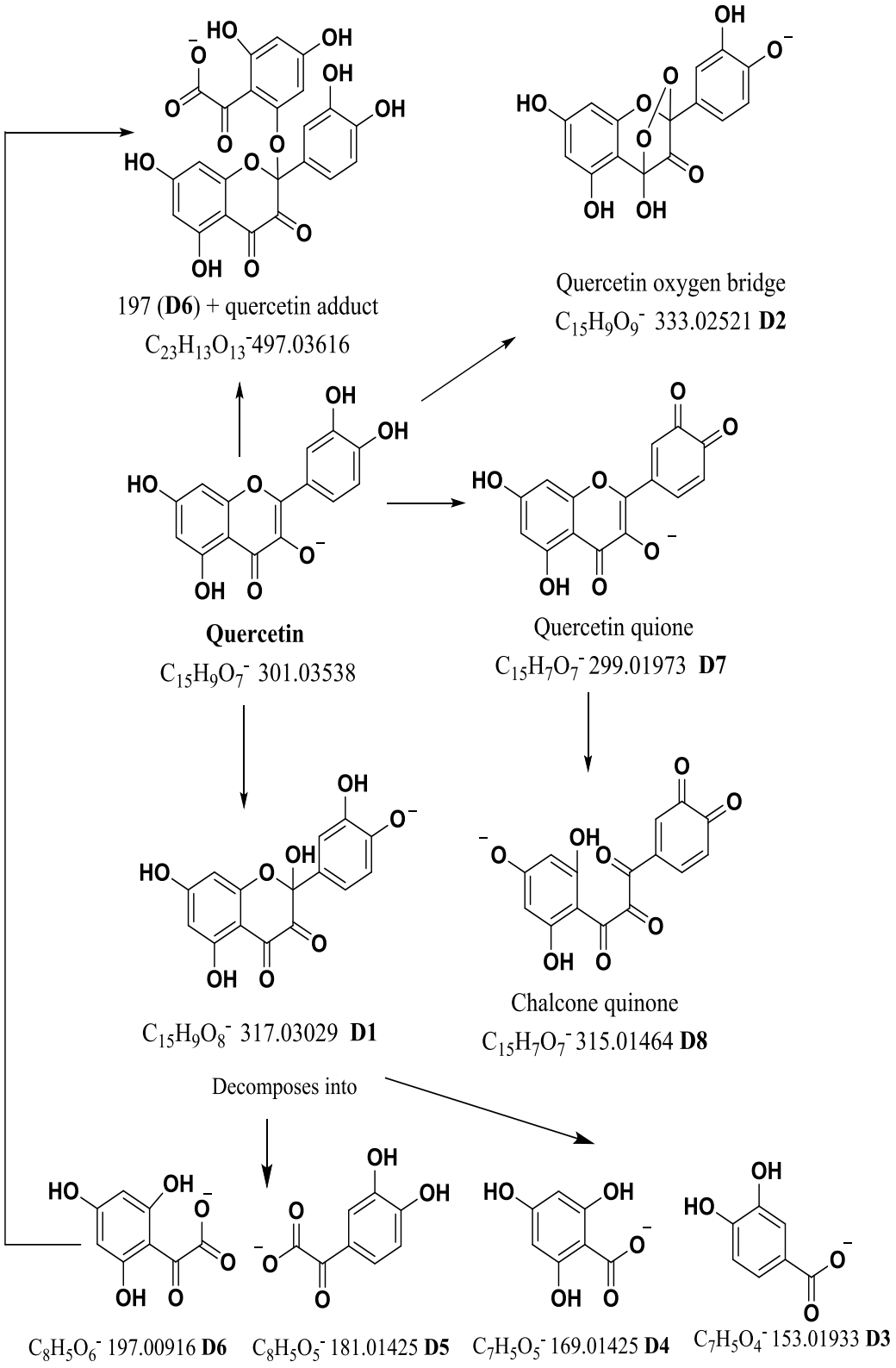

Figure 3.1 Proposed structures for major degradants formed from quercetin in KH buffer.

The major component is degradant D1 which presumably exists in equilibrium with quercetin in aqueous solution. It is likely that D1 forms via attack of oxygen on quercetin which results in D2 where an oxygen bridge is formed as proposed previously (Osman and Makris, 2010). It is possible that attack by hydroxyl plays a role in the degradation but a recent publication demonstrated that in the absence of oxygen, quercetin does not degrade even in alkaline solution (Ramešová *et al.*, 2012). D2 can be observed in the degradant mixture but at much lower levels than D1. D1 has been described as being a chalcone but a chalcone structure is not consistent with elimination of CO_2 which is observed in the MS^2 spectrum of D1 **(Figure 3.2)**, where in order to readily devise a mechanism for CO_2 elimination two oxygen atoms have to be bonded to the same carbon atom. The mass spectrum of D1 is unusually complex for a MS^2 spectrum and many of the fragments are due to alternate elimination of oxygen and CO.

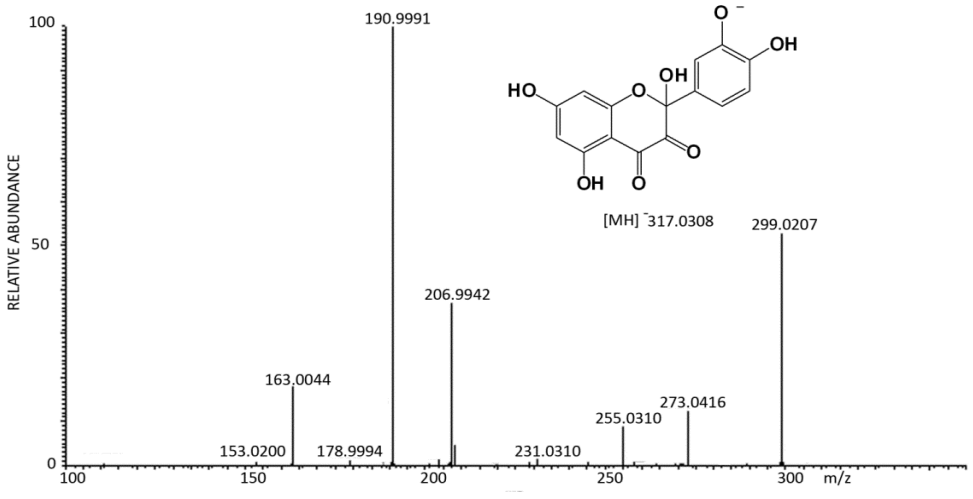

Figure 3.2 MS^2 spectrum (35eV) of the key intermediate D1 of quercetin degradation.

The fragmentation pattern observed in **Figure 3.3** and the complexity of the spectrum reinforces the impression that quercetin is an unusual molecule. D1 appears to act as the key intermediate in degradation which decomposes into mainly D3- D6 plus several minor degradants including some involving adduct formation such as the adducts formed to produce a dimer of quercetin and an adduct between quercetin and D1. Direct observation of quercetin degradation in an aqueous buffer by NMR is not an option because of its poor water solubility. Quercetin is soluble in NaOH but rapidly degrades so that it was not possible to isolate the key intermediate D1 by dissolving in NaOH.

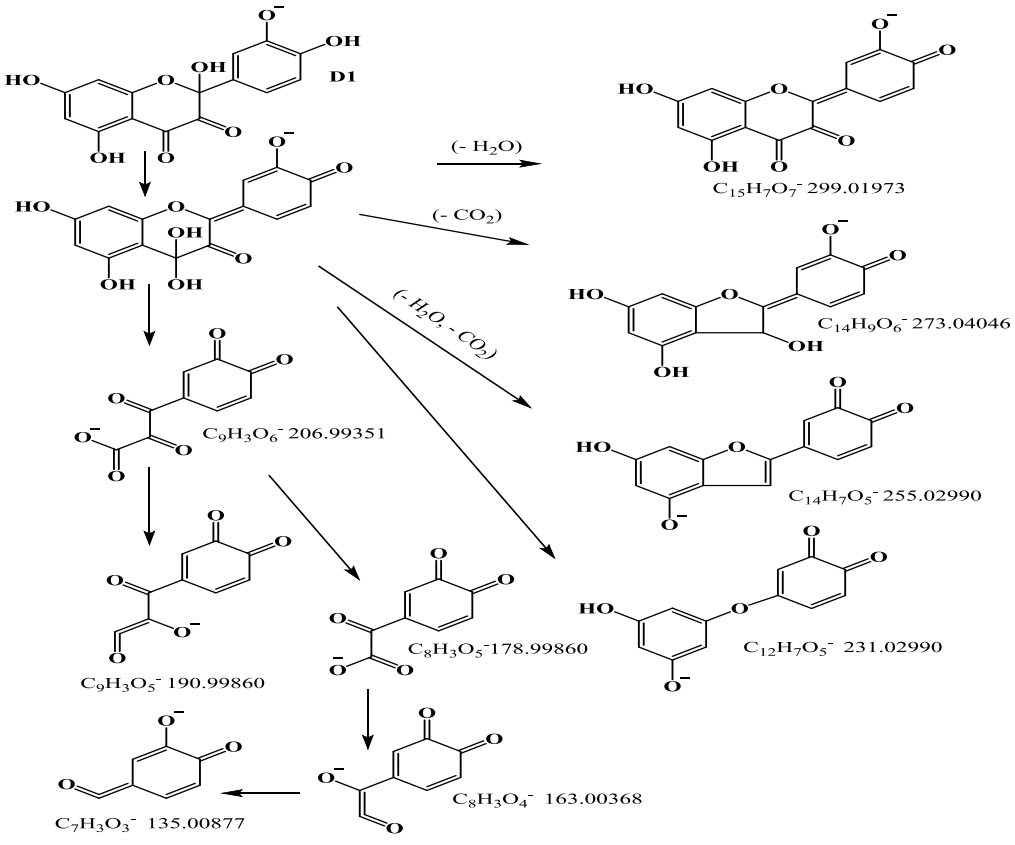

Figure 3.3 Proposed MS^2 (35eV) fragmentation pathways of the key intermediate D1 in quercetin degradation.

Table 3-4 shows the masses of the fragment ions in MS^2 spectra of those degradants which were sufficiently abundant to obtain good quality MS^2 spectra. After 120 min of incubation in KH buffer, the quercetin has almost completely decomposed. Quercetin is obviously highly reactive and as reported before (Zhou *et al*., 2007) but so far no studies have reported the degradation of quercetin under physiological conditions and the resultant contribution of the degradants to the metabolic profile of quercetin.

Table 3-2 shows the major metabolites formed during incubation of quercetin with rat hepatocytes for 30 min and 120 min. The quercetin is largely metabolised by 30 min with the major metabolites being monoglucuronides, a diglucuronide, a methyl glucuronide and a mixed glucuronide sulfate. Small amounts of monosulfates and methyl monosulfates are also present. At 120 min the main metabolites are mixed glucuronide sulfates. The proposed metabolites are shown in **Figure 3.4**. Most of these metabolites have been described before (van der Woude *et al*., 2004, Hong and Mitchell, 2006) although this a first study where they have been characterised by using liquid chromatography- high resolution mass spectrometry.

In addition to quercetin metabolites a small amount of the sulfate of D3 was formed. D3 is the major degradant of quercetin in KH buffer in the absence of hepatocytes but its levels are much lower in hepatocyte incubations. Thus, it would appear that the chemical degradation of quercetin in hepatocyte incubation is less extensive in comparison with its degradation in KH buffer alone which may be due to inhibition of degradation as a result of glucuronidation, sulfation, methylation and GSH conjugate formation. In addition to small amounts of D3 sulfate being formed there are small amounts of putatively identified metabolites resulting from the methylation

of D3 followed by glucuronidation, sulfation and sulfation in combination with glycine conjugation. Quercetin also forms three glutathione conjugates in small amounts **(Figure 3.5)** which presumably result from addition of GSH at different positions within the ring system; a GSH conjugate of D3 can also be observed in the hepatocyte incubations. It would seem likely that a favoured site for reaction of GSH would be at position 2 in the C- ring of quercetin where it was proposed that addition of oxygen occurs (Osman and Makris, 2010). Also small amounts of GSH conjugates of the quercetin quinone can be observed in **Figure 3.5**. These GSH conjugates can be readily formed when quercetin is incubated in ammonium bicarbonate solution although the relative abundance of the conjugates is different from those formed in hepatocytes.

Table 3-4 MS^2 (35eV) data for the major degradants formed from quercetin in KH buffer

Degradant	$[M-H]^-$	MS/MS fragments
$C_7H_5O_4$ D3	153.0195	109.0298 ($C_6H_5O_2$ - CO_2, 100%)
$C_7H_5O_5$ D4	169.0145	151.004 ($C_7H_3O_4$ - H_2O, 100%) 125.0246 ($C_6H_5O_3$ - CO_2, 1.24%) 107.0139 ($C_6H_3O_2$ - H_2O and - CO_2, 0.54%)
$C_8H_5O_5$ D5	181.0146	109.0295 ($C_6H_5O_2$ - $COCO_2$), 153.02 (- CO_2, 38.79%)
$C_8H_5O_6$ D6	197.0095	153.0196 ($C_7H_5O_4$ - CO_2, 100%), 125.02 ($C_6H_5O_2$ - $COCO_2$, 1.90%)
Quercetin –CO $C_{14}H_9O_6$	273.041	258.0176 ($C_{13}H_6O_6$ - CH_3, 48.19%), 245.0465 ($C_{13}H_9O_5$ - CO, 100%), 231.03076 ($C_{12}H_7O_5$ - $COCH_2$, 65.40%) 229.0515 ($C_{13}H_9O_4$ - CO_2, 84.49%), 217.0510 ($C_{12}H_9O_4$, - $COCO_2$, 11.34%)
Chalcone quinone D8 $C_{15}H_7O_8$	315.0155	287.0207 ($C_{14}H_7O_7$ - CO, 100%), 243.0308 ($C_{13}H_7O_5$ - $COCO_2$, 11.99%) 151.0043 ($C_7H_3O_4$ - $C_8H_4O_4$, 8.52%), 271.06 ($C_{14}H_7O_6$ - CO_2, 13.26%)
D1 $C_{15}H_9O_8$	317.0308	299.0182 ($C_{15}H_7O_7$ - H_2O, 53.19%) 273.0410 ($C_{14}H_9O_6$ - CO_2, 12.04%) 255.0309 ($C_{14}H_7O_5$ - CO_2H_2O, 7.86%), 231.0308 ($C_{12}H_7O_5$ - $C_3H_2O_3$, 1.32%) 206.9943 ($C_9H_3O_6$ - $C_6H_6O_2$, 36.04%) 190.9991 ($C_9H_3O_5$ - $C_6H_6O_3$, 100%) 178.9994 ($C_8H_3O_5$) 163.0044 ($C_8H_3O_4$ - $C_7H_6O_4$, 18.94%) 153.0200($C_7H_5O_4$, 1.1%) 135.0092 ($C_7H_3O_3$, 0.5%)
Quercetin oxygen bridge D2 $C_{15}H_9O_9$	333.0261	289.0363 ($C_{14}H_9O_7$ - CO_2, 29.46%) 181.0149 ($C_7H_5O_5$ - $C_8H_4O_4$, 100%) 169.0151 ($C_7H_5O_4$ - $C_8H_4O_5$, 90.47%) 109.0282 ($C_6H_5O_2$ - $C_9H_4O_7$, 7.72%)
Adduct 169/273 $C_{21}H_{13}O_{10}$	425.0525	407.0419 ($C_{21}H_{11}O_9$ - H_2O, 9.24%) 299.0207 ($C_{15}H_7O_7$, - $C_6H_6O_3$ 38.66%) 273.0412 ($C_{14}H_9O_6$, - $C_7H_4O_7$ 25.81%)
197 + Quercetin $C_{23}H_{13}O_{13}$	497.0372	345.0262 ($C_{16}H_9O_9$ - $C_7H_4O_4$, 100%) 301.0363 [$C_{15}H_9O_7$ (-196 $C_8H_4O_6$, 61.79%)]
Quercetin dimer $C_{30}H_{17}O_{14}$	601.0635	449.0553 ($C_{23}H_{13}O_{10}$ - $C_7H_4O_4$, 100%) 431.0420 ($C_{23}H_{11}O_{10}$ - $C_7H_6O_4$, 1.96%)
Quercetin + 317 $C_{30}H_{17}O_{15}$	617.0581	65.0481 ($C_{23}H_{13}O_{10}$ - $C_7H_4O_5$, 100%)

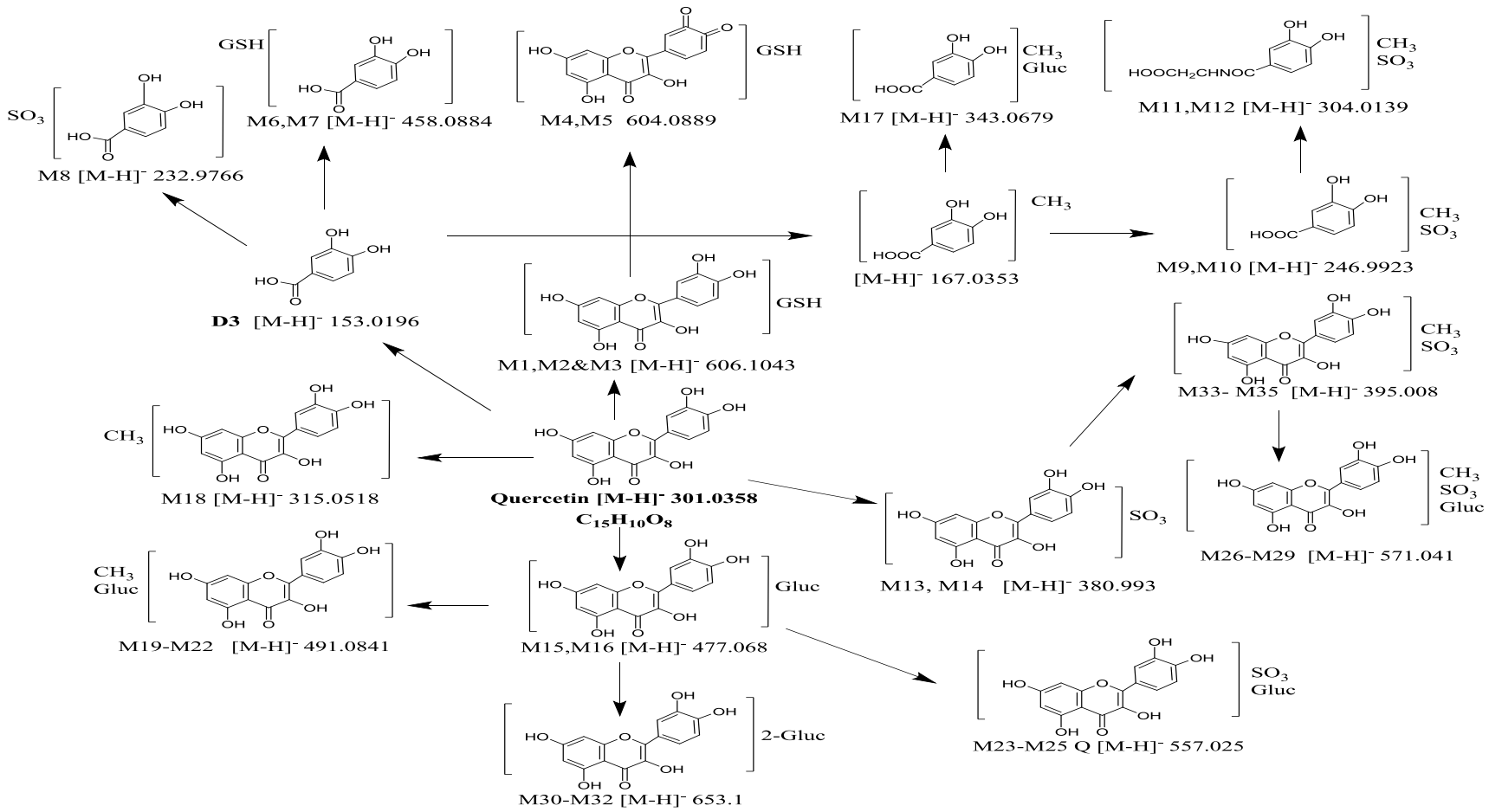

Figure 3.4 Proposed structures of the metabolites of quercetin formed in incubations with rat hepatocytes.

Gluc = glucuronic acid -OH, GSH = Glutathione.

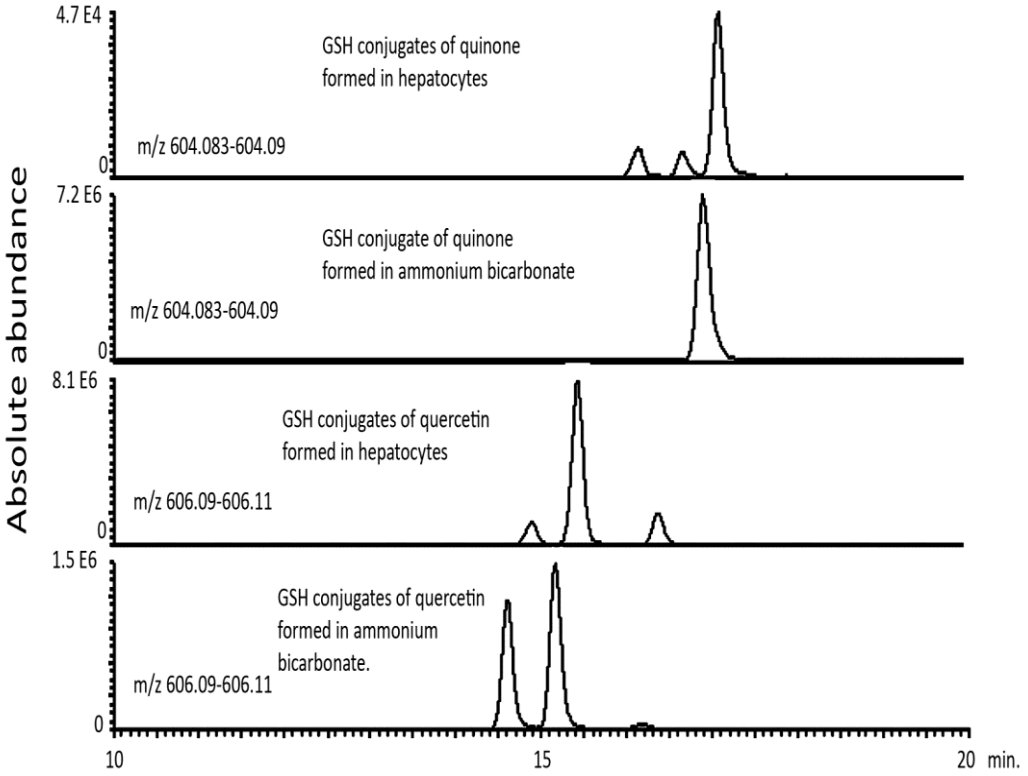

Figure 3.5 Extracted ion traces showing formation of GSH conjugates of quercetin in hepatocytes and ammonium bicarbonate solution.

In the case of the incubation in ammonium bicarbonate two peaks for the conjugate of equal intensity result and this would be consistent with addition at position 2 where two diastereomeric adducts would form since addition of GSH generates a chiral centre. Also larger amounts of a quinone GSH conjugate are formed in the ammonium bicarbonate incubation. The presence of GSH in the ammonium bicarbonate incubation does not inhibit the degradation of quercetin and the major degradants D3-D6 are all formed. In addition, GSH adducts of D3-D6 can also be observed. When quercetin is incubated in KH buffer containing GSH under an atmosphere containing 95% O_2, in contrast to the same experiment in ammonium

bicarbonate, there was no reaction with GSH and very little degradation of quercetin occurred up to 180 min. During the course of the incubation, as observed under mass spectrometry, much of the GSH was converted to oxidised glutathione (GSSG) suggesting that the GSH was removing oxygen from the medium though itself becoming oxidised. This further supports the idea that the initiation of quercetin degradation occurs via the formation of the oxygen bridge intermediate D2. The MS^2 spectra for some quercetin metabolites and quercetin degradant metabolites are shown in **Table 3-5** and these are consistent with the assigned structures.

Table 3-5 MS^2 (35eV) data for the major metabolites formed from quercetin in hepatocyte

Metabolite	$[M-H]^-$	t_R min.	Fragment ions
Quercetin GSH Conjugate M1	606.10	14.5	333.01 (-G, 38.2%), 299.02 (-GSH, 100%)
Quercetin GSH Conjugate M2	606.10	15.1	333.01 (-G, 100%), 299.02 (-GSH, 2.6%)
Quercetin GSH Conjugate M3	606.10	16.2	333.01 (-G, 50%)
Quercetin GSH Conjugate M4	604.08	16.9	330.99 (-G, 100%), 298 (-GSH, 0.98%)
Quercetin GSH Conjugate M5	604.08	21.9	301.03 (-GSH, 100%)
M8	232.97	7.0	153.02 ($-SO_3$, 100%), 109.029 ($-CO_2$, $-SO_3$ 39.5%)
M10	246.99	10.0	203.002 ($-CO_2$, 21.2%), 167.03 ($-SO_3$, 63.5%)
M11	304.01	7.4	260.02 ($-CO_2$, 1.2%), 224.05 ($-SO_3$, 100%)
M17	343.06	7.4	167.03 (-Gluc, 67.2%)
Quercetin sulfate M14	380.99	19.9	301.03 ($-SO_3$, 100%)
Quercetin glucuronide M15	477.06	16.2	301.03 (- Gluc, 100%)
Quercetin glucuronide M16	477.06	18.4	301.03 (- Gluc, 100%)
Quercetin methyl glucuronide M19	491.08	17.6	315.05 (-Gluc, 100%)

quercetin monglucuronide sulfate M22	557.02	15.0	477.06 (-SO_3, 100%), 380.99 (-Gluc, 12.6%), 301.04 (-Gluc and SO_3, 19.70%)
Quercetin monglucuronide sulfate M24	557.02	15.6	477.06 (-SO_3, 100%), 380.99 (-Gluc, 28.6%), 301.04 (-Gluc and SO_3, 4.66%)
Methylated quercetin monglucuronide sulfate M23	571.04	14.3	491.08 (-SO_3, 100%), 395.01 (-Gluc, 2.2%), 315.05 (-SO_3 and - Gluc, 6.91%)
Methylated quercetin monglucuronide sulfate M26	571.04	14.70	491.08 (-SO_3, 100%), 395.01 (-Gluc, 2.6%), 315.05 (-SO_3 and - Gluc, 23.7%)
Methylated quercetin monglucuronide sulfate M27	571.04	16.3	491.08 (-SO_3, 100%), 395.01 (-Gluc, 6.64%), 315.05 (-SO_3 and - Gluc, 6.97%)
Quercetin-3,7-diglucuronide M30	653.1	14.1	477.06 (-Gluc, 100%), 301.03 (-2Gluc, 8.3%)
Quercetin-3,7-diglucuronide M31	653.1	14.32	477.06 (-Gluc, 100%), 301.03 (-2Gluc, 7.76%)
Methylated quercetin sulfate M34	395.005	19.6	315.05 (-SO_3, 100%)
Methylated quercetin sulfate M35	395.005	20.1	315.05 (-SO_3, 100%)

Gluc = glucuronic acid -OH, G = glutathione -SH, GSH = glutathione.

3.5 Conclusion

The levels of quercetin used in the incubations in rat hepatocytes were about 10 times the likely exposure from dietary absorption when compared, for instance, the total area under the curve over 24 hours for quercetin metabolites (ca. 3 mg compared to 30 mg in the current case) absorbed from onion powder (Lee *et al*., 2012). However, from the data in **Table 3-2**, it can be seen that the level of quercetin at physiological pH rapidly declines to ca. 1.80% of the original concentration, thus the levels used in the incubation may not be that different from the levels of exposure in human dosing studies. Although quercetin has been extensively studied, it seems that its chemistry and metabolism are far from being fully understood. Its high reactivity means that, as well as acting as a free radical scavenger, it would be likely to form adducts with reactive structures such as thiol groups within proteins.

However, it would appear from the current work that its reactivity is reduced by conjugation, for instance with glucuronic acid, and this might explain the lack of an effect on the viability of the hepatocytes. It was observed in a trial using quercetin as an anti-tumour agent that nephrotoxicity was a dose limiting factor and that Phase II metabolism was important in reducing toxicity (Ferry *et al*., 1996). The mechanism of quercetin degradation remains to be fully explained but it should be possible to make a more thorough study of this by using NMR particularly in ^{13}C NMR which would be able to map the changes in carbon substitution during degradation via chemical shift changes, although this is limited by the low solubility of quercetin in water. Although quercetin has been proposed as an antioxidant compound it may have interesting pro-oxidant and oxygen sensing properties.

CHAPTER 4

The Abundant Dietary Constituent Ferulic Acid Forms a Wide Range of Metabolites Including a Glutathione Adduct when Incubated with Rat Hepatocytes

4. The Abundant Dietary Constituent Ferulic Acid Forms a Wide Range of Metabolites Including a Glutathione Adduct when Incubated with Rat Hepatocytes.

4.1 Abstract

Introduction: The metabolism of ferulic acid (FA) has been studied in a number of different systems and several metabolites of FA have been characterised. No previous work has been carried out using hepatocytes to characterise the metabolism of FA.

Objective: The current study used a metabolomics approach in combination with high resolution mass spectrometry to characterise the metabolites of FA formed in isolated rat hepatocytes.

Methodology: FA was incubated with rat hepatocytes and the metabolites formed were profiled at 30 and 120 min by comparison with hepatocytes where FA had not been added. The metabolites were characterised according to their accurate mass at < 2 ppm using high- resolution mass spectrometry.

Results: Sixteen metabolites of FA were identified. The most abundant metabolite was the sulfate of FA and this was followed by FA glucuronide and glycine conjugates. A wide range of low level metabolites was produced in the hepatocyte incubations. Novel metabolites resulted from side chain oxidation and reduction of the carboxylic acid group to an alcohol. In addition, a glutathione (GSH) adduct of FA was formed in the hepatocyte incubation and was metabolised to its glucuronide. Incubation of a solution of FA with GSH also resulted in formation of this adduct indicating that it could be formed purely by a chemical reaction.

Conclusion: The metabolism of FA is more complex than previously described. The formation of a GSH conjugate from FA, albeit in low amounts, might indicate that caution should be exercised before claiming health benefits for this compound.

4.2 Introduction

Ferulic acid (3-methoxy-4-hydroxycinnamic acid) is one of the most abundant phenolic compounds in the human diet (Zhao and Moghadasian, 2008) where it occurs largely as ester conjugates; it has been estimated that total daily intake of FA is in the rage of 150-250 mg. FA has been proposed to have anticancer activity in lung, colon, breast, tongue, stomach and prostate cancers. In addition, it potentially possesses various therapeutic activities such as against diabetes where it promotes expansion of pancreatic islets and reduces glucose levels in blood. It has also been proposed to prevent Alzheimer's disease by maintenance of cell membranes and reduces elevated levels of lipids and triglycerides in blood. It is present in traditional Chinese medicine herbs such as *Angelica sinensis*, *Cimicifuga heracleifolia* and *Lignsticum chuangxiong*. It is also concentrated mainly in the aleurone layer (~ 75%) of grain and comprises about 0.5% w/w in wheat and 0.14% w/w in barley grains (Fazary and Ju, 2007, Ou and Kwok, 2004, Li *et al*., 2011).

Moreover, ferulic acid is an antioxidant agent due to its ability to form a resonance-stabilized phenoxy radical structure, so it is used as a natural antioxidant in foods to prevent lipid peroxidation. It is also used in cosmetics for protection of skin from the aging effects of UV light (Heinonen *et al*., 1998, Adam *et al*., 2002, Fazary and Ju, 2007, Ou and Kwok, 2004).

The health claims for phytochemicals are a matter for debate and such benefits have not been conclusively proved and inevitably, much of the evidence for their benefits is epidemiological rather than the result of controlled trials. The evidence for their beneficial effects is the subject of a recent comprehensive review (Del Rio *et al*., 2013). A major factor in the proposed action of dietary xenobiotics is the influence of

metabolism which can alter their structures in a way that might affect their proposed mode of action by either negating it or changing it. In addition, xenobiotic metabolism contributes a complex profile to the urinary metabolome which may be monitored for the purposes of disease diagnosis. It has been proposed that the xenobiotic component of urine should be termed the food metabolome (Fardet *et al*., 2008). The metabolism of hydroxycinnamic acids (HCAs), which include ferulic acid (FA), has been extensively explored both *in vitro* and *in vivo*. Farrell *et al*. (2011) observed the metabolism of FA by Caco-2 cells and found that FA was converted to dihydroferulic acid and the 4-glucuronides and 4-sulfates of ferulic acid and dihydroferulic acid. The identities of the metabolites were confirmed against authentic standards. The main metabolite produced was dihydroferulic acid (Farrell *et al*., 2011). Wong *et al*. (2010) studied the phase II metabolism of FA in *vitro* using different isoforms of UDP-glucuronosyltransferases (UDPGT) and sulfotransferases and showed that sulfation was more favoured than glucuronidation, and where 3- and 4-hydroxyl groups were available, as in caffeic acid, that conjugation of the 4-position was favoured over conjugation of the 3-position (Wong *et al*., 2010). Ferulic acid metabolites were measured in human plasma and urine following coffee consumption (Stalmach *et al*., 2009). FA occurs in coffee as its quinic acid conjugate which is metabolised to ferulic acid. The ferulic acid metabolites detected in plasma and urine included: ferulic acid glycine conjugate, ferulic acid 4-*O*-sulfate, ferulic acid 4-*O*-glucuronide, and dihydroferulic acid. In addition, ferulic acid can contribute to caffeic acid metabolites following its demethylation. The metabolites of the chemical constituents of *Salvia miltiorrhiza*, which is used in Chinese traditional medicine to treat a range of diseases, was studied. The active constituents in the

water soluble fraction of the plant are believed to be phenolic acids including FA. In this study rats were dosed with phenolic acids including FA and the main metabolites found for FA were two glucuronides of FA itself (Zhang *et al*., 2005). In another study rats were administered a diet which was high in FA and it was found that FA was metabolised to sulfate and glucuronide conjugates (Zhao *et al*., 2004). Kern *et al*. (2003) reported that the most abundant metabolites of FA in urine and plasma were feruloylglycine and/or glucuronides after administration of FA from wheat bran (Kern *et al*., 2003). However, Virgili *et al*. (2000) reported that the FA was excreted in urine as free FA and glucuronic / sulfate conjugates after consumption of FA extracted from French maritime pine bark (Virgili *et al*., 2000). Three metabolites of ferulic acid in rat urine, faeces and bile have been reported by enzymatic hydrolysis, HPLC-DAD, HPLC-MS and MS/MS in positive ion mode and these were labelled as M1, M2, and M3 depending on the position of glucuronic acid conjugation to the parent compound. The M1 and M3 metabolites were conjugated with one glucuronic acid moiety at different positions but M2 FA was conjugated with two glucuronic acid moieties (Zhang *et al*., 2005). More recently, it has been reported that FA was metabolised by uridine diphosphate glucuronyl transferase (UDPGT) in human liver microsomes to two polar glucuronide metabolites (M1 and M2) which were analysed by mass spectrometry in negative ion mode. The metabolites had molecular ions with m/z 369 formed by addition of glucuronic acid moiety (176) to FA (m/z 193). The presence of an ion at m/z 178 peak in M1 spectrum following MS/MS provided the differentiation between M1 & M2. Furthermore, in M1, the methyl group can be lost before or after the loss of the CO_2 moiety. However, the methyl group could be only lost from M2 after the loss of the CO_2 moiety (Li *et al*., 2011).

Fardet *et al*. (2008) used a metabolomics approach to study the metabolism of phenolic acids, and used chemometric data extraction and QTOF-MS to identify metabolites of FA in rat urine. Rats fed on a diet enriched with FA produced the following metabolites: FA glucuronide, FA sulfate, feruloylglycine, feruloylglycine sulfate, dihydroferulolyl glycine and dihydroferruloyl sulfate (Fardet *et al*., 2008). Thus, this approach allowed identification of several novel metabolites.

The current chapter adopts a metabolomics approach to exploring the metabolism of FA in rat hepatocytes and provides evidence that the biotransformation of FA is more complex than previously observed in this system.

4.3 Experimental

4.3.1 Incubation of ferulic acid with rat hepatocytes protocols

The incubation of ferulic acid with rat hepatocytes and extraction of incubation solutions are described in detail in (General Methodology Chapter 2 pages 58:60).

4.3.2 Instrumentation and data processing

These details have been reported in (General Methodology Chapter 2 pages 61, 62).

4.3.3 Preparation of GSH conjugate of FA

Ferulic acid (1 mg) was dissolved in 1 mL of 0.2% ammonium bicarbonate and then GSH (3 mg) dissolved in 1 mL of water was added. The sample was left at room temperature for 24 hours before analysis. For analysis the sample was diluted 10:1 with 0.1% formic acid and then analysed by LC-MS.

4.3.4 Analysis of ferulic acid metabolites in a sample of human plasma

0.2 mL of a pooled plasma sample were mixed with 0.8 mL of acetonitrile and 10 µL of sample were injected onto a ZICpHILIC column (L150 x 4.6 mm) eluted with a mobile phase consisting of 20 mM ammonium carbonate buffer, pH 9.2 (A) and acetonitrile (B) at a flow rate of 0.3 mL/min. The elution conditions were 80% B (0 min) 20% B (30 min) with a linear gradient. The HPLC column was interfaced to an Orbitrap Exactive instrument used in positive negative switching mode with ESI voltages of 4.5 kV positive ions and 4.0 kV negative ions.

4.4 Results and discussion

Table 4-1 shows the hepatocyte viability with time indicating that there was no significant loss of viability over 120 min of incubation either in the controls or in the presence of FA.

Table 4-1 Viability of suspension hepatocytes during two hours of treatment period with 100 µM ferulic acid

Incubation time (min)	Viability of control	Viability with FA
0	92%	84%
30	90%	76%
120	76%	82%

FA was metabolised very rapidly by hepatocytes and on a peak area % basis only 2.6% FA remained at 30 min and only 0.1% remained at 120 min. Using Sieve software to compare blank incubations with incubations containing FA allowed the putative identification of 16 metabolites of FA **(Table 4-2, Figure 4.1)**.

The metabolites listed in **Table 4-2** were also characterised using MS^2 at 35 eV and the fragments obtained largely support the assignments of the metabolites **(Table 4-3)**. The most dominant metabolite, as might be expected from the literature, was the sulfate, presumably the 4-*O*-sulfate. There was a second less abundant sulfate metabolite which probably corresponds to the 4-*O*-sulfate of cis ferulic acid (Omar *et al*., 2012). Again, as might be expected a glucuronide, presumably the 4-*O*-glucuronide, was relatively abundant as was the previously identified sulfate conjugate of FA glycine. A second glucuronide correlates in terms of its later retention time with the acyl glucuronide observed by Li *et al*. however, we did not observe any difference in MS^2 spectra of acyl glucuronide from that of 4-*O*-glucuronide mentioned by these researchers (Li *et al*., 2011). In addition there were sulfate, glucuronide and glycine metabolites of dihydro FA which have all been previously described (Fardet *et al*., 2008).

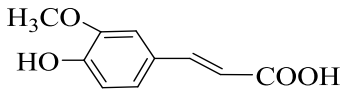

Ferulic Acid [M-H]⁻ = 193.0509
$C_{10}H_{10}O_4$

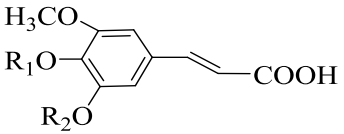

M6 R_1 = H R_2 = H [M-H]⁻ = 209.0461
M7 R_1 = SO_3H R_2 = H [M-H]⁻ = 289.0031
M8 R_1 = H R_2 = SO_3H [M-H]⁻ = 289.0031

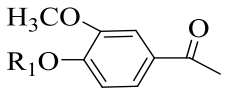

M11 R_1 = H [M-H]⁻ = 165.0560
M12 R_1 = SO_3H [M-H]⁻ = 245.013
M13 245.013 ISOMER OF M12

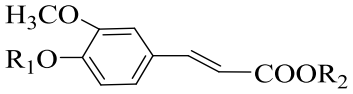

M1 R_1 = SO_3H R_2 = H [M-H]⁻ = 273.0078
M2 R_1 = Gluc R_2 = H [M-H]⁻ = 369.0835
M3 R_1 = H R_2 = Gluc [M-H]⁻ = 369.0835

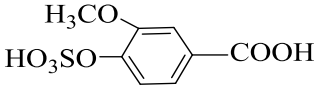

M9 [M-H]⁻ =246.9923

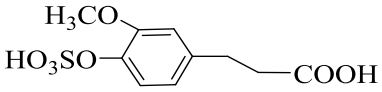

M14 [M-H]⁻ =275.0235

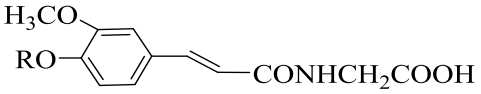

M4 R = H [M-H]⁻ = 250.0726
M5 R = SO_3H [M-H]⁻ = 330.0297

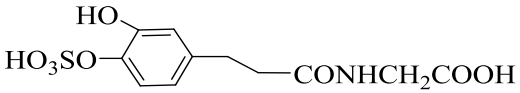

M10 [M-H]⁻= 332.0445

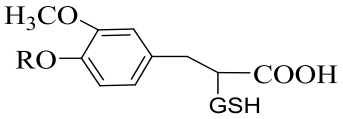

M15 R = H [M-H]⁻ = 500.1354
M16 R = Gluc [M-H]⁻ = 676.1672

Figure 4.1 Proposed structures of the metabolites of ferulic acid formed in incubations with rat hepatocytes.

Gluc = Glucuronic acid -OH, GSH = Glutathione.

Table 4-2 Metabolites of ferulic acid putatively identified according to accurate mass in incubations with rat hepatocytes

Metabolite	$[M-H]^-$	Elemental Composition	t_R min	Area %30 min	RSD *n*=4	Area %120 min	RSD *n*=4
Ferulic acid	193.0509	$C_{10}H_9O_4$	19.0	2.648	10.0	0.110	11.6
FA sulfate M1	273.0078	$C_{10}H_9SO_7$	14.2	84.356	6.9	83.3	10.3
FA glucuronide M2	369.0835	$C_{16}H_{17}O_{10}$	12.8	4.990	7.7	3.65	10.3
FA glucuronide M3	369.0837	$C_{16}H_{17}O_{10}$	15.2	0.935	12.7	0.823	9.4
FA glycine M4	250.0726	$C_{12}H_{12}NO_5$	14.3	0.670	15.5	0.509	7.2
Sulfate of FA glycine M5	330.0297	$C_{12}H_{12}NSO_8$	12.8	3.252	9.6	3.80	10.9
Hydroxy FA M6	209.0461	$C_{10}H_9O_5$	15.5	0.241	11.8	0.0745	9.0
FA OH sulfate M7	289.0031	$C_{10}H_9SO_8$	13.5	0.122	13.2	0.0943	10.3
FA OH sulfate M8	289.0031	$C_{10}H_9SO_8$	14.1	0.113	13.3	0.0911	10.7
DHBA sulfate M9	246.9923	$C_8H_7SO_7$	11.2	0.472	11.2	0.515	10.3
FA reduced glycine sulfate M10	332.0455	$C_{12}H_{14}NSO_8$	11.1	0.283	16.5	0.423	11.8
FA demethylated reduced M11	165.0560	$C_9H_9O_3$	15.5	0.611	9.9	0.179	7.3
FA demethylated reduced sulfate M12	245.0130	$C_9H_9SO_6$	13.5	0.403	6.7	0.321	6.6
FA demethylated reduced sulfate M13	245.0130	$C_9H_9SO_6$	11.9	0.209	10.0	0.166	13.7
FA reduced sulfate M14	275.0235	$C_{10}H_{11}SO_7$	13.3	0.40	11.7	0.53	11.3
FA GSH conjugate M15	500.1354	$C_{20}H_{26}O_{10}N_3S$	11.3	0.208	21.0	0.130	15.1
FA GSH conjugate Glucuronide M16	676.1672	$C_{26}H_{34}O_{16}N_3S$	7.1	0.122	10.1	0.0631	10.7

Table 4-3 MS^2 (35eV) data for major metabolites formed from FA in hepatocyte incubations.

Metabolite	$[M-H]^-$	t_R min	Fragment ions
FA sulfate M1	273.0078	14.2	229.02 (-CO_2, 15%), 193.05 (-SO_3, 100%)
FA glucuronide M2	369.0837	12.8	351.07 (-H_2O, 1%) 193.05 (-Gluc, 55%), 175.03 (-Gluc & OH, 100%), 113.02 (54%)
FA glucuronide M3	369.0837	15.2	351.07 (-H_2O, 2%) 193.05 (-Gluc, 100%), 175.03 (-Gluc & OH, 38%), 113.02 (22%)
FA glycine M4	250.0726	14.3	206.08 (-CO_2, 100%)
Sulfate of FA glycine M5	330.0297	12.8	286.04 (-CO_2, 0.5%), 250.07 (-SO_3, 100%)
Hydroxy FA M6	209.0461	15.5	165.02 (-CO_2)
FA OH sulfate M7	289.0031	13.5	209.02 (-SO_3, 100%)
FA OH sulfate M8	289.0031	14.1	209.02 (-SO_3, 100%)
DHBA sulfate M9	246.9923	11.2	203.00 (-CO_2, 44%), 167.04 (-SO_3, 100%), 123.05 (SO_3, -CO_2 0.5%), 96.96 (due to HSO_4^-)
FA reduced glycine sulfate M10	332.0455	11.1	288.06 (-CO_2, 0.5%), 252.09 (-SO_3, 100%)
FA demethylated reduced M11	165.0560	15.5	150.03 (-CH_3 100%)
FA demethylated reduced sulfate M12	245.0130	13.5	165.06 (-SO_3, 100%)
FA demethylated reduced sulfate M13	245.0130	11.9	165.06 (-SO_3, 100%)
FA reduced sulfate M14	275.0235	13.3	231.01 (-CO_2, 100%), 193.05 (-SO_3 & H_2, 75%)
FA GSH conjugate M15	500.1354	11.3	306.06 (-FA, 100)
FA GSH conjugate Glucuronide M16	676.1672	7.1	500.13 (-Gluc, 100%)

Figure 4.2 shows extracted ion chromatograms for the major metabolites produced from FA by hepatocytes. In addition, several novel metabolites were also observed at low levels. M9 results from the oxidation of the propenoic side chain followed by sulfation. It was not possible to get additional structural identification of M9 from MS^3 experiments but applying source fragmentation energy of 35 eV resulted in the spectrum shown in **Figure 4.3A** where losses of sulfate, methyl and CO_2 can be clearly observed.

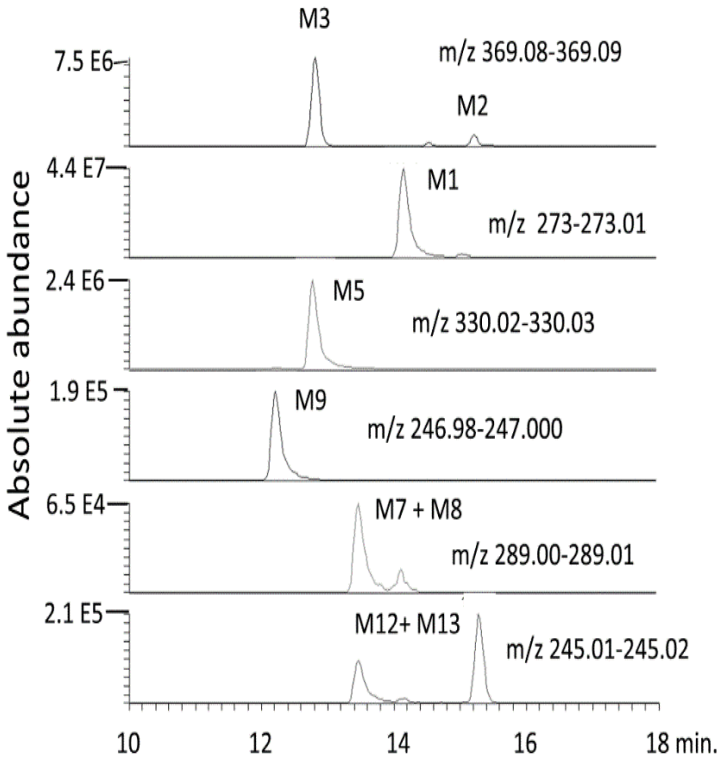

Figure 4.2 Extracted ion chromatograms for some of the major metabolites of ferulic acid produced by rat hepatocytes analysed using an ACE C18-AR column.

There are three hydroxylated metabolites of FA and dihydroferulic acid (M6, M7 and M8) and surprisingly these do not seem to have been reported before although this would be an expected modification of an aromatic ring. Also there are three metabolites, M11, M12 and M13, where it would appear that partial oxidation of the side chain has occurred, this might be an expected intermediate in the formation of M9 via β-oxidation of the side chain. However, it is not possible to explain why there appear to be isomers M12 and M13.

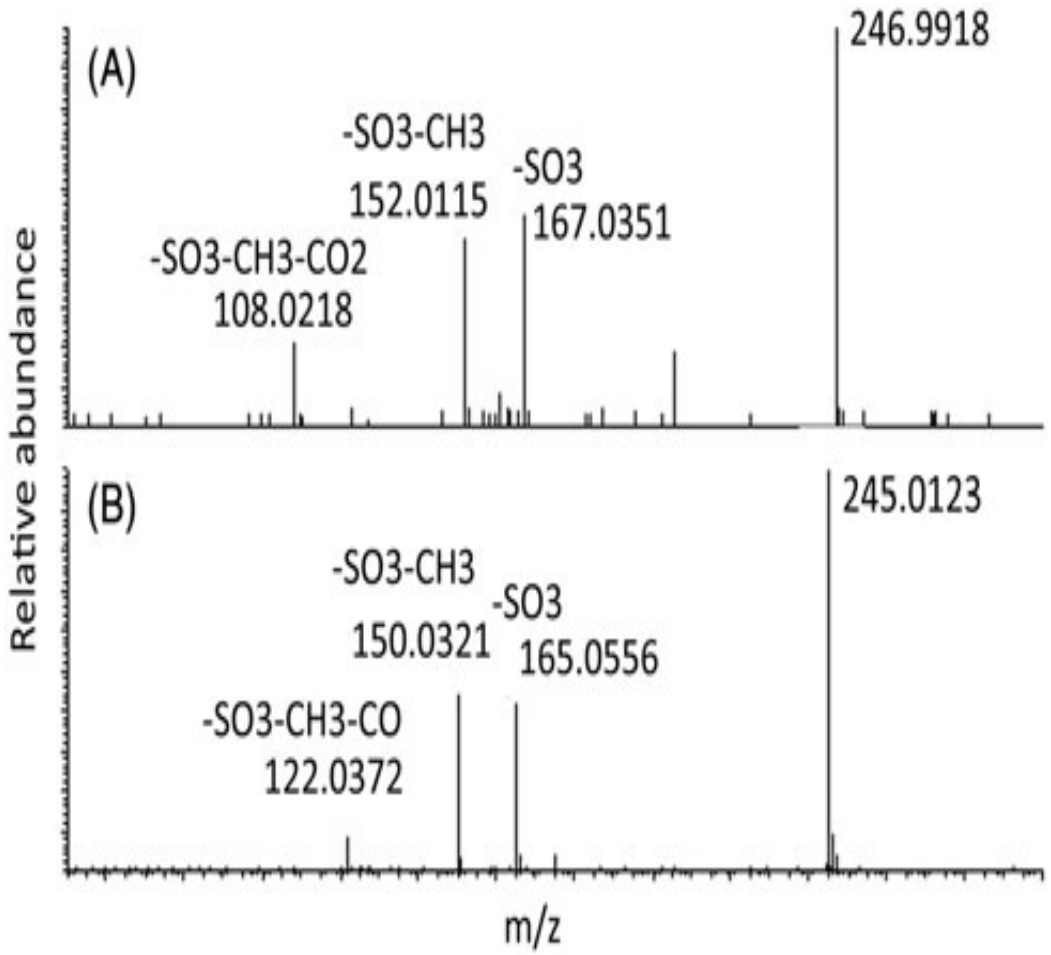

Figure 4.3 Spectra of M9 (A) and M12 (B) obtained by ion source fragmentation at 35 eV.

Figure 4.3B shows the source fragmentation spectrum at 35 eV of M12 where losses of sulfate, methyl and carbonyl can be clearly seen. Of most interest from a toxicological perspective is the occurrence of metabolites M15 and M16 which are glutathione (GSH) conjugates of ferulic acid. These conjugates are formed by nucleophilic addition of the GSH across the double bond in the side chain of FA. This observation suggests that the double bond in the side chain of FA is reactive and damaging reactions with thiol groups within cellular structures could occur. It is important to note that this addition is not of the type which occurs in quinonoid derivatives of phenolic acids (Moridani *et al*., 2002) since it does not require oxidation prior to addition but occurs in un-metabolised FA.

Figures 4.4 and **4.5** show the MS^2 spectra obtained for the GSH conjugate of FA (M15) and its glucuronide (M16). The GSH conjugate fragments to give an ion at m/z 306 for the GSH portion of the molecule resulting from the loss of FA. The glucuronide conjugate of the GSH adduct shows ions at m/z 500, resulting from the neutral loss of glucuronide and ion at m/z 306 from the GSH portion of the molecule. Incubation of GSH with FA in ammonium bicarbonate solution at pH 7.6 resulted in formation of the same FA-GSH adduct indicating that this reaction can occur non enzymatically. Dimethyl fumarate, which is used to treat psoriasis is a conjugated acid like ferulic acid, and has been shown to react with GSH (Schmidt *et al*., 2007).Thus, this suggests that the numerous naturally occurring phenylpropenoid acids might have the ability to react in this way. Although this class of compounds is promoted as having health benefits, reaction with GSH is not a desirable property, and indicates that FA behaves like an electrophilic reactive metabolite. Despite the fact that reaction with GSH occurred, the viability of the hepatocytes was not

significantly affected suggesting that the reaction rate with FA is slow enough not to damage the hepatocytes. Comparing the ratio of the extracted ion chromatogram for GSH (308.09–308.1, peak at t_R = 6.2 min) after 30 min in hepatocytes incubated on their own and incubated with FA there was no significant difference in GSH levels between the untreated and treated hepatocytes (ratio 1.1, *p* value 0.47, n = 4).

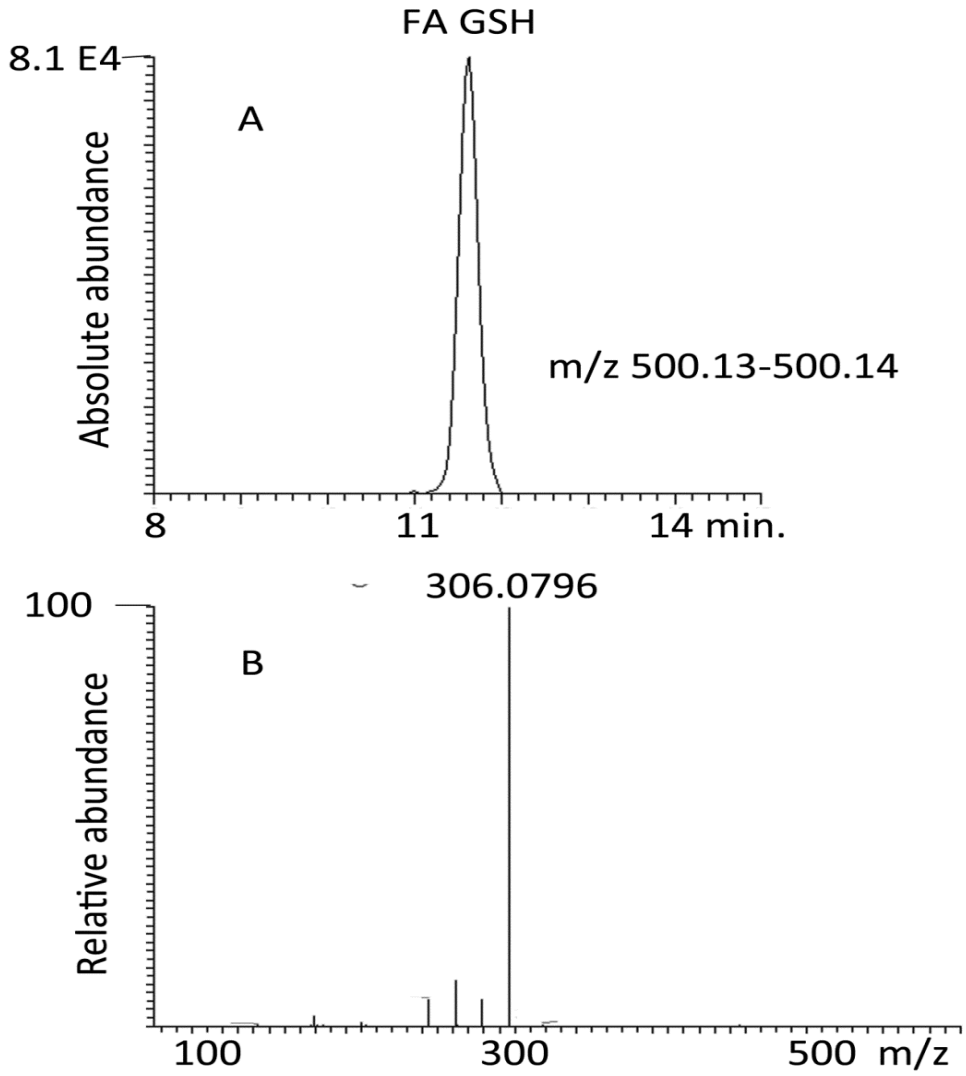

Figure 4.4 Extracted ion chromatogram and MS^2 spectrum of the GSH conjugate of FA formed in hepatocyte incubations.

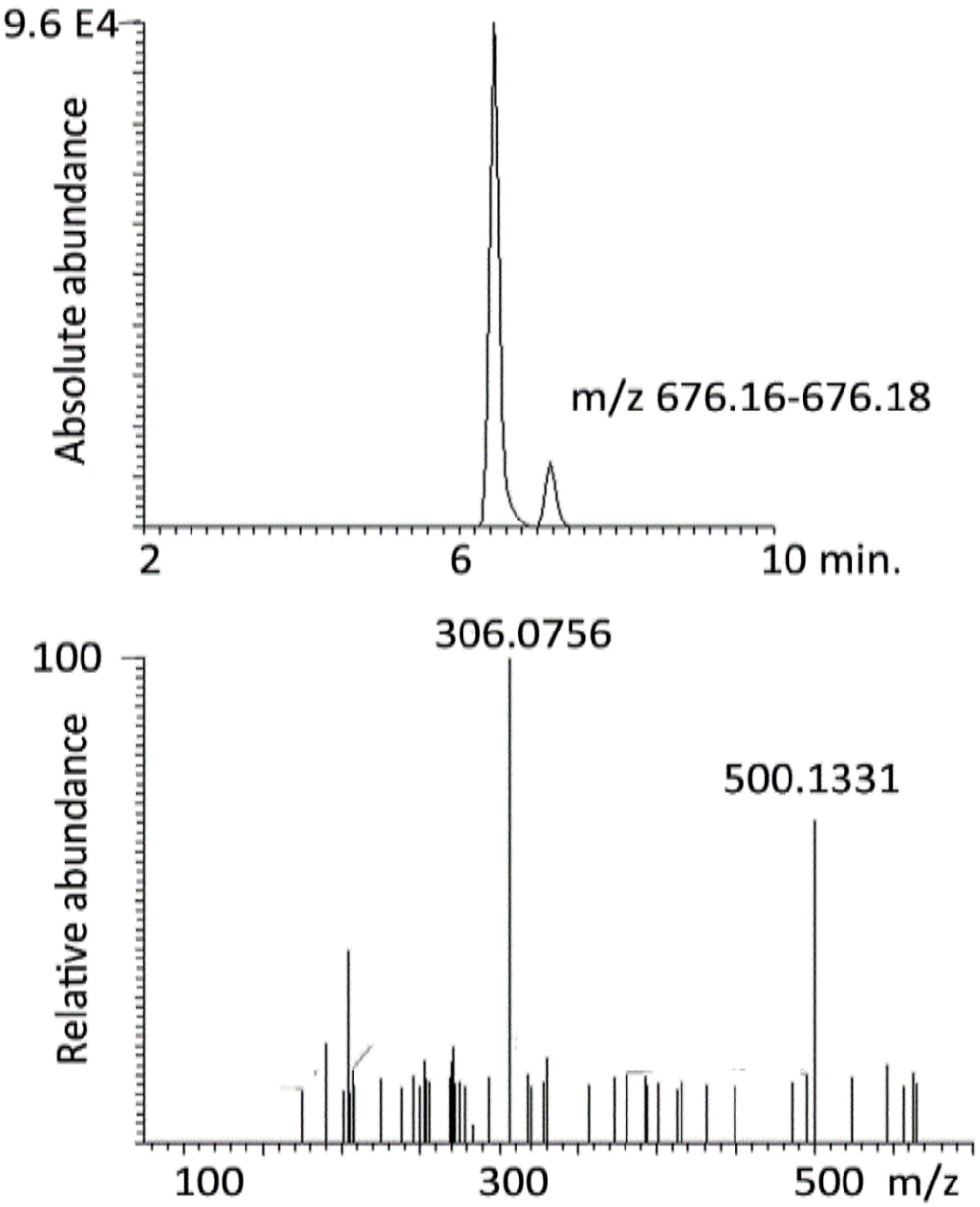

Figure 4.5 Extracted ion chromatogram and MS^2 spectrum of the glucuronide conjugate of ferulic acid GSH adduct formed in incubations with rat hepatocytes.

Given the abundance of ferulic acid in the diet a number of metabolites of ferulic acid can be observed in human plasma **(Figure 4.6)** including a sulfate and two glucuronides, and a demethylated reduced sulfate. Thus ferulic acid makes a major contribution to the complexity of the plasma metabolome.

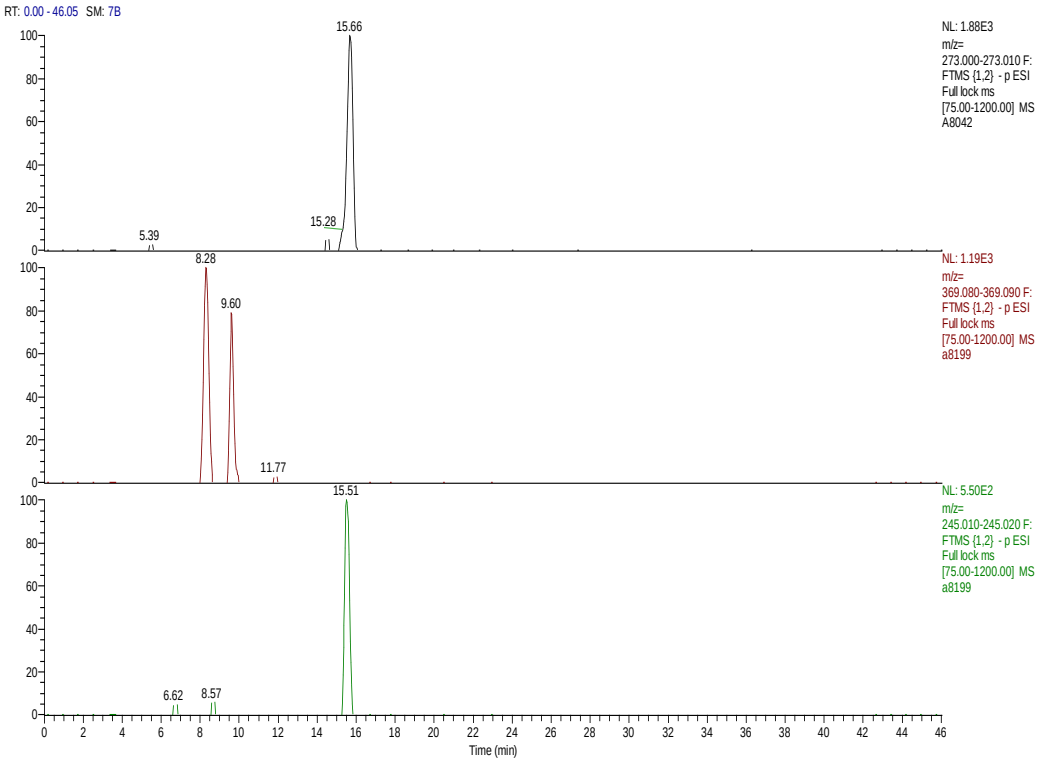

Figure 4.6 Extracted ion traces showing a sulfate two glucuronides, and a demethylated reduced of ferulic acid in human plasma using chromatography on ZICpHILIC.

4.5 Discussion

It is evident from the above data that metabolism of the simple phenolic acid FA in rat hepatocytes is more complex than previously observed. The most novel observation is the formation of a GSH addition product with FA and this has a wider implication in that all phenylpropionic acids could behave in this manner with varying degrees of reactivity. Of course it is difficult to extrapolate from an in vitro model to the situation in vivo. In the current case there was no evidence that the reaction led to FA being toxic and this is presumably because the rate of reaction is slow and also the polar metabolites of FA such as the glucuronide and sulfate conjugates partition out of the cells and thus do not undergo reaction with GSH

which is primarily within the cells. It would be of interest to evaluate the toxicity of similar acids which are not as readily sulfated as FA such as cinnamic acid where the aromatic ring requires hydroxylation prior to sulfation.

4.6 Conclusion

Hepatocyte incubations in combination with high resolution mass spectrometry and data extraction provide a powerful combination for extending the knowledge of xenobiotic metabolites. The approach also has the potential for building up a retention time/mass spectral library which would be useful for the characterisation of urinary metabolites of xenobiotics present in the diet in order to get a better understanding of the food metabolome. Of course, the metabolites from rat hepatocytes may differ from those in humans as a model they are more accessible than human hepatocytes and thus may provide a useful adjunct to studies in humans and possible means of generating small quantities of metabolite standards.

CHAPTER 5

Metabolism of Hesperidin in Rat Hepatocytes

5. Metabolism of Hesperidin in Rat Hepatocytes

5.1 Abstract

Hesperidin is a naturally occurring flavanone glycoside predominant in citrus fruits (Yang *et al*., 2002). Dietary hesperidin is hydrolyzed by gut microflora to give hesperetin, the aglycone form of hesperidin (Haidari *et al*., 2009). In recent years, there have been an increasing number of reports on the physiological functions or pharmacological effects of hesperidin including antioxidant, anti-cancer, antiallergenic, anti-inflammatory, neuroprotective, antihypotensive, vasodilator properties and antimicrobial activities (Cho, 2006, Lee *et al*., 2010, Garg *et al*., 2001). In the present study, we observed seven metabolites of hesperidin formed *in vitro* by incubating hesperidin with rat hepatocytes. The most abundant metabolite was the sulfate of hesperidin followed by hesperidin glucuronide and glutathione conjugation as phase II metabolites. Moreover, a range of novel hesperidin metabolites have been formed such as *O*-demethylation, desaturation, aromatic hydroxylation and hydroxylation and methylation of hesperidin. These were detected and reported for the first time; also this is the first study of hesperidin metabolism *in vitro* using rat hepatocytes. The hepatocytes completely lacked the ability to convert hesperidin to its aglycone, heperitin can only be absorbed if the gut microflora convert hesperidin to the aglycone.

5.2 Introduction

Hesperidin **(Figure 5.1)** (4'-methoxy-7-O-rutinosyl-3',5-dihydroxyflavanone), is a naturally occurring flavanone glycoside predominant in citrus fruits (Yang *et al*., 2002). Dietary hesperidin is hydrolysed by gut microflora to give hesperetin (4'-methoxy-3',5,7 trihydroxyflavanone), the aglycon form of hesperidin (Haidari *et al*., 2009).

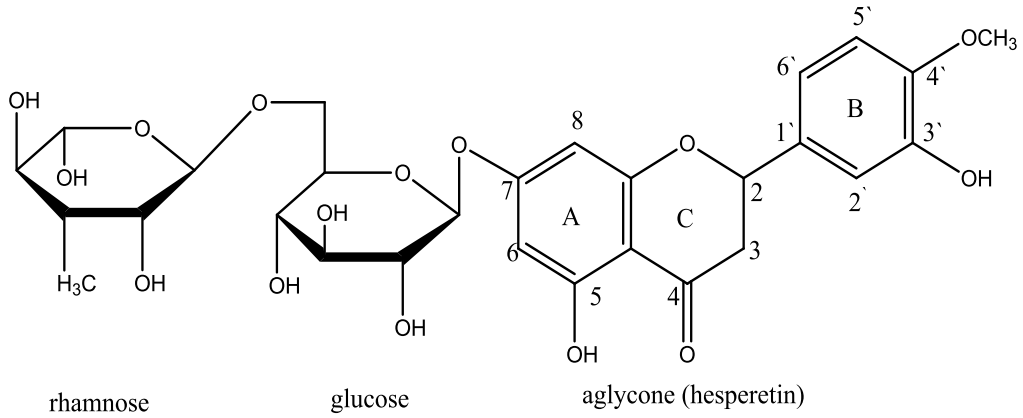

Figure 5.1 Chemical structure of hesperidin.

Hesperidin can be extracted in large amounts from the rinds of some citrus species [e.g., *Citrus aurantium* L. (bitter orange), *Citrus sinensis* L. (sweet orange), and *Citrus unshiu* Marcov. (*Satsuma mandarin*)] (Garg *et al*., 2001).

In recent years, there has been an increasing number of reports on the physiological functions or pharmacological effects of hesperidin including antioxidant, anti-cancer, antiallergenic, anti-inflammatory, neuroprotective, antihypotensive, vasodilator properties and antimicrobial activities (Cho, 2006, Lee *et al*., 2010, Garg *et al*., 2001). The potential anticancer properties of hesperidin have been confirmed *in vivo* in rats by administering citric juice which contains high levels of hesperidin and

these studies have shown that colon and lung cancers were significantly reduced. Other studies showed that the level of triglycerides and cholesterol were reduced after the consumption of orange juice in a hamster model by inhibiting hepatic production of cholesterol-containing lipoproteins and thus potentially reducing the occurrence of cardiovascular diseases (Khono *et al*., 2002, Wilmsen *et al*., 2005, Miguel *et al*., 2009).

The antioxidant property of flavonoids is dependent on the positions of the hydroxyl groups in their structures. Usually flavonoids with a hydroxyl group at position C-4' possess antioxidant properties. Hence hesperidin which has no hydroxyl at this position is not expected to show antioxidant properties (Cao *et al*., 1997, Cos *et al*., 1998, Van Acker *et al*., 1996). However, Wilmsen *et al*. reported that the methoxy group at position C-4' of hesperidin activates the hydroxyl group at C-3` thus making hesperidin a more active scavenger of the superoxide radical (van Acker *et al*., 1998, Wilmsen *et al*., 2005).

Generally gastrointestinal tract cells play certain roles in the biotransformation of polyphenols before entering into systemic circulation (Tripoli *et al*., 2007). Nielsen *et.al*. 2006 reported the *in vitro* biotransformation of flavonoids by rat liver microsomes and in this study demonstrated that the C-4' methoxy group of hesperetin was demethylated and, consequently, converted to eriodictyol. They also reported that hesperidin was absorbed from the small intestine instead of the colon and enzymatically converted to hesperetin-7-glucoside (Nielsen *et al*., 2006). In another study, it was demonstrated that hesperidin was transformed to hesperetin after the removal of disaccharide by intestinal bacteria and that hesperetin was directly

glucuronidated in the intestinal epithelium and, consequently transformed to hesperetin glucuronides by enzymes (Garg *et al*., 2001), in the liver.

Hesperetin glucuronides have been deglucuronidated, demethylated, remethylated and reglucuronidated by the hepatic enzymes and transformed to hesperetin glucuronides. Moreover, another study suggests that the concentration of the hesperetin sulfoglucuronides was much lower than that of hesperidin glucuronides (Matsumoto *et al*., 2004). On the other hand several reports have noted that hesperidin can be conjugated by glucuronidation and sulfoglucuronidation in animals and humans after being orally administered (Matsumoto *et al*., 2004). Hesperidin has been found as hesperidin glucuronide in rat plasma and activated by UDP-glucuronosyltansferases enzyme (UGTs) (Spencer *et al.*, 2004). Other authors have determined 87% of glucuronidation and 13% sulfoglucuronidation of hesperetin in human plasma after consuming orange juice (Manach *et al*., 2003).

In the present study, we have monitored seven metabolites of hesperidin and identified *in vitro* by incubating pure hesperidin with rat hepatocytes. The most abundant metabolite was the sulfate of hesperidin followed by hesperidin glucuronide and glutathione conjugation as a phase II conjugate. The existence of GSH conjugation, aromatic hydroxylation, *O*-demethylation, desaturation, hydroxylation and methylation of hesperidin has not been reported previously *in vitro* using rat hepatocytes.

5.3 Experimental

5.3.1 Chemicals and reagents

Hesperidin (99%) and dimethylsulphoxide (DMSO) were purchased from Sigma Aldrich, Dorset UK. HPLC grade acetonitrile and Analar formic acid were obtained from Fisher Scientific (Loughborough, UK). Water was obtained from a Milli-Q water-purification system (Millipore, Watford UK).

5.3.2 Preparation of hepatocytes

Hepatocytes were isolated from adult male Sprague-Dawley (SD) rat (≈ 200 g of body weight) livers by collagenase digestion a two - step perfusion process as described by Moldeus *et al.* (1978) Subsequently, the hepatocyte suspension was washed with 50 mL Krebs Henseleit buffer, pH 7.4, containing 12.5 mM HEPES (Liu *et al*., 2002). In order to determine cell viability a Trypan blue exclusion test was carried out, and hepatocyte preparations used were ≥ 78.4% viable. More described details in (General Methodology Chapter 2 pages (54:57).

5.3.3 Incubation with hepatocytes

A 100 mM stock solution of hesperidin was prepared by dissolving 61.06 mg in 1 mL of DMSO. The hesperidin solution was incubated at 100 µM with 2 x 10^6 isolated hepatocytes per mL at 37°C under an atmosphere of 95% O_2, 5% CO_2 in rotating 50 mL round bottomed flasks. Blank incubation was carried out without cells. Control incubation was concomitantly run with hepatocytes but without drug. Four aliquots (0.5 mL) were taken from the incubation solutions at 0, 30 and 120 min and the reaction terminated by addition of 1 mL of acetonitrile. The samples were stored at -80°C. Prior to analysis samples were thawed at room temperature,

sonicated and centrifuged at 5000 rpm for five min to remove protein and collect the supernatants for analysis of conjugates. More details described in (General Methodology Chapter 2 pages (58:60).

5.3.4 LC-MS analysis

These details have been reported in (General Methodology Chapter 2 pages: (61, 62).

5.4 Results and discussion

Table 5-1 shows the hepatocyte viability indicating that there was no significant loss of viability over 120 min of incubation either in the controls or in the presence of hesperidin.

Table 5-1 Viability of suspension hepatocytes during two hours of treatment period with 100 µM hesperidin

Incubation time (min)	Viability of control	Viability with Hesperidin
0	84%	84%
30	86%	74%
120	70%	80%

Hesperidin was metabolised very rapidly by hepatocytes and on a peak area % basis only 93.2% of hesperidin remained after few min and only 36.1% remained at 120 min of incubation. Using Sieve software to compare blank incubations with incubations containing hesperidin allowed the putative identification of seven metabolites of hesperidin **(Table 5-2, Figure 5.1)**.

Table 5-2 illustrates elemental compositions and retention times of the detected hesperidin and its metabolite peaks that elute at different position and retentions times through C18-AR coulmn in LC-MS. The abundances of the metabolites were compared regarding the percentage of the peak areas at different intervals time points 0, 30 and 120 min of incubation with $[M-H]^-$ ions of m/z 609.18, 785,21, 689.14, 595.17, 607.17, 914.25, 625.18 and 639.19 which correspond to hesperdin, glucuronidation M1, sulfation M2, *O*-demethylation M3, desaturation M4, glutathione conjugation of hesperidin M5, aromatic hydroxylation M6 and hydroxylation and methylation M7 at 30, 120 min of incubation. Within a few minutes of incubation LC-MS detected hesperdin, sulfation M2, *O*-demethylation M3, desaturation M4, aromatic hydroxylation M6 and hydroxylation and methylation M7. The mass error of all metabolites were within ± 1-1.5 ppm when compared to their theoretical masses. The most abundant metabolites after 30 min incubation were sulfation [M2, t_R =15.21 min; m/z = 689.14], glucronidation [M1, t_R = 14.95 min; m/z = 785.21] and GSH conjugation [M5, t_R =14.09 min; m/z = 914.25]. The levels of these metaboltes increased further between 30 and 120 min with a corresponding decease in the level of unmetabolised hesperidin. On the other hand, the abundance of *O*-demethylation [M3, t_R = 15.88 min; m/z = 595.17], desaturation [M4, t_R = 17.15 min; m/z = 607.17], aromatic hydroxylation [M6 , t_R = 17.17 min; m/z = 625.18] and hydroxylation and methylation [M7, t_R = 20.70 min; m/z = 639.19] are likely to decline steadily after zero min of incubation.

The significant variations (p values < 0.05) by one-way analysis of variance (ANOVA) between the metabolites peak areas were clearly stated in **Figure 5.3** in prism statistical software ver 5.

The proposed scheme of hesperidin biotransformation in **Figure 5.2** indicates that hesperidin can be directly metabolised to phase II metabolites via sulfate, glucuronic acid -OH and glutathione conjugations. In contrast, hesperidin can be metabolised to other phase II metabolism such as hydroxylation and methylation after aromatic hydroxylation as phases I . Hesperidin to lose $-H_2$ at C ring as phase I (desaturation).

Table 5-3 and **Figure 5.4** show the proposed MS^2 of major fragmentation ions obtained for hesperidin metabolites and this added further support of the assigned identities. **Appendix A** illustrates the MS^2 spectra of hesperidin metabolites fragmentation.

Table 5-2 Metabolites of hesperidin putatively identified according to accurate mass in incubations with rat hepatocytes

Metabolites	$[M-H]^-$	Elemental Composition	t_R min	Area % 0 min	RSD n=4	Area % 30 min	RSD n=4	Area % 120 min	RSD n=4	RDB
Hesperidin	609.18	$C_{28}H_{33}O_{15}$	17.00	93.23	0.717	69.62	2.51	36.1	0	12.5
Glucuronidation of Hesperidin M1	785.21	$C_{34}H_{41}O_{21}$	14.95	0	0	3.07	7.64	8.01	5.57	14.5
Sulfation of Hesperidin M2	689.14	$C_{28}H_{33}O_{18}S$	15.21	0.738	3.169	22.04	1.79	50.71	0.707	12.5
***O*-Demethylation of Hesperidin** M3	595.17	$C_{27}H_{31}O_{15}$	15.88	0.0230	8.080	0.0154	1.07	0.010	4.42	12.5
Desaturation of Hesperidin M4	607.17	$C_{28}H_{31}O_{15}$	17.15	0.7214	3.418	0.2644	1.59	0.0366	0.46	13.5
GSH conjugation of Hesperidin M5	914.25	$C_{38}H_{48}O_{21}N_3S$	14.09	0	0	0.0034	14.0	0.028	11.26	16.5
Aromatic hydroxylation of Hesperidin M6	625.18	$C_{28}H_{33}O_{16}$	17.17	2.366	0.2167	1.52	1.96	0.614	2.989	12.5
Hydroxylation and Methylation of Hesperidin M7	639.19	$C_{29}H_{35}O_{16}$	20.70	2.906	1.096	2.138	6.20	1.072	6.06	12.5

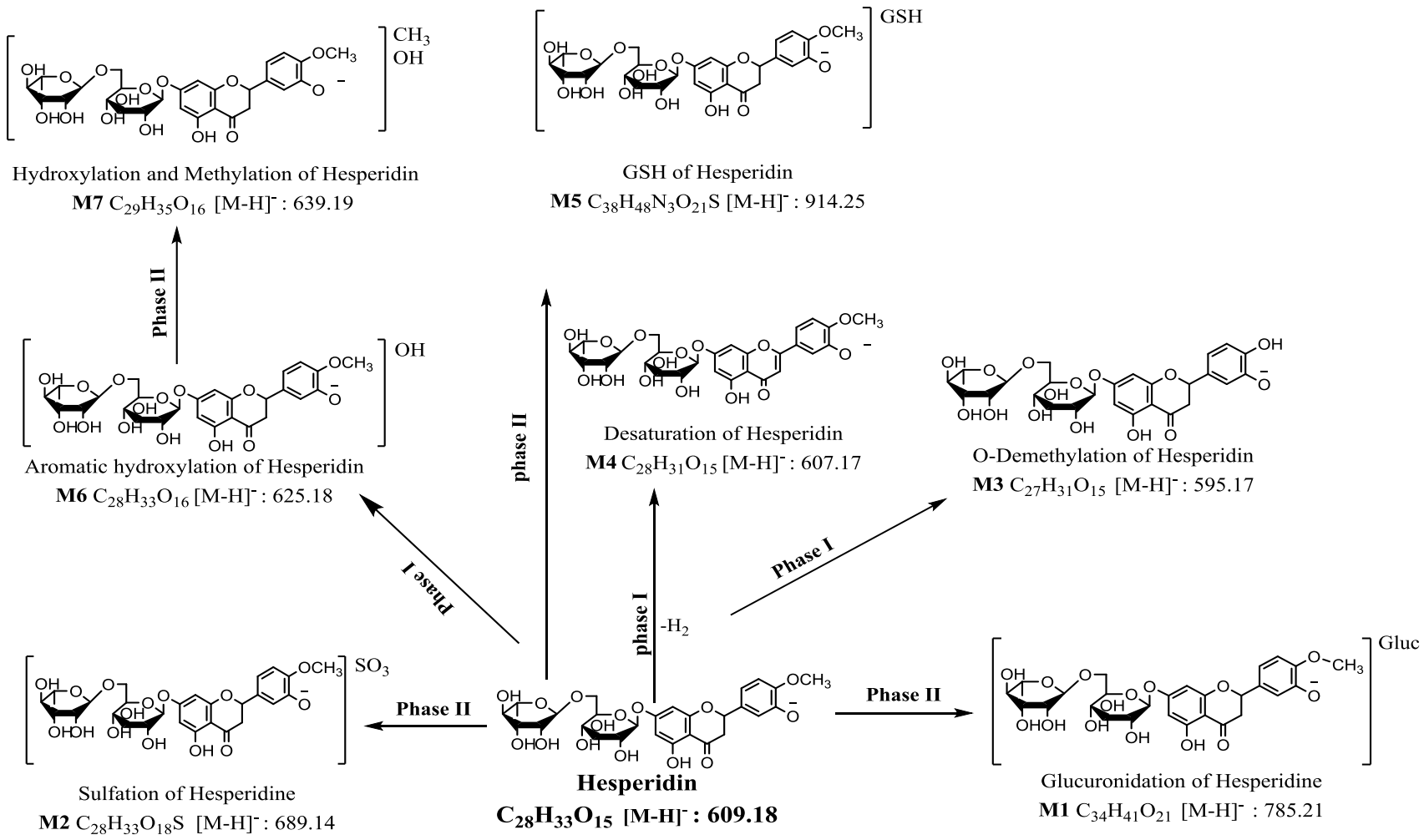

Figure 5.2 Proposed structures of the metabolites of hesperidin formed in incubations with rat hepatocytes.

Gluc = glucuronic acid -OH, GSH = Glutathione.

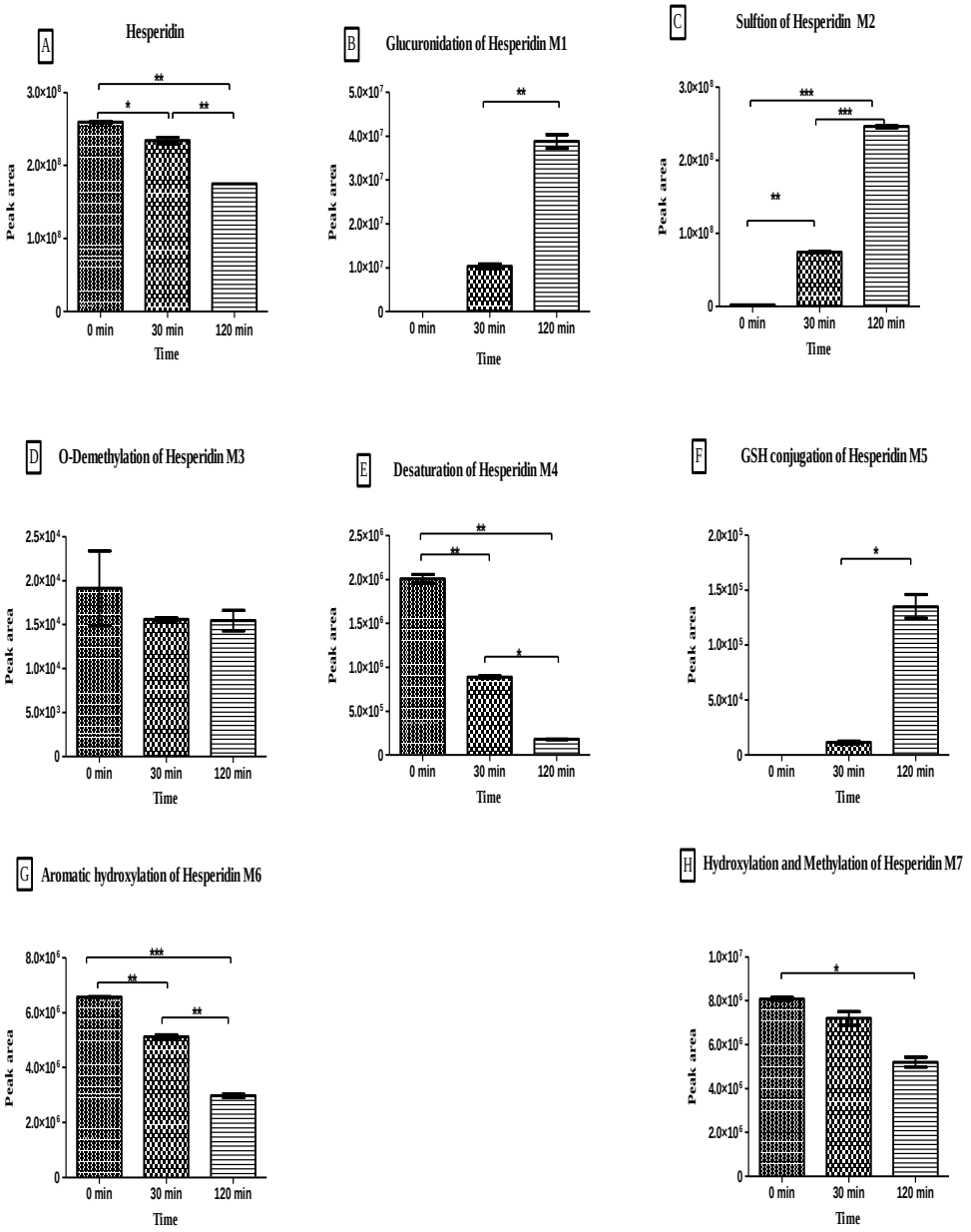

Figure 5.3 The graphs above are one-way ANOVA output comparing peak area of hesperidin and its metabolites at 0, 30 and 120 minutes.

*Significant P- value < 0.05, ** Significant P- value < 0.01and *** Significant P- value < 0.001.

Table 5-3 MS^2 (35eV) data for major metabolites formed from hesperidin in hepatocyte incubations

Metabolite	$[M-H]^-$	t_R min	Fragment ions
Hesperidin	609.18	17.00	301.07 (- Rutinose, 100%)
Glucuronidation of Hesperidin M1	785.21	14.95	477.1 (- Rutinose, 29.01%), 609.1 (-Gluc, 78.57%), 301.06 (- Gluc, Routinose, 100%)
Sulfation of Hesperidin M2	689.14	15.21	301.07 (- Rutinose, - SO_3, 100%), 381.02 (- Rutionse, 85.76%), 609.18 (-SO_3, 39.78%)
***O*-Demethylation of Hesperidin** M3	595.17	15.88	Nil
Desaturation of Hesperidin M4	607.17	17.15	299.06 (- Rutinose, 100%)
GSH conjugation of Hesperidin M5	914.25	14.09	Nil
Aromatic hydroxylation of Hesperidin M6	625.18	17.17	579.22 (- $COOH_2$, 100%)
Hydroxylation and Methylation of Hesperidin M7	639.19	20.70	593.19 (- COOH, 100%)

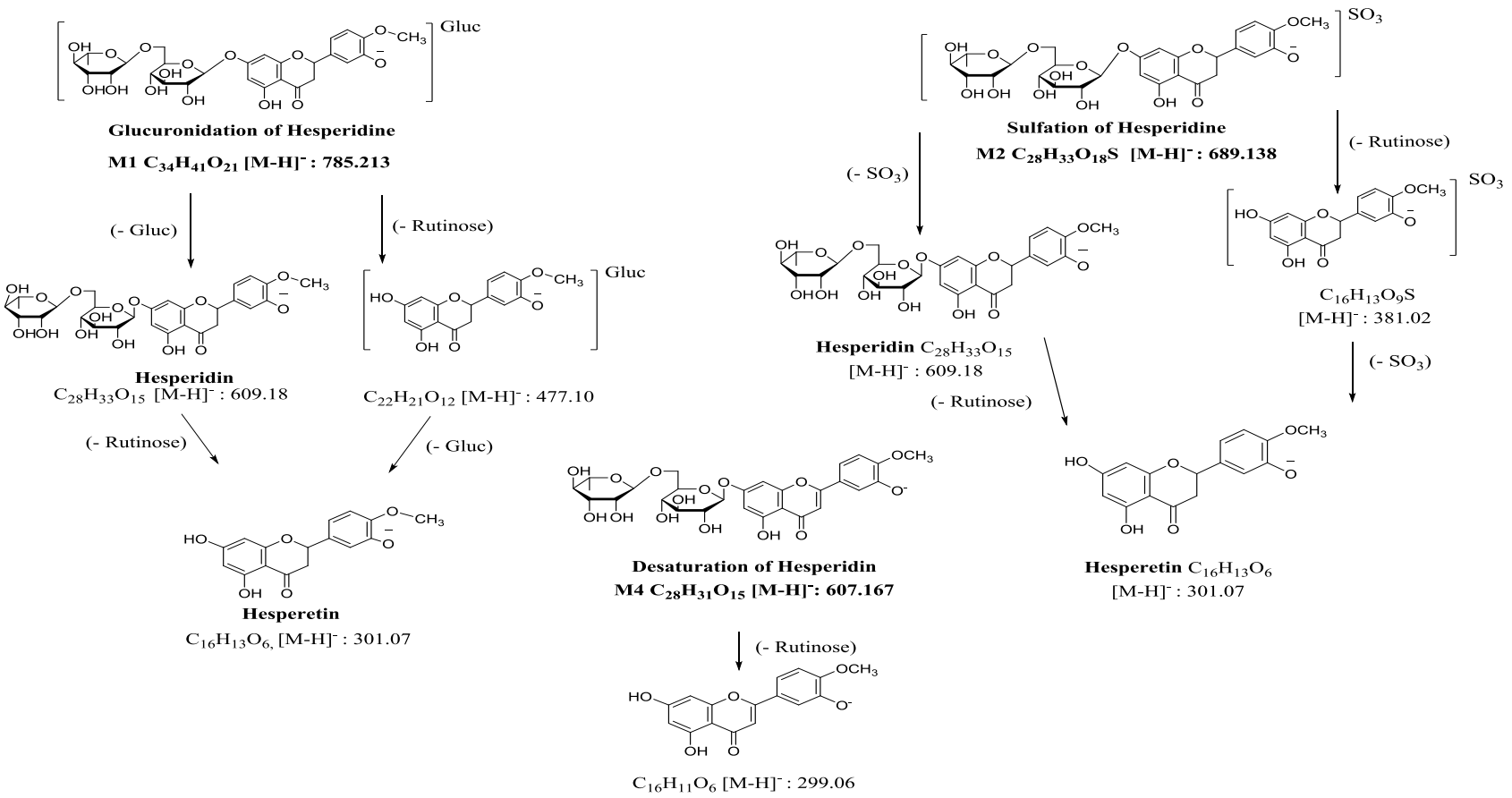

Figure 5.4 Proposed structures derived from the fragmentation of the hesperidin and its metabolites formed in incubations with rat hepatocytes.

Gluc = glucuronic acid -OH, Rutinose = (Glucose and Rhamnose).

5.5 Conclusion

The metabolism of hesperidin is to a large extent predictable. The major metabolites are due to sulfation and glucuronidation with the majority of the hesperidin being converted into a sulfate. It might seem unnecessary for phase II metabolism of hesperidin to be required since it is already quite a water-soluble compound but phase II metabolism dominates over phase I metabolism and there is little phase I metabolism. The formation of small amounts of a glutathione adduct is again of interest since this seems to occur consistently with these dietary phenolic compounds despite their reported health benefits although the amount of GSH adduct formed is extremely small based on peak area.

CHAPTER 6

Metabolism of *p*-coumaric acid by Isolated Rat Hepatocytes

6. Metabolism of *p*-Coumaric acid by Isolated Rat Hepatocytes

6.1 Abstract

In the present study, we have monitored seven metabolites of *p*-coumaric acid, and identified their metabolites *in vitro* by incubating *p*-coumaric acid with rat hepatocytes. The most abundant metabolite was the sulfate of *p*-CA followed by *p*-CA glucuronide and glutathione conjugation. Novel *p*-CA metabolites were also detected involving aromatic hydroxylation, sulfation and glutathione conjugation. The metabolites of *p*-coumaric acid found in this study are summarized **in Figure 6.2, 6.3** and **Table 6-3**.

6.2 Introduction

Hydroxycinnamates (hydroxycinnamic acid derivatives) (HCAs) are a subclass of non-flavonoid compounds and they have a chemical backbone composed of a phenylpropanoid C6-C3 structure. One member of the subgroup of these phenolic compounds is *p*-coumaric acid *(p*-CA).

HCAs are found in plants such as tea leaves, coffee and in fruits and vegetables (Mateos *et al*., 2006, Teixeira *et al*., 2013). Infrequently, they are found in free states in processed foods or esterified with organic acids, sugars, and lipids (Mateos *et al*., 2006, Sato, 1966). In addition HCAs have been considered as an important intermediate in the biosynthesis of phenolic compounds such as cinnamic acid and caffeic acid after catalyses of hydroxylation at 4- position of the aromatic ring creating the *p*-coumaric acid by the phenolase enzyme (Sato, 1966, Halliwell, 1975). Moreover, HCAs are found in several conjugated forms, including amides

(conjugated with mono- or polyamines, amino acids, or peptides), esters, mainly esters of hydroxyl acids, such as tartaric acid and sugar derivatives, and glycosides. Extensively, esterification of cinnamates occurs in higher plants but amides of cinnamic acids seem to be rare (Teixeira *et al*., 2013). Neish (1961) reported that *p*-coumaric acid is formed by L-tyrosine ammonia lyase enzyme in plants in the presence of O_2 and a reducing agent such as ascorbate, nicotinamide adenine dinucleotide (NADH) or nicotinamide adenine dinucleotide phosphate-oxidase (NADPH). Walker (1964) found that apple polyphenoloxidase converts *p*-coumaric acid to caffeic acid (3, 4-dihydroxycinnamic acid) (Sato, 1966, Halliwell, 1975).

In recent years, there are increasing numbers of reports on the pharmacological effects of hydroxycinnamic acid as *p*-coumaric acid including antioxidant, anti-inflammatory, and anti-cancer properties. The anti-cancer properties include a reduction in the risk of stomach cancer and antileukemic activities (Halliwell and Ahluwalia, 1976, Zang *et al*., 2000, Abdel-Wahab *et al*., 2003, Yoon *et al*., 2013, Fernandez *et al*., 1998). Due to its antioxidant activity, *p*-CA could be used to reduce the cholesterol levels in plasma (Zang *et al*., 2000). Moreover, Chesson *et al*. (1982) and others reported that *p*-CA has antimicrobial activity by inhibiting the growing of various paunch bacteria. On the other hand, Leifertova *et al*. (1975) found no evidence for antimicrobial activity with hydroxycinnamic acid (Herald and Davidson, 1983). The physiological activity of *p*-CA depends upon the absorption and subsequent interaction with target tissues and *p*-CA absorbed in gastrointestinal tract by monocarboxlic acid transporter. However, the absorption of *p*-CA could be blocked by benzoic acids (Konishi *et al*., 2003).

A number of HCAs metabolites have been studied *in vivo* in rats, rabbits, and in humans and with isolated rat and rabbit livers *in vitro.* The metabolic pathways include the cleavage of ester bonds, *O*-methylation via catechol O-methyl transferase, dehydroxlyation, reduction of the residual double bond, β-oxidation, decarboxlation, and glycination (Rechner, 2003).

The metabolites of *p*-CA such as glucuronidation and glycination have been considered in *in vivo* studies and summarized in **Figure 6.1** and these bio-transformations occur in the liver or epithelium of small intestine of animals. Moreover, *p*-CA could be converted to 3-(4-hydroxphenyl)-propionic acid due to reduction of its double bond by colonic microorganisms and then converted to 4-hydroxybenzoic acid after β-oxidation in liver by adenosine triphosphate coenzyme (ATP) in mitochondria. Unconjugated *p*- CA and its pathways have been detected and identified in urine of rats after consuming *p*-CA (Rechner, 2003).

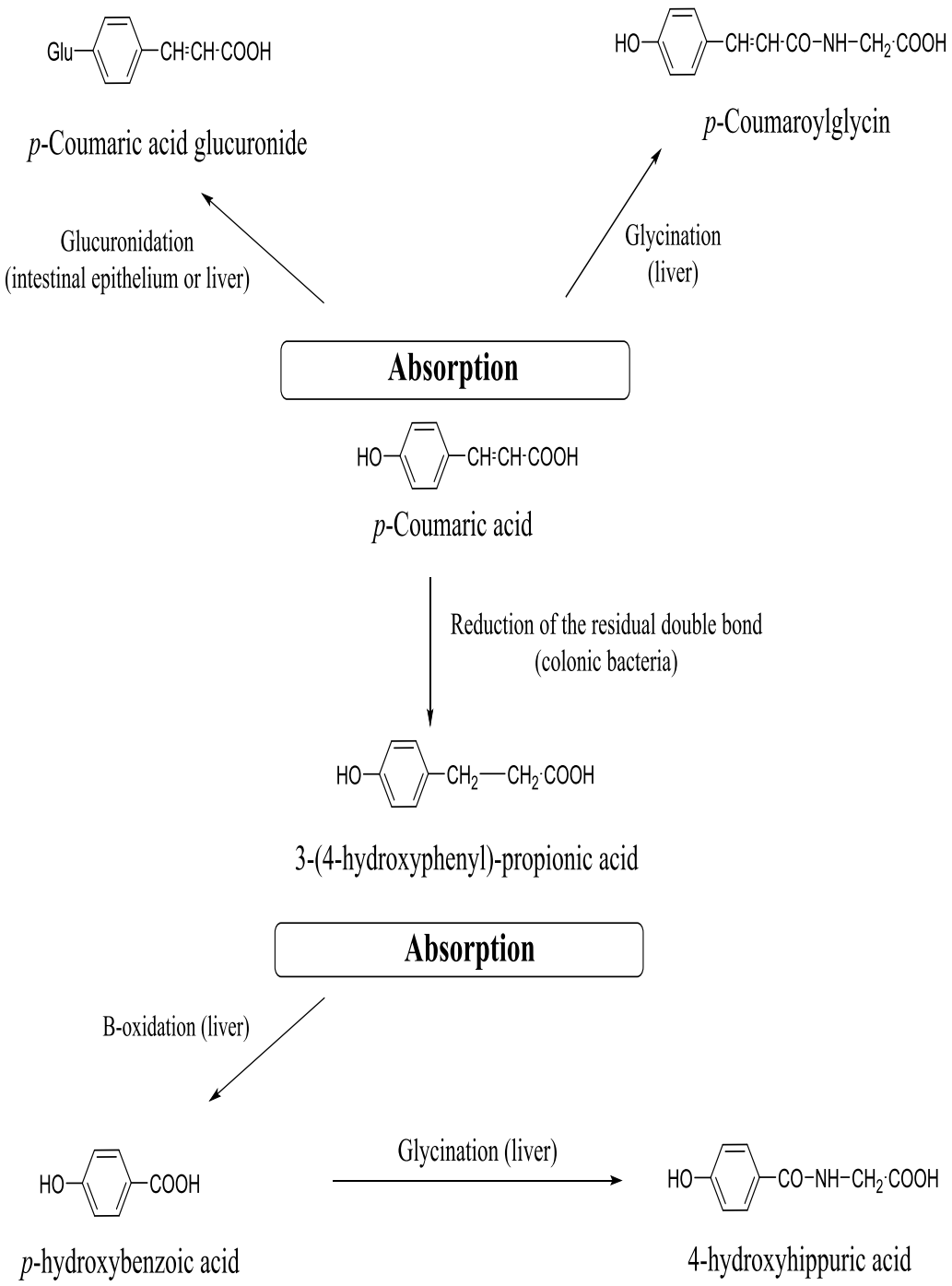

Figure 6.1 The metabolic pathways of *p*-coumaric acid.

6.3 Experimental

6.3.1 Chemicals and reagents

P- coumaric acid and dimethylsulphoxide (DMSO) were purchased from Sigma Aldrich, Dorset UK. HPLC grade acetonitrile and Analar formic acid were obtained from Fisher Scientific (Loughborough, UK). Water was obtained from a Milli-Q water-purification system (Millipore, Watford UK).

6.3.2 Preparation of hepatocytes

Hepatocytes were isolated from adult male Sprague-Dawley (SD) rat (≈ 200 g of body weight) livers by collagenase digestion a two - step perfusion process as described by (Moldeus *et al.* 1978). Subsequently, the hepatocyte suspension was washed with 50 mL Krebs Henseleit buffer, pH 7.4, containing 12.5 mM HEPES (Liu *et al*., 2002). In order to determine cell viability a Trypan blue exclusion test was carried out, and hepatocyte preparations used were ≥ 80.1% viable with *p*-coumaric. More details described in General Methodology Chapter 2 pages (54:57).

6.3.3 Incubation with hepatocytes

A stock solution (100 mM) of *p*-coumaric acid was prepared by dissolving 16.4 mg of *p*-coumaric acid in 1 mL of DMSO. The *p*-CA solution was incubated at 100 µM with 2 x 10^6 isolated hepatocytes per mL at 37°C under an atmosphere of 95% O_2, 5% CO_2 in rotating 50 mL round bottomed flasks. Blank incubation was carried out without cells. A control incubation was concomitantly run with hepatocytes but without drug. Four aliquots (0.5 mL) were taken from the incubation solutions at 0, 30 and 120 min and the reaction terminated by addition of 1 mL of acetonitrile. The

samples were stored at -80°C. Prior to analysis samples were thawed at room temperature, sonicated and centrifuged at 5000 rpm for five min to remove protein and collect the supernatants for analysis of conjugates. More details described in General Methodology Chapter 2 pages (58:60).

6.3.4 LC-MS analysis

These details have been reported in General Methodology Chapter 2 pages (61, 62).

6.4 Results and discussion

Table 6-1 show the hepatocyte viability indicating that there was no significant loss of viability over 120 min of incubation either in the controls or in the presence of *p*-coumaric acid.

Table 6-1 Viability of suspension hepatocytes during two hours of treatment period with 100 µM *p*-coumaric acid

Incubation time (min)	Viability of control	Viability with *p*-CA
0	70%	78%
30	68%	70%
120	68%	74%

P-coumaric was metabolised very rapidly by hepatocytes and on a peak area % basis only 98.1% of *p*-CA after few min and only 2.89% of *p*-CA remained at 120 min of incubation. Using Sieve software to compare blank incubations with incubations containing *p*-coumaric acid the putative identification of seven metabolites of *p*-coumaric acid **(Table 6-2, Figure 6.2)**.

Table 6-2 illustrates the elemental composition and retention times of the detected *p*-coumaric acid and its metabolite peaks eluting at different retentions times through C18-AR coulmn in LC-MS. The abundance of the metabolites were compared regarding the percentage of the peak areas at different intervals time points 0, 30 and 120 min of incubation with $[M-H]^-$ ions of m/z 136.04, 339,07, 339.07, 242.99, 220.06, 470.10, 470.10 and 179.03 which correspond to *p*-coumaric acid, glucuronidation M1, glucuronidation M2, sulfation M3, glycination M4, glutathione M5, glutathione conjugation M6 and aromatic hydroxylation at 30, 120 min of incubation. Following a few mintues of incubation, *p*-coumaric acid, sulfation M3 and aromatic hydroxylation M7 were detected by LC-MS. The mass error of all metabolites were within ± 1-1.5 ppm when compared to their therotical masses. The most abundant metabolites after 30 min incubation were sulfation [M3, t_R = 12.45 min; m/z = 242.99], glucronidation [M1, M2, t_R = 13.1, 13.55 min; m/z^- = 339.07], glycination [M4, t_R = 13.58 min; m/z = 220.06] and glutathione conjugation [M5, M6, t_R = 9.89, 10.35 min; m/z = 470.10].The amounts of these metaboltes increased further between 30 and 120 min with a corresponding decease in the level of unmetabolised *p*-CA. On the other hand, the abundance of aromatic hydroxylation [M7 , t_R = 14.23 min; m/z = 179.03] is likely to decline steadily after 30 min of incubation. The significant variations (P value < 0.05) by one-way ANOVA between the metabolites peak areas were clearly stated in **Figure 6.3** in prism statistical software ver 5.

The proposed scheme of *p*-CA biotransformation in **Figure 6.2** indicates that *p*-CA can be directly metabolised to phase II metabolites via conjugation to sulfate, glucuronic acid -OH, glycine -OH (+ m/z 57.02) and GSH (+ m/z 307.08).

Moreover, *p*-CA can be hydroxylated at aromatic ring as phase I metabolism. The most dominant metabolite, as might be expected from the literature, was the glucuronidation and glucination *in vivo* studies which can be accrued in the liver or epithelium of small intestine of animals (Rechner, 2003). In contrast, we detected the glutathione and sulfation from *p*-CA by hepatocytes and surprisingly these do not seem to have been reported before. In addition, *p*-CA can be converted to caffeic acid after aromatic hydroxylation. Of most interest from a toxicological perspective is the occurrence of metabolites M5 and M6 which are glutathione (GSH) conjugates of *p*-coumaric acid. These conjugates are formed by nucleophilic addition of the GSH across the double bond in the side chain of *p*-CA. Similar to ferulic acid (Chapter 4) this observation suggests that the double bond in the side chain of *p*-CA is reactive and damaging reactions with thiol groups within cellular structures could occur. The GSH conjugate fragments to give an ion at m/z 306 for the GSH portion of the molecule resulting from the loss of *p*-CA. **Table 6-3** and **Figure 6.4** show the proposed MS^2 which were obtained for the *p*-CA metabolites fragmentation and this added further support of the assigned identities. The MS^2 spectra of metabolites fragmentation ions are shown in **Appendix B**.

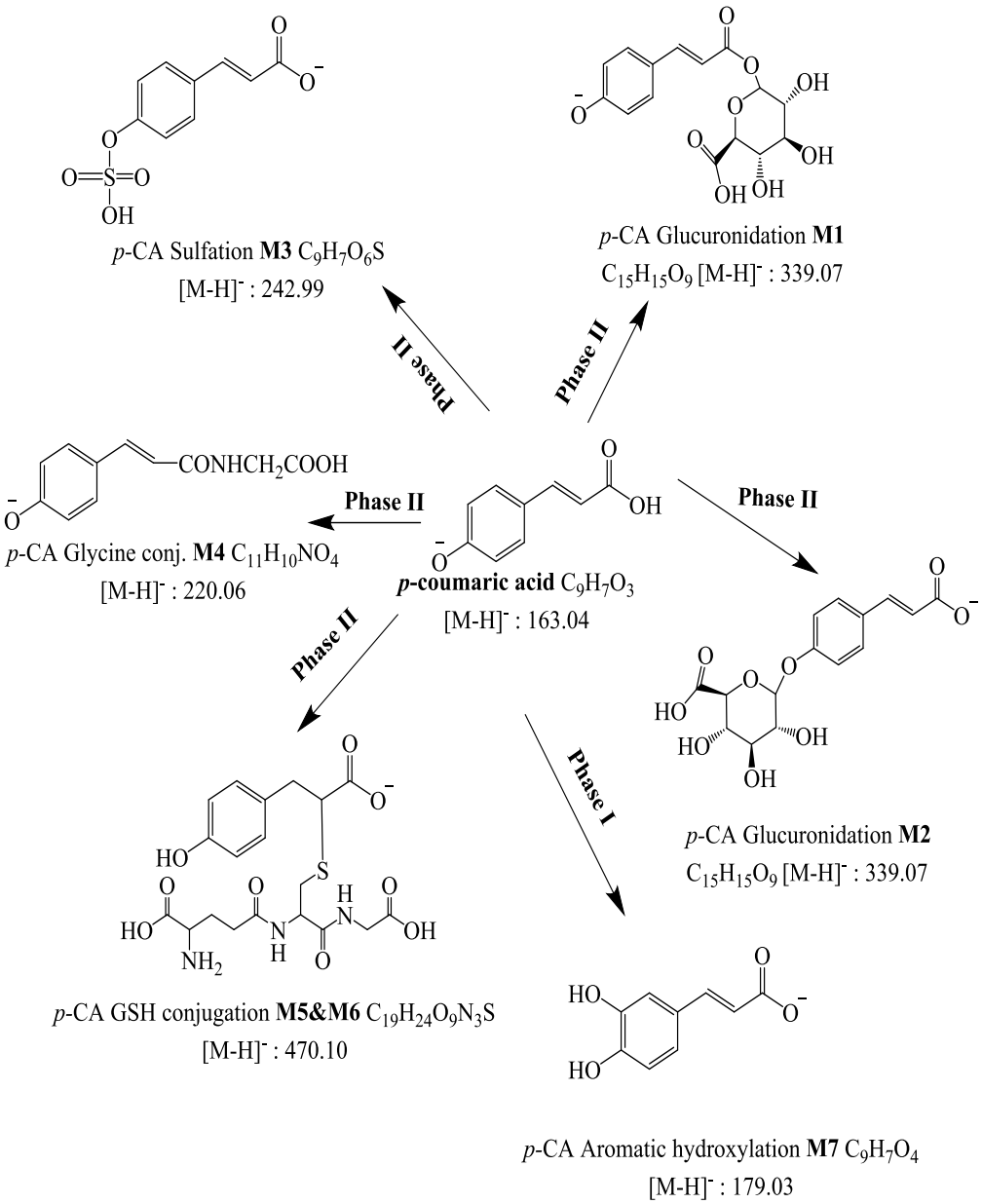

Figure 6.2 Proposed structures of the metabolites of *p*- coumaric acid formed in incubations with rat hepatocytes.

Table 6-2 Metabolites of *p*-Coumaric acid putatively identified according to accurate mass in incubations with rat hepatocytes

Metabolite	**$[M-H]^-$**	**Elemental Composition**	**t_R min.**	**Area % 0 min**	**RSD n=4**	**Area % 30 min**	**RSD n=4**	**Area % 120 min**	**RSD n=4**	**RDB**
***p*-coumaric acid (*p*-CA)**	163.04	$C_9H_7O_3$	16.85	98.1	2.5	58.79	9.48	2.89	2.60	6.5
***p*-CA Glucuronidation** M1	339.07	$C_{15}H_{15}O_9$	13.1	0	0	0.064	3.96	0.133	2.18	8.5
***p*-CA Glucuronidation** M2	339.07	$C_{15}H_{15}O_9$	13.55	0	0	0.016	7.53	0.051	5.76	8.5
***P*-CA Sulfation** M3	242.99	$C_9H_7O_6S$	12.45	1.84	3.79	41.01	13.00	96.70	2.37	6.5
***p*-CA Glycine conj.** M4	220.06	$C_{11}H_{10}O_4N$	13.58	0.007	9.41	0.050	13.56	0.176	2.97	7.5
***p*-CA GSH conjugation** M5	470.10	$C_{19}H_{24}O_9N_3S$	9.89	0	0	0.014	8.00	0.018	6.31	9.5
***p*-CA GSH conjugation** M6	470.10	$C_{19}H_{24}O_9N_3S$	10.35	0	0	0.009	20.83	0.011	7.76	9.5
***p*-CA Aromatic hydroxylation** M7	179.03	$C_9H_7O_4$	14.23	0.013	73.9	0.051	39.80	0.028	8.34	6.5

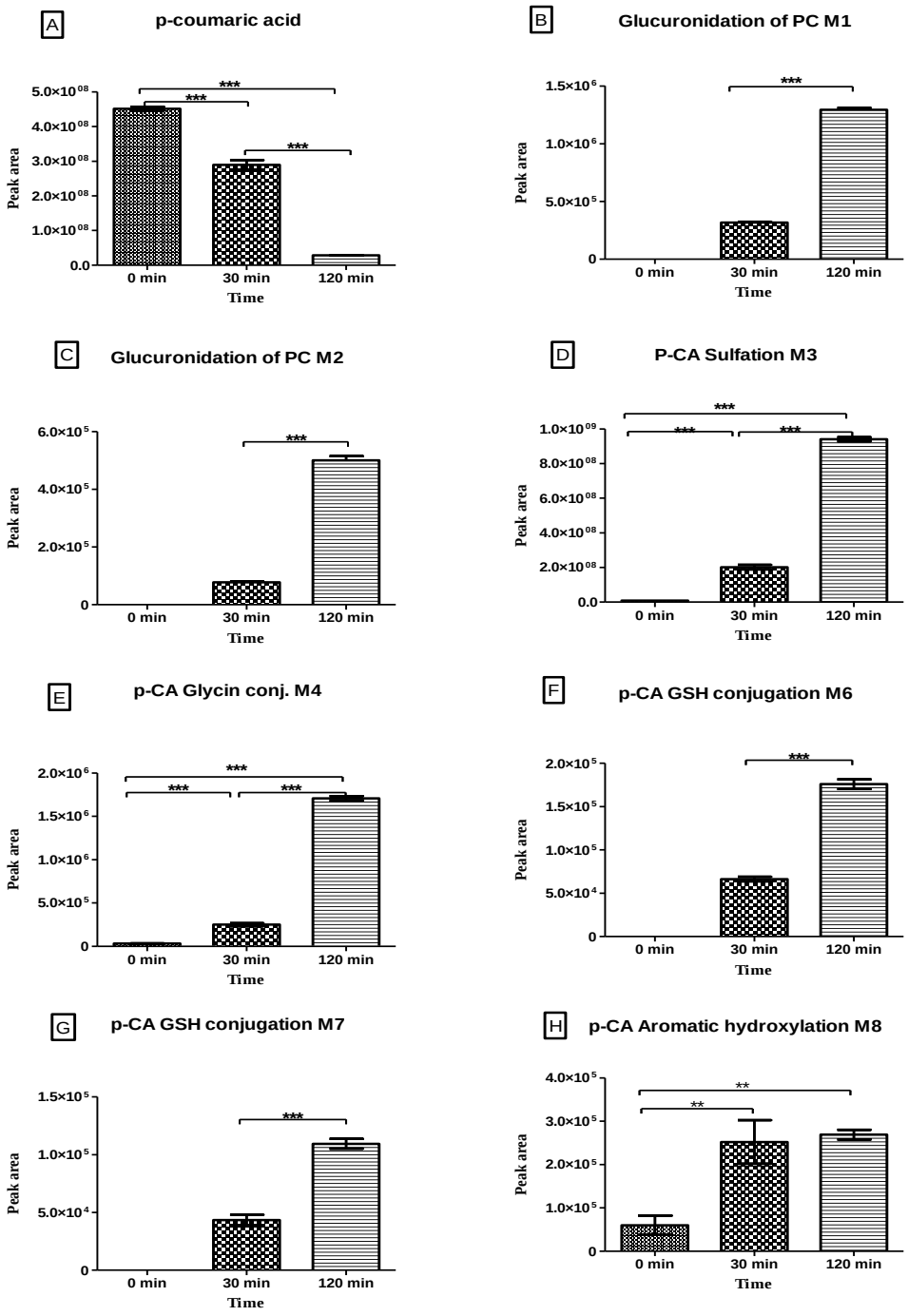

Figure 6.3 The graphs above are one-way ANOVA output comparing peak area of *p*- coumaric acid and its metabolites at 0, 30 and 120 minutes.

** Significant P-value < 0.01and *** Significant P-value < 0.001.

Table 6-3 MS^2 (35eV) data for major metabolites formed from *p*-Coumaric acid in hepatocyte incubations

Metabolite	$[M-H]^-$	t_R min.	Fragment ions
***P*-coumaric acid (*p*-CA)**	163.04	12.71	119.05 (- CO_2, 100%)
***p*-CA Glucuronidation** M1	339.07	13.1	Nil
***p*-CA Glucuronidation** M2	339.07	13.55	Nil
***P*-CA Sulfation** M3	242.99	12.55	163.04 (- SO_2, 100%), 199.01 (- CO_2, 15.73%), 119.05 (- SO_3 & -CO_2, 4.10%)
***p*-CA Glycine conj.** M4	220.06	11.34	119.16 (- CO_2, - Glycine 13.67%), 176.16 (- CO_2, 100%)
***p*-CA GSH conjugation** M5	470.10	9.89	306.1 (- *p*-CA, 100%)
***p*-CA GSH conjugation** M6	470.10	10.35	306.13 (- *p*-CA, 100%)
***p*-CA Aromatic hydroxylation** M7	179.03	14.23	135.08 (- CO_2, 100%)

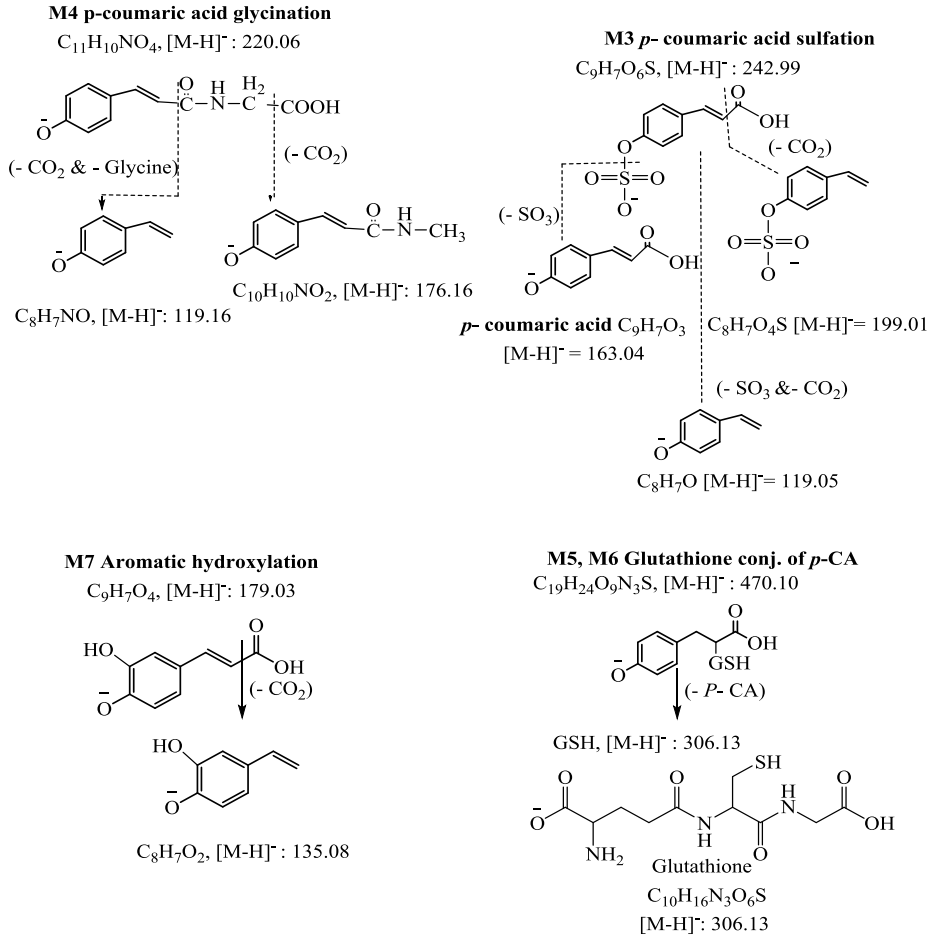

Figure 6.4 Proposed structures of the fragmentation of the metabolites of *p*-coumaric acid formed in incubations with rat hepatocytes.

6.5 Conclusion

The metabolism of *p*-coumaric acid was very rapid and was largely as would have been predicted. Sulfation was the major route of metabolism as was the case for ferulic acid (Chapter 4). Again, there was clear formation of two glutathione adducts and these appear to be due to addition across the double bond as described for ferulic acid in Chapter 4. The formation of glutathione adducts is not a good sign with regards to potential toxicity and the proposed health benefits of cinnamic acid and its derivatives may require further investigation.

CHAPTER 7

The Metabolomics Effects Flavonoids and Cinnamates on the Hepatocyte Metabolome

7. The Metabolomics Effects Flavonoids and Cinnamates on the Hepatocyte Metabolome

7.1 Abstract

Metabolomics profiling of the effects of quercetin, ferulic acid and *p*-coumaric acid with respect to their effects on the metabolome was carried out. This has not been reported before and hepatocytes provide a very clear system in which to observe the impact of a xenobiotic on metabolism. The attention was mainly focused on quercetin in view of its complex and intricate metabolism and degradation. The effects of quercetin on the metabolome of hepatocytes were in line with that which would be expected regarding requirement for co-factors with the levels of co-factors for the formation of sulfate and glucuronide metabolites being depleted. There was a good indication that quercetin has powerful antioxidant effects and in addition it might reduce proteolysis within the hepatocytes. Ferulic acid and *p*-coumaric acid did not produce similar effects and thus the effects of quercetin seem to be quite specific.

7.2 Introduction

7.2.1 Metabolomics definition

The expression of metabolomics is derived from metabolism which originally comes from Greek word *metabolé* which means "change". Dunn (2008) explained that the metabolomics is the identification and quantification of all metabolites which is present in biological systems. Metabolomics has been used in numerous arenas such as agriculture, drug discovery, drug development, drug efficacy, toxicity analysis, biomarker discovery and diagnosis of diseases by studying the expected xenobiotic metabolites (Kell, 2006).

7.2.2 Identification of metabolomics techniques

The most common analytical techniques in the field of metabolomics is liquid chromatography - mass spectrometry (LC-MS). This is capable of detecting low and high molecular weight compounds such as phospholipids, glycosides and sugars using suitable columns and mobile phase composition. Reversed phase chromatography (RPC) was the first liquid separation technique coupled with High Resolution Mass Spectrometry (HRMS) and it can be applied for metabolomics analysis particularly lipophilic substances and xenobiotics in biological systems which are normally eluted based on their lipophilicity. However, phospholipids are strongly retained in RPC columns due to presence of ion suppression and interference. Moreover, polar metabolites such as amino acids (glycine and alanine) which are major components in biological samples have limited retention and separation and may be eluted at the void volume of the RPC column because they have little retention on stationary phase of RPC columns. Instead the use of

hydrophilic interaction chromatography (HILIC) is recommended and has been increasingly applied for metabolomics studies. The main concept of HILIC separation mechanism is the partitioning of the analytes between an organic mobile phase and a water surface layer (pseudo – stationary phase) associated with a zwitterionic or polar surface coating on the column such as ZICIHLIC which is able to separate positively and negatively charged ions of the analyte (Dunn, 2008, Watson, 2010). HILIC columns can be categorised into three groups depending on stationary phase chemistry as bare silica / neutral, charged and zwitterionic phases. The ZIC-HILIC column is the most commonly used on targeted and untargeted profiling metabolites identification.

7.2.3 Data processing obtained from LC-MS analysis used in metabolomics

7.2.3.1 mzMatch and IDEOM

All raw data files (Thermo-Xcalibur format) were manually sorted into folders according to study groups. Then they were converted to mzXML files and split polarity using mzMatch split function to separate Exactive files that contain both positive and negative polarity. After this, XCMS was run through R, using the centwave function, peaks were picked and each individual file converted to peakml format. The settings for the centwave function were employed as mass deviation from scan to scan (< 2) ppm, range for baseline peak width (minimum 5 seconds and maximum 100 seconds), Signal to Noise ratio (3), prefilter intensity (1000), Mzdiff (0.001). This was followed by running mzMatch to match peaks from each sample to produce a single dataset and group individual peakml files together. Furthermore, the noise filter, RSD filter, intensity filter and detection filter were run to remove

irreproducible signals (Creek *et al*., 2012). Parameter settings for the mzMatch filters were mass deviation from sample to sample (5 ppm) and t_R deviation from sample to sample (0.5 min). If there is a large shift in retention time, the signal intensities will not be comparable and the datasets will not make sense. mzMatch filtrations are [1] RSD filter (0.5), where peak reproducibility is assessed by the RSD of peak intensities for each group of replicates; [2] noise filter (0.8), where peak shape is assessed by CoDA-DW score (0-1); [3] intensity filter (3000), where features are removed if no sample has a peak above the intensity threshold; and, [4] detection filter (3), where peaks must be present in a minimum number of samples. In addition, mzMatch fills the gap for peaks which may fall off during the process. Finally, IDEOM is used to filter the data further, and then the metabolites are compared and identified.

IDEOM is a Microsoft Excel template enabled for automated data processing of high-resolution LC-MS data from untargeted metabolomics studies (Creek *et al*., 2012). In IDEOM, more noise filtration is done and the authentic chemical standard is matched with a sample metabolite. It is necessary to update database (DB) with retention times using a list of retention times from authentic standards (≈180 standards) run with each experiment; this list is created using Toxid (which is an automated compound identification tool that dramatically simplifies LC-MS data and identifies compounds according to retention time and chemical formula). The retention time calculator also uses physicochemical properties (depending on the functional group and chemical formula of compound) in the DB sheet to predict retention times based on a multiple linear regression model with the authentic standards. The retention time calculator also uses the Quantitative Structure

Retention Relationships (QSRR) approach to predict retention times based on the known retention times of authentic standards and the physicochemical nature of the interactions of analyte with columns that determine retention (Creek *et al*., 2011). Identification of more accurate putative metabolite requires more filtration of mzMatch files. The blank run with the study group to filter all intensities in a study group must be greater than that in the solvent blanks to 56 remove contaminants. Other filters for noise, such as RSD, intensity and detection filters, are repeated. Chromatography filters, shoulder peak filter and duplicate peak filter, are also applied in IDEOM. Identification of metabolites is performed by matching the accurate mass (accurate mass error for mass identification with DB < 3ppm is suitable for formula identification from a biochemical database with unique entries in DB of 97%) and retention time (t_R for identification of authentic standards is 5%) of detected metabolite peak to metabolites in the database. Final lists of identified and rejected peaks are annotated with confidence level from 0 to 10 (10 = most confident) according to the identification of each metabolite; confidence < 5 is rejected as false identification and metabolites matched with authentic standards are identified metabolites and highlighted yellow.

7.3 Materials and methods

7.3.1 Materials

Flavonoids [Quercetin (99%)], non-flavonoids [*P*- coumaric acid (99%) and Ferulic acid (99%)], dimethylsulphoxide (DMSO) and ammonium carbonate were obtained from Sigma Aldrich, Dorset UK. HPLC grade acetonitrile (ACN) was purchased from Fisher Scientific (Loughborough, UK). Distilled Water was obtained from a Milli - Q water - purification system (Millipore, Watford UK) in laboratory.

7.3.2 Preparation of hepatocytes

Hepatocytes were isolated from adult male Sprague-Dawley (SD) rat (≈ 200 g of body weight) livers by collagenase digestion a two - step perfusion process as described by (Moldeus *et al.* 1978). More details described in General Methodology Chapter 2 pages (54:57).

7.3.3 Sample preparation

Three stock solutions (100 mM) of *p*-coumaric acid, feurlic acid and quercetin were prepared by dissolving 16.4 mg of *p*-coumaric acid in 1 mL of DMSO, 19.9 mg of ferulic acid in1 mL of DMSO and 30.2 mg of quercetin in 1 mL of DMSO. They were incubated at 100 µM with 2 x 10^6 isolated hepatocytes per mL at 37°C under an atmosphere of 95% O_2, 5% CO_2 in rotating 50 mL round bottomed flasks. Blank incubations were carried out without cells. Control incubation was concomitantly run with hepatocytes but without drug. Four aliquots (0.5 mL) were taken from the incubation solutions at 0, 30, 120 and 180 min and the reaction terminated by addition of 1 mL of acetonitrile. The samples were stored at -80°C. Prior to analysis samples were thawed at room temperature, sonicated and centrifuged at 5000 rpm for

five min to remove protein and collect the supernatants for analysis of conjugates. More details described in General Methodology Chapter 2 pages (58:60).

7.3.4 Preparation of mobile phase solutions for ZIC-pHILIC chromatography

All mobile phase solutions were freshly prepared and were stored at room temperature for up to 48 hours. Mobile phase A (20 mM Ammonium carbonate buffer, pH 9.2) was prepared by addition of 1.92 g of ammonium carbonate to 800 mL of HPLC - grade water followed by adjustment to pH 9.2 with ammonia solution and then more water was added to make the volume up to 1 L. Mobile phase B was HPLC-grade acetonitrile only. The column used was a ZIC-pHILIC column (L150 × I.D. 4.6 mm, 5 µm, polymeric bead support) from Hichrom Ltd, Reading, UK.

7.3.5 LC-MS method

Liquid chromatographic separation was carried out on an Accela HPLC system interfaced to an Exactive Orbitrap mass spectrometer (Thermo Fisher Scientific, Bremen, Germany) using a hydrophilic interaction liquid chromatography (HILIC) column (ZIC-pHILIC, 150 x 4.6 mm, 5 µm particle size) supplied by Hichrom Ltd. (Reading, UK). The method was reported previously (Zhang *et al*., 2014). The mobile phase for ZIC-pHILIC consisted of 20 mM ammonium carbonate in water purified (solvent A) and acetonitrile (Sigma-Aldrich, Poole, UK) (solvent B) at a flow rate of 0.3 mL/min. The elution gradient was an A: B ratio of 20:80 at 0 min, 80:20 at 30 min, 92:8 at 35 min and finally 20:80 at 45 min. The mass spectrometer was operated in positive negative ion switching mode with needle voltages of 4.5 kV in positive mode and 4.0 kV in negative mode. The sheath and auxiliary gases were

50 and 17 arbitrary units respectively and the heated capillary temperature was 300°C.

7.4 Results and discussion

The other phenolic compounds ferulic acid and *p*-coumaric acid produced quite a lot of metabolic shifts but the changes specific to quercetin will be focused on since its chemistry and metabolism are complex as indicated in Chapter 3. There were very clear effects of quercetin metabolism on several pathways within the hepatocyte metabolome **(Table 7-1)**. The major metabolites of quercetin were sulfates and glucuronides with the largest percentage being due to glucuronidation (Chapter 3). However, the depletion of the co-factor for sulfate phosphoadenylyl sulfate transfer by 180 min is greater than that for UDP-glucuronate which is initially depleted at 30 min but more appears to be restored by 120 min and so that it is not much different from that of the control cells. D-Glucuronate levels are lower at all three-time points and this might be the rate limiting step for maintaining UDP-glucuronate levels since UDP levels are higher in the quercetin treated cells. Uridine levels are significantly lower at 30 and 120 min compared with control and this suggests that uridine is consumed in order to maintain UDP levels and uridine formation requires uracil which is also lowered in the treated cells. Altogether this provides a fascinating insight into metabolism in action since the hepatocytes are maintained in simple medium where the only substrates for metabolism are derived from their own resources. The requirements for quercetin metabolism are perfectly reflected by the consumption and production of the relevant intracellular substrates.

Quercetin has been proposed as an antioxidant compound although it is evident from the metabolism data in Chapter 3 that it consumes GSH. The levels of GSSG are lower at all the sampling time points in the hepatocytes treated with quercetin supporting quercetin antioxidant properties and this is further supported by the lower levels of glutathione cysteine in the treated cells. In addition, glutathione levels are much higher in the treated hepatocytes at 180 min although the levels are quite variable between all samples makes the P value less significant (< 0.05). In addition, there is a strong indication that quercetin is reducing the level of protein oxidation in the samples since the levels of L-formylkynurenine (FK) are much lower in the treated samples at 180 min. FK can form via enzymatic action but it has also been used as an indicator of the oxidation of tryptophan (Ou *et al*., 2017). Recently it has been shown that quercetin can inhibit protein oxidation in vitro and it has also been demonstrated the quercetin forms adducts with methylglyoxal, an oxidation product of glucose (also derived from the glycolysis pathway) thus reducing the damaging effects of methylglyoxal to cellular proteins (Li *et al*., 2014). A marker for this effect is carboxyethyllysine. However, in the current study this marker is slightly elevated in the quercetin treated samples at 120 min rather than reduced.

Other indicators of the antioxidant effects of quercetin are lowered levels of methionine S-oxide which, forms under oxidative stress and lower levels of urocanic acid which is a product of the oxidation of histidine. Both of these oxidation products could result from oxidation of amino acids in proteins. N1-Methyl-2-pyridone-5-carboxamide is an oxidation product of N-methylnicotinamide which generates oxidative stress during its metabolic conversion and has been implicated in the development of type 2 diabetes (Zhou *et al*., 2009). This metabolite is much lower in

the quercetin treated hepatocytes than in the controls. Quercetin treatment appears to promote glycogen and starch breakdown in the liver with oligomers of glycogen/starch being significantly lower in the treated hepatocytes. Glycogen is broken down into glucose phosphate which is slightly elevated in the treated hepatocytes but this effect does not carry through into glycolytic intermediates with phosphoglyceric acid, glyceraldehyde phosphate and being lowered in the treated hepatocytes although pyruvate is higher. The apparent lower rate of glycolysis is reflected in slightly lowered levels of ATP in the treated hepatocytes. The effect of quercetin on the Krebs cycle intermediates is fairly minor. Of course glucose is also required for the biosynthesis of glucuronic acid which is required to form the glucuronide metabolites of quercetin. It has previously been observed that quercetin has antidiabetic effects through lowering plasma glucose levels in diabetic rats and was also found to cause a large elevation in hexokinase in the livers of treated rats (Vessal *et al*., 2003).

There are marked effects on several amino acids with amino acids being lower in the treated hepatocytes. This suggests that quercetin is strongly inhibiting autophagy in the hepatocytes. Hepatocytes are known to undergo autophagy during incubation and inhibitors of autophagy include methylated adenosines (Seglen and Gordon, 1982) Interestingly the treated hepatocytes have greatly elevated levels of methylguanosine.

In has been observed that fisetin, which is very close in structure to quercetin promotes autophagy in cancer cells (Suh *et al*., 2010). It might be that in normal cells the effect is opposite as evidenced by the current work where there are very clear effects on autophagy inhibition. Thus quercetin might be beneficial for extending the viability of isolated hepatocytes. In contrast to the effect of quercetin on the

hepatocyte metabolome the effects of *p*-coumaric acid **(Table 7-2)** were less noticeable with regard to the pathways affected by quercetin. Phosphoadenylyl sulfate is depleted with time which reflects the fact that the predominant route of metabolism is sulfation. However, there are no significant effects on the co-factors required for glucuronidation which is the less dominant pathway in the metabolism of coumaric acid in comparison to quercetin and this also largely true for the precursors of the UDP-glucuronide. Coumaric acid does not affect the markers of oxidative stress significantly and the levels GSSG, glutathionyl cysteine and methionine S-oxide do not differ from those in the control. The effects on amino acid levels are also largely absent to there is no apparent reduction in autophagy resulting from the *p*-coumaric acid treatment. The metabolomics profile produced by treatment with ferulic acid **(Table 7-3)** is similar to that produced by *p*-coumaric acid with respect the effects produced by quercetin. Thus the effect of quercetin is significant particularly with regards to antioxidant effects and on autophagy. Quercetin is a very interesting molecule both chemically and with regards to its biological effects.

Table 7-1 Effect of Quercetin on the metabolome of hepatocytes (n = 4)

T = Treated, C = Control.The full metabolic are shown in **Appendix C** [Table C1]

Mass	t_R (min)	Putative metabolite	P value 180 min	Ratio C/T 180 min	P value 120 min	Ratio C/T 120 min	P value 30 min	Ratio C/T 30 min
Cofactors involved in quercetin metabolism								
580.03	19.2	UDP-glucuronate	0.3	1.156	0.700	1.119	0.017	2.091
566.06	16.5	UDP-glucose	0.007	1.897	0.020	2.038	0.021	1.979
506.99	21.3	3'-Phosphoadenylyl sulfate	0.04	1.924	0.010	2.41	0.003	0.6
468.16	4.5	Bilirubin beta-diglucuronide	0.008	0.418	0.500	0.761	0	#DIV/0!
404.00	16.7	UDP	0.03	0.321	0.050	0.25	0.024	0.634
274.01	17.7	D-Glucuronate 1-phosphate	0.3	0.844	0.070	0.726	0.061	1.301
244.07	12.0	Uridine	0.1	1.309	0.050	1.786	0.002	1.589
196.06	14.1	D-Gluconic acid	<0.001	2.147	0.000	2.262	0.005	1.749
194.04	15.8	D-Glucuronate	<0.001	2.444	0.001	2.749	0.001	2.779
146.07	14.9	L-Glutamine	<0.001	1.587	0.008	1.859	0.68	0.98
112.03	8.6	Uracil	0.002	1.4	0.010	1.982	0.007	0.618
105.04	15.5	L-Serine	<0.001	1.802	0.010	2.006	0.073	1.316
Oxidative stress								
612.15	17.4	Glutathione disulfide	<0.001	1.896	0.000	2.126	0.023	1.253
426.09	16.9	S-glutathionyl-L-cysteine	<0.001	4.429	0.001	6.73	0.071	2.882
307.08	14.8	Glutathione	0.05	0.085	0.200	0.069	0.793	1.495
255.99	18.7	Ascorbate 2-sulfate	<0.001	4.28	0.000	4.636	0.431	1.272
236.08	9.6	L-Formylkynurenine	0.003	8.963	0.070	4.359	0.357	1.576
218.13	8.8	N2-(D-1-Carboxyethyl)-L-lysine	0.01	0.584	0.300	0.809	0.629	0.942
181.04	7.6	DL-Methionine sulfone	0.1	0.735	0.700	0.944	0.35	1.248

176.03	15.3	Ascorbate	0.2	0.062	0.200	0.064	0.397	33.694
175.10	15.6	L-Citrulline	<0.001	2.525	0.001	2.725	0.164	1.129
175.02	11.4	Monodehydroascorbate	0.07	1.437	0.060	1.498	0.296	0.86
165.05	13.3	L-Methionine S-oxide	<0.001	1.767	0.007	2.445	0.337	1.176
152.06	7.5	N1-Methyl-2-pyridone-5-carboxamide	<0.001	2.476	0.001	2.624	0.013	1.472
138.04	11.3	Urocanate	0.009	2.132	0.001	2.591	0.862	0.981
Glycogen/glucose metabolism								
990.33	18.4	Glycogen 6 units	<0.001	1.492	0.003	1.581	0.229	1.269
828.27	17.8	Glycogen 5 units	0.003	1.842	0.080	2.182	0.021	1.42
666.22	17.4	Glycogen 4 units	0.007	1.813	0.020	2.017	0.003	1.477
536.16	15.8	Glycogen 3 units	0.001	2.611	0.001	2.772	0.004	3.062
507.00	16.6	ATP	0.07	1.283	0.200	1.394	0.136	0.795
427.03	15.3	ADP	0.01	1.389	0.060	1.545	0.604	0.934
347.06	13.2	AMP	0.07	1.213	0.300	1.607	0.128	1.393
260.03	16.9	D-Glucose 6-phosphate	0.02	0.707	0.100	0.823	0.083	0.78
185.99	17.0	3-Phospho-D-glycerate	0.08	1.278	0.300	1.214	<0.001	0.478
170.00	15.5	D-Glyceraldehyde 3-phosphate	0.004	1.584	0.020	1.907	0.484	0.945
167.98	17.6	Phosphoenolpyruvate	0.08	1.2	0.080	1.234	<0.000	0.41
88.016	8.6	Pyruvate	0.003	0.767	0.020	0.695	0.099	0.651
TCA cycle								
665.12	13.5	NADH	0.6	1.093	1.000	1.012	0.252	0.605
192.03	17.9	Citrate	0.9	1.006	0.900	0.989	0.33	1.11
192.03	16.2	Citrate isomer	0.002	2.289	0.000	2.535	0.023	1.639
148.04	15.5	(R)-2-Hydroxyglutarate	0.1	1.763	0.020	1.861	0.443	1.157
146.02	15.9	2-Oxoglutarate	0.02	0.72	0.070	0.853	0.018	2.136

134.02	16.3	(S)-Malate	0.3	1.091	0.300	1.191	0.014	1.16
118.03	15.4	Succinate	0.02	1.418	0.010	1.834	0.01	1.736
Amino acids and Metabolites								
220.08	10.3	5-Hydroxy-L-tryptophan	<0.001	3.697	0.060	5.19	0.069	3.235
204.09	11.5	L-Tryptophan	0.2	0.915	0.100	1.462	0.742	0.968
189.04	6.7	Kynurenate	0.1	0.83	0.300	0.826	<0.001	0.303
181.07	12.9	L-Tyrosine	<0.001	1.698	0.004	2.121	0.235	1.152
180.04	8.1	3-(4-Hydroxyphenyl)pyruvate	0.002	0.456	0.040	0.476	0.372	0.661
169.00	15.1	L-Cysteate	0.04	1.298	0.050	1.431	0.53	1.09
155.07	14.5	L-Histidine	<0.001	2.149	0.002	1.969	0.595	1.076
149.05	11.3	L-Methionine	<0.001	1.574	0.008	2.355	0.216	1.154
147.05	11.2	L-Glutamate	0.09	1.224	0.007	1.582	0.303	0.813
146.11	22.3	L-Lysine	0.02	2.877	0.030	2.724	0.75	1.037
132.05	15.0	L-Asparagine	0.3	1.996	0.000	2.454	0.115	1.176
132.05	12.7	L-Asparagine isomer	0.02	1.302	0.009	1.781	0.013	1.581
131.09	10.6	L-Leucine	<0.001	2.104	0.010	2.617	0.06	1.257
131.06	9.4	L-Glutamate 5-semialdehyde	<0.001	4.332	0.010	4.791	0.16	1.113
129.04	10.6	L-1-Pyrroline-3-hydroxy-5-carboxylate	0.003	1.544	0.070	1.697	0.024	1.41
128.05	8.0	(4E)-2-Oxohexenoic acid	0.006	0.719	0.500	1.207	0.572	1.079
119.06	14.4	L-Threonine	<0.001	1.916	0.000	2.234	0.016	1.152
117.08	12.4	L-Valine	<0.001	2.133	0.001	2.845	0.067	1.239
118.06	8.0	5-Hydroxypentanoate	<0.001	1.739	0.002	2.331	0.531	0.897
115.06	12.7	L-Proline	0.001	1.61	0.030	2.224	0.038	1.326
Purines and pyrimidines								
384.12	13.2	S-Adenosyl-L-homocysteine	<0.001	2.882	0.008	2.698	0.455	0.924

297.09	6.8	5'-Methylthioadenosine	0.1	1.522	0.070	4.194	0.042	2.143
297.11	9.4	Methyl guanosine	<0.001	0.28	0.020	0.32	0.001	<0.001
284.08	12.8	Xanthosine	<0.001	0.458	0.300	0.746	0.047	0.794
283.09	12.5	Guanosine	0.2	0.871	0.400	1.464	0.466	1.44
267.10	8.9	Adenosine	0.07	0.73	0.400	1.355	0.313	1.177
243.09	11.8	Cytidine	<0.001	1.722	0.002	2.339	0.065	1.277
227.09	10.3	Deoxycytidine	0.08	1.286	0.080	1.587	0.354	1.292
246.09	10.0	5-6-Dihydrouridine	0.008	1.842	0.002	2.409	0.306	2.025
228.07	8.1	Deoxyuridine	0.06	0.817	0.200	1.29	0.101	1.394
181.06	12.1	8-Hydroxy-7-methylguanine	0.07	1.506	0.200	1.368	0.315	0.557
135.05	8.9	Adenine	0.06	0.729	0.400	1.289	0.122	1.234
Amino sugars								
614.15	15.4	CMP-N-acetylneuraminate	0.06	0.748	0.800	0.97	0.688	0.941
607.08	15.3	UDP-N-acetyl-D-glucosamine	0.02	0.669	0.200	0.744	0.106	0.804
301.06	14.9	N-Acetyl-D-glucosamine 6-phosphate	0.02	0.593	0.100	0.743	0.985	0.998
259.05	15.6	D-Glucosamine 6-phosphate	0.07	1.332	0.020	1.772	0.135	1.234
221.09	12.9	N-Acetyl-D-glucosamine	0.4	1.115	0.100	1.401	0.416	1.133
179.08	11.2	D-Glucosamine	0.009	0.868	0.300	1.245	0.945	1.008
Miscellaneous								
515.29	4.8	Taurocholate	0.04	1.236	0.040	1.686	0.015	1.183
219.11	8.9	Pantothenate	<0.001	1.845	0.007	2.166	0.507	1.115
183.07	15.0	Choline phosphate	0.02	1.404	0.008	1.784	0.983	0.996
169.05	14.9	Phosphodimethylethanolamine	0.006	1.686	0.030	1.896	0.114	1.239

Table 7-2 Effect of *p*-coumaric acid on the metabolome of hepatocytes with respect to the metabolites altered by quercetin

[Complete changes are shown in **Appendix C** (Table C2)]

Mass	t_R (min)	Putative metabolite	P value 180 min	Ratio C/T 180 min	P value 120 min	RatioC/T 120 min	P value 30 min	Ratio C/T 30 min
Cofactors involved in PA metabolism								
580.03	19.2	UDP-glucuronate	0.131	1.173	0.05	1.734	0.084	1.303
566.06	16.5	UDP-glucose	0.178	1.18	0.163	1.415	0.628	1.066
506.99	21.3	3'-Phosphoadenylyl sulfate	0.149	1.345	0.016	2.355	0	2.674
468.16	4.5	Bilirubin beta-diglucuronide	Nil	Nil	Nil	Nil	Nil	Nil
404.00	16.7	UDP	0.688	0.7	0.139	#DIV/0!	0.863	1.093
274.01	17.7	D-Glucuronate 1-phosphate	0.999	1	0.041	1.348	0.79	1.038
244.07	12.0	Uridine	0.253	0.855	0.016	1.161	0.822	0.976
196.06	14.1	D-Gluconic acid	0.559	0.931	0.007	1.507	0.6	1.061
194.04	15.8	D-Glucuronate	0.066	1.239	0.001	1.872	0.005	1.547
146.07	14.9	L-Glutamine	0.517	0.95	0.178	1.08	0.007	1.335
112.03	8.6	Uracil	0.022	0.792	0.044	0.845	0.533	0.926
105.04	15.5	L-Serine	0	5.189	0	5.257	0	3.846
Oxidative stress								
612.15	17.4	Glutathione disulfide	0.884	0.991	0.008	1.373	0.4	1.11
426.09	16.9	S-glutathionyl-L-cysteine	0.442	1.065	0.823	1.014	0.675	1.205
307.08	14.8	Glutathione	0.124	0.482	0.356	#DIV/0!	0.445	0.42
255.99	18.7	Ascorbate 2-sulfate	0.001	1.354	0.001	1.84	0.441	1.223
236.08	9.6	L-Formylkynurenine	0.304	1.296	0.082	1.618	0.143	3.653
218.13	8.8	N2-(D-1-Carboxyethyl)-L-lysine	0.892	0.971	0.003	1.887	0.506	1.133
181.04	7.6	DL-Methionine sulfone	0.01	1.376	0	1.687	0.385	1.228

176.03	15.3	Ascorbate	0.19	0.098	0.314	1.138	0.34	0.323
175.10	15.6	L-Citrulline	0.001	0.518	0.016	0.712	0.008	0.546
175.02	11.4	Monodehydroascorbate	0.402	1.093	0.524	1.123	0.145	0.821
165.05	13.3	L-Methionine S-oxide	0.589	1.09	0.129	1.424	0.035	2.136
152.06	7.5	N1-Methyl-2-pyridone-5-carboxamide	0.209	1.126	0.068	1.197	0.557	1.053
138.04	11.3	Urocanate	0.995	1.002	0.002	1.564	0.005	0.476
Glycogen/glucose metabolism								
990.33	18.4	glycogen 6 units	Nil	Nil	Nil	Nil	Nil	Nil
828.27	17.8	glycogen 5 units	Nil	Nil	Nil	Nil	Nil	Nil
666.22	17.4	Glycogen 4 units	0.05	1.347	0.002	1.321	0.054	1.189
536.16	15.8	glycogen 3 units	Nil	Nil	Nil	Nil	Nil	Nil
507.99	16.6	ATP	0.354	1.109	0.198	1.533	0.994	1.001
427.03	15.3	ADP	0.397	1.135	0.087	1.718	0.985	1.003
347.06	13.2	AMP	0.252	0.9	0.329	0.753	0.443	1.171
260.03	16.9	D-Glucose 6-phosphate	0.433	1.084	0.026	1.272	0.556	0.965
185.99	17.0	3-Phospho-D-glycerate	0.795	1.039	0.021	1.452	0.82	1.017
170.00	15.5	D-Glyceraldehyde 3-phosphate	0.045	1.431	0.001	1.63	0.59	1.046
167.98	17.6	Phosphoenolpyruvate	0.702	0.958	0.06	1.559	0.546	1.084
88.02	8.6	Pyruvate	0	0.291	0	0.259	0.006	0.4
TCA cycle								
665.12	13.5	NADH	0.805	1.035	0.124	1.734	0.501	1.092
192.03	17.9	Citrate	0	1.561	0.014	1.925	0.001	1.792
192.03	16.2	Citrate isomer	0.81	1.015	0.265	1.239	0.847	1.041

148.04	15.5	(R)-2-Hydroxyglutarate	0.003	1.756	0.001	3.338	0.007	2.624
146.02	15.9	2-Oxoglutarate	0	0.409	0	0.451	0.341	1.16
134.02	16.3	(S)-Malate	0.256	1.109	0	1.971	0	1.985
118.03	15.4	Succinate	0.135	1.201	0.122	1.544	0.001	2.324
Amino acids and metabolites								
220.08	10.3	5-Hydroxy-L-tryptophan	0.912	0.979	0.014	0.674	0.416	1.678
204.09	11.5	L-Tryptophan	0.145	1.098	0.001	1.325	0.908	1.008
188.04	6.7	Kynurenate	0.004	0.559	0.001	0.538	0.662	0.921
181.07	12.9	L-Tyrosine	0.269	1.08	0.002	1.194	0.081	1.145
180.04	8.1	3-(4-Hydroxyphenyl)pyruvate	0	0.371	0.089	0.632	0.261	0.615
169.00	15.1	L-Cysteate	0.04	0.863	0.082	1.3	0.924	0.983
155.07	14.5	L-Histidine	0.156	0.864	0.886	0.992	0.707	1.034
149.05	11.3	L-Methionine	0.677	1.017	0.016	1.202	0.204	0.947
147.05	11.2	L-Glutamate	0.023	1.331	0	1.4	0.717	0.963
146.11	22.3	L-Lysine	0.064	0.867	0.04	1.208	0.769	1.045
132.05	15.0	L-Asparagine	0.085	1.095	0.001	1.275	0.254	1.067
132.05	12.7	L-Asparagine isomer	0.102	1.171	0.002	1.434	0.086	1.249
131.09	10.6	L-Leucine	0.088	0.848	0.012	1.316	0.355	1.105
131.06	9.4	L-Glutamate 5-semialdehyde	0.001	1.465	0	2.349	0.132	1.146
129.04	10.6	L-1-Pyrroline-3-hydroxy-5-carboxylate	0.146	1.111	0.592	1.104	0.645	1.067
128.05	8.0	(4E)-2-Oxohexenoic acid	0.034	0.833	0.011	1.273	0.409	1.113
119.06	14.4	L-Threonine	0.406	0.917	0.031	1.173	0.709	0.978
117.08	12.4	L-Valine	0.26	0.932	0.003	1.384	0.037	1.213
118.06	8.0	5-Hydroxypentanoate	0	1.613	0	2.487	0.046	1.372
115.06	12.7	L-Proline	0.517	1.052	0.046	1.178	0.251	1.093

Purines and pyrimidines								
384.12	13.2	S-Adenosyl-L-homocysteine	0.722	1.077	0.02	1.583	0.623	0.931
297.09	6.8	5'-Methylthioadenosine	0.299	0.811	0.554	0.938	0.555	0.919
297.11	9.4	Methyl guanosine	0.262	0.862	0.03	0.828	0.716	1.045
284.08	12.8	Xanthosine	0.006	0.506	0.199	0.901	0.136	0.832
283.09	12.5	Guanosine	0.497	0.852	0.312	0.727	0.416	1.542
267.10	8.9	Adenosine	0.362	0.867	0.416	1.108	0.805	1.054
243.09	11.8	Cytidine	0.258	1.071	0.057	1.097	0.251	1.137
227.09	10.3	Deoxycytidine	0.035	1.209	0.58	1.043	0.231	1.186
246.09	10.0	5-6-Dihydrouridine	0.093	1.232	0.07	1.361	0.028	#DIV/0!
228.07	8.1	Deoxyuridine	0.041	0.82	0.754	0.974	0.692	0.941
181.06	12.1	8-Hydroxy-7-methylguanine	Nil	Nil	Nil	Nil	Nil	Nil
135.05	8.9	Adenine	0.072	0.751	0.101	1.237	0.81	1.053
Amino sugars								
614.15	15.4	CMP-N-acetylneuraminate	0.979	0.997	0.004	1.242	0.64	0.953
607.08	15.3	UDP-N-acetyl-D-glucosamine	0.248	1.174	0.243	1.289	0.375	0.898
301.06	14.9	N-Acetyl-D-glucosamine 6-phosphate	0.15	0.819	0.86	1.009	0.606	1.097
259.05	15.6	D-Glucosamine 6-phosphate	0.242	1.112	0.004	1.331	0.46	1.088
221.09	12.9	N-Acetyl-D-glucosamine	0.172	1.148	0.002	1.353	0.215	1.144
179.08	11.2	D-Glucosamine	0.583	0.981	0.034	1.112	0.321	1.061
Miscellaneous								
515.29	4.8	Taurocholate	0.921	0.993	0.001	1.336	0.084	1.099
219.11	8.9	Pantothenate	0.107	1.197	0	1.643	0.126	1.308
183.07	15.0	Choline phosphate	0.007	1.327	0.001	1.489	0.232	1.151
169.05	14.9	Phosphodimethylethanolamine	0.065	1.217	0.006	1.645	0.043	1.361

Table7-3 Effect of ferulic acid on the metabolome of hepatocytes comparing with the metabolites which are changed by quercetin

The full metabolic changes are shown in **Appendix C** [Table C3]

Mass	t_R (min)	Putative metabolite	P value 180 min	Ratio C/T 180 min	P value 120 min	Ratio C/T 120 min	P value 30 min	Ratio C/T 30 min
Cofactors involved in quercetin metabolism								
580.03	19.2	UDP-glucuronate	0.723	0.951	0.004	0.826	0.000	1.481
566.06	16.5	UDP-glucose	0.157	1.156	0.378	0.958	0.002	1.298
506.99	21.3	3'-Phosphoadenylyl sulfate	0.222	1.225	0.691	1.046	0.000	1.876
468.16	4.5	Bilirubin beta-diglucuronide	Nil	Nil	Nil	Nil	Nil	Nil
404.00	16.7	UDP	0.139	0.000	0.034	0.000	0.230	0.864
274.01	17.7	D-Glucuronate 1-phosphate	0.071	0.734	0.053	0.825	0.044	1.073
244.07	12.0	Uridine	0.076	0.899	0.089	1.043	0.004	1.118
196.06	14.1	D-Gluconic acid	0.256	0.898	0.321	0.965	0.005	1.206
194.04	15.8	D-Glucuronate	0.215	1.210	0.009	0.711	0.008	1.325
146.07	14.9	L-Glutamine	0.000	1.392	0.000	1.415	0.000	1.993
112.03	8.6	Uracil	0.064	1.179	0.006	1.151	0.003	1.092
105.04	15.5	L-Serine	0.733	1.007	0.010	1.052	0.008	1.162
Oxidative stress								
612.15	17.4	Glutathione disulfide	0.826	0.980	0.000	0.880	0.011	1.262
426.09	16.9	S-glutathionyl-L-cysteine	0.030	1.371	0.720	0.970	0.005	1.313
307.08	14.8	Glutathione	0.022	0.000	0.076	0.044	0.042	0.501
255.99	18.7	Ascorbate 2-sulfate	0.832	1.011	0.001	1.260	0.000	1.514
236.08	9.6	L-Formylkynurenine	Nil	Nil	Nil	Nil	Nil	Nil
218.13	8.0	N2-(D-1-Carboxyethyl)-L-lysine	Nil	Nil	Nil	Nil	Nil	Nil
181.04	7.6	DL-Methionine sulfone	Nil	Nil	Nil	Nil	Nil	Nil
176.03	15.3	Ascorbate	0.017	0.026	0.000	0.114	0.034	0.312

175.1	15.6	L-Citrulline	0.469	0.968	0.533	0.960	0.572	0.957
175.02	11.4	Monodehydroascorbate	0.146	0.000	#DIV/0!	#DIV/0!	0.139	0.441
165.05	13.3	L-Methionine S-oxide	0.965	1.061	0.546	1.061	0.043	1.103
152.06	7.5	N1-Methyl-2-pyridone-5-carboxamide	0.319	0.879	0.967	0.997	0.044	0.876
138.04	11.3	Urocanate	0.462	0.846	0.811	1.052	0.749	0.883
Glycogen/glucose metabolism								
990.33	18.4	glycogen 6 units	Nil	Nil	Nil	Nil	Nil	Nil
828.27	17.8	glycogen 5 units	Nil	Nil	Nil	Nil	Nil	Nil
666.22	17.4	Glycogen 4 units	0.735	1.023	0.025	1.081	0.011	1.142
536.16	15.8	glycogen 3 units	Nil	Nil	Nil	Nil	Nil	Nil
507.99	16.6	ATP	0.599	1.059	0.828	0.976	0.011	1.420
427.03	15.3	ADP	0.242	0.844	0.180	0.909	0.684	1.048
347.06	13.2	AMP	0.015	0.713	0.052	0.843	0.029	1.175
260.03	16.9	D-Glucose 6-phosphate	0.789	0.995	0.984	1.001	0.036	1.156
185.99	17.0	3-Phospho-D-glycerate	0.419	0.896	0.921	0.996	0.043	1.243
170.00	15.5	D-Glyceraldehyde 3-phosphate	0.952	1.010	0.379	1.099	0.023	1.441
167.98	17.6	Phosphoenolpyruvate	0.260	0.864	0.275	0.858	0.006	1.296
88.016	8.6	Pyruvate	0.142	0.882	0.023	0.852	0.047	0.919
TCA cycle								
665.12	13.5	NADH	0.000	0.000	0.095	0.353	0.891	1.031
192.03	17.9	Citrate	0.028	1.132	0.153	1.153	0.062	1.521
192.03	16.2	Citrate isomer	0.374	1.141	0.001	0.639	0.015	1.262
148.04	15.5	(R)-2-Hydroxyglutarate	0.002	0.665	0.000	0.720	0.006	1.470
146.02	15.9	2-Oxoglutarate	0.000	0.506	0.000	0.518	0.497	1.032
134.02	16.3	(S)-Malate	0.016	0.812	0.000	0.855	0.000	1.438
118.03	15.4	Succinate	0.971	0.991	0.129	0.908	0.003	1.465

Amino acids and metabolites								
220.08	10.3	5-Hydroxy-L-tryptophan	0.012	3.041	0.004	1.993	0.136	#DIV/0!
204.09	11.5	L-Tryptophan	0.001	0.757	0.021	0.903	0.259	0.944
189.04	6.7	Kynurenate	0.137	0.861	0.019	0.792	0.024	0.761
181.07	12.9	L-Tyrosine	0.091	0.942	0.003	0.880	0.370	1.023
180.04	8.1	3-(4-Hydroxyphenyl)pyruvate	0.002	0.291	0.004	0.520	0.065	0.884
169.00	15.1	L-Cysteate	Nil	Nil	Nil	Nil	Nil	Nil
155.07	14.5	L-Histidine	0.001	0.614	0.000	0.699	0.037	1.287
149.05	11.3	L-Methionine	0.933	0.997	0.309	0.946	0.319	0.973
147.05	11.2	L-Glutamate	0.004	0.806	0.054	0.903	0.244	1.127
146.11	22.3	L-Lysine	0.080	0.905	0.008	0.908	0.735	1.027
132.05	15.0	L-Asparagine	0.424	0.971	0.577	1.031	0.953	1.001
132.05	12.7	L-Asparagine isomer	0.672	1.020	0.317	0.960	0.899	0.994
131.09	10.6	L-Leucine	0.027	1.191	0.088	1.170	0.772	1.031
131.06	9.4	L-Glutamate 5-semialdehyde	0.175	0.926	0.135	1.135	0.001	1.260
129.04	10.6	L-1-Pyrroline-3-hydroxy-5-carboxylate	0.001	1.296	0.000	1.285	0.003	1.416
128.05	8.0	(4E)-2-Oxohexenoic acid	Nil	Nil	Nil	Nil	Nil	Nil
119.06	14.4	L-Threonine	0.019	0.890	0.065	0.928	0.481	0.987
117.08	12.4	L-Valine	0.263	0.941	0.419	1.015	0.000	1.176
118.06	8.0	5-Hydroxypentanoate	0.238	1.127	0.076	1.415	0.531	0.897
115.06	12.7	L-Proline	0.160	0.947	0.579	0.988	0.802	1.009
Purines and pyrimidines								
384.12	13.2	S-Adenosyl-L-homocysteine	0.099	0.609	0.019	0.689	0.134	1.134
297.09	6.8	5'-Methylthioadenosine	0.681	0.923	0.085	0.826	0.351	1.123
297.11	9.4	Methyl guanosine	0.214	0.888	0.761	0.983	0.123	1.086
284.08	12.8	Xanthosine	0.083	0.789	0.000	0.759	0.410	1.055

283.09	12.5	Guanosine	0.924	1.024	0.345	0.791	0.836	0.961
267.10	8.9	Adenosine	0.708	0.932	0.529	0.924	0.028	0.777
243.09	11.8	Cytidine	0.754	1.008	0.469	0.980	0.089	0.975
227.09	10.3	Deoxycytidine	0.151	1.088	0.262	0.953	0.321	0.956
246.09	10.0	5-6-Dihydrouridine	0.378	0.918	0.470	1.100	0.144	3.749
228.07	8.1	Deoxyuridine	0.859	1.041	0.200	1.114	0.363	1.037
181.06	12.1	8-Hydroxy-7-methylguanine	Nil	Nil	Nil	Nil	Nil	Nil
135.05	8.9	Adenine	0.714	0.933	0.954	0.994	0.651	0.962
Amino sugars								
614.15	15.4	CMP-N-acetylneuraminate	0.995	1.001	0.666	0.962	0.171	1.129
607.08	15.3	UDP-N-acetyl-D-glucosamine	0.766	0.972	0.004	0.846	0.362	1.049
301.06	14.9	N-Acetyl-D-glucosamine 6-phosphate	0.200	1.147	0.016	1.258	0.425	1.053
259.05	15.6	D-Glucosamine 6-phosphate	0.789	0.995	0.984	1.001	0.036	1.156
221.09	12.9	N-Acetyl-D-glucosamine	0.864	1.014	0.593	1.056	0.081	1.258
179.08	11.2	D-Glucosamine	0.223	0.929	0.977	1.001	0.233	1.053
Miscellaneous								
515.29	4.8	Taurocholate	0.489	1.035	0.039	1.079	0.002	1.098
219.11	8.9	Pantothenate	0.013	0.786	0.187	0.951	0.037	1.177
183.07	15.0	Choline phosphate	0.547	1.048	0.216	0.925	0.245	0.942
169.05	14.9	Phosphodimethylethanolamine	0.388	0.883	0.588	0.964	0.182	1.104

CHAPTER 8

Future work

8. Future work

The most interesting phenolic compounds studied in the set of compounds subjected to hepatocyte metabolism was quercetin because of its very complex degradation and metabolism pattern. In addition, its effects on the metabolome of hepatocytes were complex. Further work on this compound would definitely be of interest. The first step would be to repeat the hepatocyte incubations in order to test the reproducibility of the metabolic perturbations. It would be interesting to test whether or not the quercetin was able to extend the period in which isolated hepatocytes remain viable through reducing proteolysis. It would also be of interest to determine whether or not quercetin had an effect on the metabolome of other cell lines. This might contribute to its further development as a powerful anti-oxidant and potential antidiabetic and anticancer agent. Another goal would be produce a library of xenobiotic metabolites. There are many unidentified metabolites in biological matrices such as urine and plasma and using hepatocytes to produce partially characterised metabolites of common phenolic compounds. To do this it might be best to produce a standard method based on ultra-performance liquid chromatography to increase resolution between isomeric metabolites. In addition to reducing variability during method transfer it would be useful to use some standard metabolites to lock retention times and base characterisation on relative retention times. Such a standard approach would facilitate monitoring of phenolic metabolites during dietary intervention studies.

References:

ABDEL-WAHAB, M. H., EL-MAHDY, M. A., ABD-ELLAH, M. F., HELAL, G. K., KHALIFA, F. & HAMADA, F. M. A. 2003. Influence of p-coumaric acid on doxorubicin-induced oxidative stress in rat's heart. *Pharmacological Research,* 48**,** 461-465.

ADAM, A., CRESPY, V., LEVRAT-VERNY, M.-A., LEENHARDT, F., LEUILLET, M., DEMIGNÉ, C. & RÉMÉSY, C. 2002. The bioavailability of ferulic acid is governed primarily by the food matrix rather than its metabolism in intestine and liver in rats. *The journal of nutrition,* 132**,** 1962-1968.

AL-ASMARI, A. I. 2009. *Applications of LC-MS/MS in Forensic Toxicology for the Analysis of Drugs and their Metabolites.* University of Glasgow.

BARNES, J. S., FOSS JR, F. W. & SCHUG, K. A. 2013. Thermally accelerated oxidative degradation of quercetin using continuous flow kinetic electrospray-ion trap-time of flight mass spectrometry. *Journal of The American Society for Mass Spectrometry,* 24**,** 1513-1522.

BERRY, M. N. & FRIEND, D. S. 1969. High-yield preparation of isolated rat liver parenchymal cells: a biochemical and fine structural study. *J Cell Biol,* 43**,** 506-20.

BERRY, N., BARRITT, G. J., EDWARDS, A. M. & BURDON, R. H. 1991. *Isolated Hepatocytes: Preparation, Properties and Applications: Preparation, Properties and Applications*, Elsevier Science.

BO WEN , S. D. N. 2011. Common Biotransformation Reactions. *In:* MIKE S. LEE, M. Z. (ed.) *Mass Spectrometry in Drug Metabolism and Disposition.* First Edition ed. New Jersey: John Wiley & Sons.Inc.

BRONK, J. R. 1999. *Human metabolism: functional diversity and integration,* Addison-Wesley Longman.

CAO, G. H., SOFIC, E. & PRIOR, R. L. 1997. Antioxidant and prooxidant behavior of flavonoids: Structure-activity relationships. *Free Radical Biology and Medicine,* 22**,** 749-760.

CHANET, A., MILENKOVIC, D., MANACH, C., MAZUR, A. & MORAND, C. 2012. Citrus flavanones: what is their role in cardiovascular protection? *Journal of agricultural and food chemistry,* 60**,** 8809-8822.

CHARRON, C. S., KURILICH, A. C., CLEVIDENCE, B. A., SIMON, P. W., HARRISON, D. J., BRITZ, S. J., BAER, D. J. & NOVOTNY, J. A. 2009. Bioavailability of anthocyanins from purple carrot juice: effects of acylation and plant matrix. *Journal of agricultural and food chemistry,* 57**,** 1226-1230.

CHO, J. 2006. Antioxidant and neuroprotective effects of hesperidin and its aglycone hesperetin. *Archives of Pharmacal Research,* 29**,** 699-706.

CIALDELLA-KAM, L., NIEMAN, D. C., SHA, W., MEANEY, M. P., KNAB, A. M. & SHANELY, R. A. 2013. Dose–response to 3 months of quercetin-containing supplements on metabolite and quercetin conjugate profile in adults. *British Journal of Nutrition,* 109**,** 1923-1933.

CLIFFORD, M. N. 2000. Chlorogenic acids and other cinnamates–nature, occurrence, dietary burden, absorption and metabolism. *Journal of the Science of Food and Agriculture,* 80**,** 1033-1043.

COLEMAN, M. D. 2010a. Drug Biotransformational Systems – Origins and Aims. *Human Drug Metabolism.* John Wiley & Sons, Ltd.

COLEMAN, M. D. 2010b. How Oxidative Systems Metabolize Substrates. *Human Drug Metabolism.* John Wiley & Sons, Ltd.

COLEMAN, M. D. 2010c. *Human drug metabolism: an introduction,* John Wiley & Sons.

CONWAY, J. G., KAUFFMAN, F. C. & THURMAN, R. G. 1987. 2 - Regulation of Sulfation and Glucuronidation of Xenobiotics in Periportal and Pericentral Regions of the Liver Lobule. *In:* PADILLA, E. J. R. M. (ed.) *The Isolated Hepatocyte.* Academic Press.

COS, P., YING, L., CALOMME, M., HU, J. P., CIMANGA, K., VAN POEL, B., PIETERS, L., VLIETINCK, A. J. & VANDEN BERGHE, D. 1998. Structure-activity relationship and classification of flavonoids as inhibitors of xanthine oxidase and superoxide scavengers. *Journal of Natural Products,* 61**,** 71-76.

CREEK, D. J., JANKEVICS, A., BREITLING, R., WATSON, D. G., BARRETT, M. P. & BURGESS, K. E. 2011. Toward global metabolomics analysis with hydrophilic interaction liquid chromatography–mass spectrometry: improved metabolite identification by retention time prediction. *Analytical chemistry,* 83**,** 8703-8710.

CREEK, D. J., JANKEVICS, A., BURGESS, K. E., BREITLING, R. & BARRETT, M. P. 2012. IDEOM: an Excel interface for analysis of LC–MS-based metabolomics data. *Bioinformatics,* 28**,** 1048-1049.

CROZIER, A., CLIFFORD, M. N. & ASHIHARA, H. 2008. *Plant secondary metabolites: occurrence, structure and role in the human diet*, John Wiley & Sons.

CROZIER, A., JAGANATH, I. B. & CLIFFORD, M. N. 2009. Dietary phenolics: chemistry, bioavailability and effects on health. *Natural product reports,* 26**,** 1001-1043.

CUYCKENS, F., ROZENBERG, R., DE HOFFMANN, E. & CLAEYS, M. 2001. Structure characterization of flavonoid O-diglycosides by positive and negative nano-electrospray ionization ion trap mass spectrometry. *Journal of Mass Spectrometry,* 36**,** 1203-1210.

DEL RIO, D., RODRIGUEZ-MATEOS, A., SPENCER, J. P., TOGNOLINI, M., BORGES, G. & CROZIER, A. 2013. Dietary (poly) phenolics in human health: structures, bioavailability, and evidence of protective effects against chronic diseases. *Antioxidants & redox signaling,* 18**,** 1818-1892.

DOO-HOON LEE & LEE, K.-W. 2014. Hepatocyte Isolation, Culture, and Its Clinical Applications. *Hanyang Medical Reviews,* 34**,** 165-172.

DUNN, W. B. 2008. Current trends and future requirements for the mass spectrometric investigation of microbial, mammalian and plant metabolomes. *Physical biology,* 5**,** 011001.

FARDET, A., LLORACH, R., ORSONI, A., MARTIN, J.-F., PUJOS-GUILLOT, E., LAPIERRE, C. & SCALBERT, A. 2008. Metabolomics provide new insight on the metabolism of dietary phytochemicals in rats. *The Journal of nutrition,* 138**,** 1282-1287.

FARRELL, T., POQUET, L., DIONISI, F., BARRON, D. & WILLIAMSON, G. 2011. Characterization of hydroxycinnamic acid glucuronide and sulfate conjugates by HPLC–DAD–MS 2: Enhancing chromatographic quantification and application in Caco-2 cell metabolism. *Journal of pharmaceutical and biomedical analysis,* 55**,** 1245-1254.

FAZARY, A. E. & JU, Y.-H. 2007. Feruloyl esterases as biotechnological tools: current and future perspectives. *Acta biochimica et biophysica Sinica,* 39**,** 811-828.

FERNANDEZ, M. A., SAENZ, M. T. & GARCIA, M. D. 1998. Anti-inflammatory activity in rats and mice of phenolic acids isolated from Scrophularia frutescens. *Journal of Pharmacy and Pharmacology,* 50**,** 1183-1186.

FERRY, D. R., SMITH, A., MALKHANDI, J., FYFE, D. W., ANDERSON, D., BAKER, J. & KERR, D. 1996. Phase I clinical trial of the flavonoid quercetin: pharmacokinetics and evidence for in vivo tyrosine kinase inhibition. *Clinical Cancer Research,* 2**,** 659-668.

GARG, A., GARG, S., ZANEVELD, L. J. D. & SINGLA, A. K. 2001. Chemistry and pharmacology of the Citrus bioflavonoid hesperidin. *Phytotherapy Research,* 15**,** 655-669.

GUILLOUZO, A. 1996. 17 - Biotransformation of Drugs by Hepatocytes. *In:* CASTELL, J. V. & GÓMEZ-LECHÓN, M. J. (eds.) *In Vitro Methods in Pharmaceutical Research.* San Diego: Academic Press.

GUNTER, G. C. K. 2003. Investigation of Flavonoids and Their In Vivo Metabolite Forms Using Tandem Mass Spectrometry. *In:* CATHERINE, A. R.-E., LESTER PACKER (ed.) *Flavonoids in Health and Disease, Second Edition.* CRC Press.

HAIDARI, F., KESHAVARZ, S. A., RASHIDI, M. R. & SHAHI, M. M. 2009. Orange Juice and Hesperetin Supplementation to Hyperuricemic Rats Alter Oxidative Stress Markers and Xanthine Oxidoreductase Activity. *Journal of Clinical Biochemistry and Nutrition,* 45**,** 285-291.

HALLIWELL, B. 1975. HYDROXYLATION OF PARA-COUMARIC ACID BY ILLUMINATED CHLOROPLASTS - ROLE OF SUPEROXIDE. *European Journal of Biochemistry,* 55**,** 355-360.

HALLIWELL, B. & AHLUWALIA, S. 1976. HYDROXYLATION OF PARA-COUMARIC ACID BY HORSERADISH-PEROXIDASE - ROLE OF SUPEROXIDE AND HYDROXYL RADICALS. *Biochemical Journal,* 153**,** 513-518.

HARGREAVES, T. 1968. Drug Metabolism. *In:* HARGREAVES, T. (ed.) *The Liver and Bile Metabolism.* Amsterdam: North-Holland Publishing Company.

HEINONEN, M., REIN, D., SATUÉ-GRACIA, M. T., HUANG, S.-W., GERMAN, J. B. & FRANKEL, E. N. 1998. Effect of protein on the antioxidant activity of phenolic compounds in a lecithin-liposome oxidation system. *Journal of Agricultural and Food Chemistry,* 46**,** 917-922.

HERALD, P. J. & DAVIDSON, P. M. 1983. Antibacterial Activity of Selected Hydroxycinnamic Acids. *Journal of Food Science,* 48**,** 1378-1379.

HERRMANN, K. & NAGEL, C. W. 1989. Occurrence and content of hydroxycinnamic and hydroxybenzoic acid compounds in foods. *Critical Reviews in Food Science & Nutrition,* 28**,** 315-347.

HOFFMANN, M. F., PREISSNER, S. C., NICKEL, J., DUNKEL, M., PREISSNER, R. & PREISSNER, S. 2014. The Transformer database: biotransformation of xenobiotics. *Nucleic Acids Research,* 42**,** D1113-D1117.

HOLT, A. & SMITH, A. 2008. An introduction to the anatomy of the liver. *In:* NORTH-LEWIS, P. (ed.) *Drugs and the Liver.* Royal Pharmaceutical Society Great Britain: Pharmaceutical Press.

HONG, Y.-J. & MITCHELL, A. E. 2006. Identification of glutathione-related quercetin metabolites in humans. *Chemical research in toxicology,* 19**,** 1525-1532.

HOPFGARTNER, G. 2013. Overview of the Various Types of Mass Spectrometers that are Used in Drug Discovery and Drug Development. *Mass Spectrometry for Drug Discovery and Drug Development.* John Wiley & Sons, Inc.

ICHIYANAGI, T., SHIDA, Y., RAHMAN, M. M., HATANO, Y. & KONISHI, T. 2005. Extended glucuronidation is another major path of cyanidin 3-O-β-D-glucopyranoside metabolism in rats. *Journal of agricultural and food chemistry,* 53**,** 7312-7319.

IONESCU, C. 2006. *Drug metabolism : current concepts*, Dordrecht : Springer.

ISWALDI, I., ARRÁEZ-ROMÁN, D., GÓMEZ-CARAVACA, A. M., DEL MAR CONTRERAS, M., UBEROS, J., SEGURA-CARRETERO, A. & FERNÁNDEZ-GUTIÉRREZ, A. 2013. Identification of polyphenols and their metabolites in human urine after cranberry-syrup consumption. *Food and chemical toxicology,* 55**,** 484-492.

JAGANATH, I. B., JAGANATH, I. B., MULLEN, W., EDWARDS, C. A. & CROZIER, A. 2006. The relative contribution of the small and large intestine to the absorption and metabolism of rutin in man. *Free radical research,* 40**,** 1035-1046.

JEREMY, P. E. S., HAGEN, S. & CATHERINE, A. R.-E. 2003a. Cytoprotective and Cytotoxic Effects of Flavonoids. *In:* CATHERINE, A. R.-E. (ed.) *Flavonoids in Health and Disease, Second Edition.* CRC Press.

JEREMY, P. E. S., SURJITKAILA SINGH, S. & CATHERINE, A. R.-E. 2003b. Metabolism in the Small Intestineand Gastrointestinal Tract. *In:* CATHERINE, A. R.-E. (ed.) *Flavonoids in Health and Disease, Second Edition.* CRC Press.

KANG, J.-S. 2012. Principles and applications of LC-MS/MS for the quantitative bioanalysis of analytes in various biological samples. *Tandem Mass Spectrometry–Applications and Principles***,** 441-492.

KELL, D. B. 2006. Systems biology, metabolic modelling and metabolomics in drug discovery and development. *Drug discovery today,* 11**,** 1085-1092.

KERN, S. M., BENNETT, R. N., MELLON, F. A., KROON, P. A. & GARCIA-CONESA, M.-T. 2003. Absorption of hydroxycinnamates in humans after high-bran cereal consumption. *Journal of agricultural and food chemistry,* 51**,** 6050-6055.

KHONO, H., TAIMA, M., SUMIDA, T., AZUMA, Y., OGAWA, H. & TANAKA, T. 2002. Inhibitory effect of mandarin juice rich in beta-cryptoxanthin and hesperidin on 4-(methylnitrosamino)-1-(3-pyridyl)-1-butanone-induced pulmonary tumorigenesis in mice. *Proceedings of the American Association for Cancer Research Annual Meeting,* 43**,** 308-308.

KLOHR, M. S. L. A. S. E. 2010. 2- The Drug Discovery Process: From Molecules to Drugs. *In:* WALTER, A. K. (ed.) *Using mass spectrometry for drug metabolism studies.* New York: Boca Raton, FL : CRC Press.

KNIGHT, S. 2003. *Metabolism of dietary polyphenols by gut flora.* University of Surrey.

KOHLMEIER, M. 2003. *Nutrient metabolism*, Amsterdam ; Boston : Academic Press.

KONISHI, Y., KOBAYASHI, S. & SHIMIZU, M. 2003. Transepithelial transport of p-coumaric acid and gallic acid in caco-2 cell monolayers. *Bioscience Biotechnology and Biochemistry,* 67**,** 2317-2324.

LEE, J., EBELER, S. E., ZWEIGENBAUM, J. A. & MITCHELL, A. E. 2012. UHPLC-(ESI) QTOF MS/MS profiling of quercetin metabolites in human plasma postconsumption of applesauce enriched with apple peel and onion. *Journal of agricultural and food chemistry,* 60**,** 8510-8520.

LEE, K.-H., YEH, M.-H., KAO, S.-T., HUNG, C.-M., LIU, C.-J., HUANG, Y.-Y. & YEH, C.-C. 2010. The inhibitory effect of hesperidin on tumor cell invasiveness occurs via suppression of activator protein 1 and nuclear factor-kappaB in human hepatocellular carcinoma cells. *Toxicology Letters,* 194**,** 42-49.

LEE, M. S., LEE, Y.-J., KIM, B. J., SHIN, K. J., CHUNG, B. C., BAEK, D.-J. & JUNG, B. H. 2009. The relationship between glucuronide conjugate levels and hepatotoxicity after oral administration of valproic acid. *Archives of Pharmacal Research,* 32**,** 1029-1035.

LI, A. P. 2000. Human hepatocytes as an experimental system for the evaluation of xenobiotics. *In:* BERRY, N. & EDWARDS, A. M. (eds.) *The Hepatocyte Review.* DORDRECHT/BOSTON/LONDON: Kluwer Academic.

LI, X., SHANG, L., WU, Y., ABBAS, S., LI, D., NETTER, P., OUZZINE, M., WANG, H. & MAGDALOU, J. 2011. Identification of the Human UDP-glucuronosyltransferase Isoforms Involved in the Glucuronidation of the Phytochemical Ferulic Acid. *Drug Metabolism and Pharmacokinetics,* 26**,** 341-350.

LI, X., ZHENG, T., SANG, S. & LV, L. 2014. Quercetin inhibits advanced glycation end product formation by trapping methylglyoxal and glyoxal. *Journal of Agricultural and Food Chemistry,* 62**,** 12152-12158.

LIU, X.-L., LI, L.-J. & CHEN, Z. 2002. Isolation and primary culture of rat hepatocytes. *Hepatobiliary & pancreatic diseases international : HBPD INT,* 1**,** 77-9.

MA, S. & ZHU, M. 2009. Recent advances in applications of liquid chromatography-tandem mass spectrometry to the ana lysis of reactive drug metabolites. *Chemico-Biological Interactions,* 179**,** 25-37.

MANACH, C., MORAND, C., GIL-IZQUIERDO, A., BOUTELOUP-DEMANGE, C. & REMESY, C. 2003. Bioavailability in humans of the flavanones hesperidin and narirutin after the ingestion of two doses of orange juice. *European Journal of Clinical Nutrition,* 57**,** 235-242.

MANACH, C., SCALBERT, A., MORAND, C., REMESY, C. & JIMENEZ, L. 2004. Polyphenols: food sources and bioavailability. *American Journal of Clinical Nutrition,* 79**,** 727-747.

MATEOS, R., GOYA, L. & BRAVO, L. 2006. Uptake and metabolism of hydroxycinnamic acids (chlorogenic, caffeic, and ferulic acids) by HepG2 cells as a model of the human liver. *Journal of Agricultural and Food Chemistry,* 54**,** 8724-8732.

MATSUMOTO, H., IKOMA, Y., SUGIURA, M., YANO, M. & HASEGAWA, Y. 2004. Identification and quantification of the conjugated metabolites derived from orally administered hesperidin in rat plasma. *Journal of Agricultural and Food Chemistry,* 52**,** 6653-6659.

MAURICE, D., GARY, M. & ELIZABETH, P. 2004. Phase II Enzymes. *A Handbook of Bioanalysis and Drug Metabolism.* CRC Press.

MCQUEEN, C. A. & WILLIAMS, G. M. 1987. 3 - Toxicology Studies in Cultured Hepatocytes from Various Species. *In:* PADILLA, E. J. R. M. (ed.) *The Isolated Hepatocyte.* Academic Press.

MIGUEL, M. G., DUARTE, A., NUNES, S., SUSTELO, V., MARTINS, D. & DANDLEN, S. A. 2009. Ascorbic acid and flavanone glycosides in citrus: Relationship with antioxidant activity. *Journal of Food Agriculture & Environment,* 7**,** 222-227.

MORENO-ARRIBAS, M. V. & POLO, M. C. 2009. *Wine chemistry and biochemistry*, Springer.

MORIDANI, M. Y., SCOBIE, H. & O'BRIEN, P. J. 2002. Metabolism of caffeic acid by isolated rat hepatocytes and subcellular fractions. *Toxicology letters,* 133**,** 141-151.

MULLEN, W., BOITIER, A., STEWART, A. J. & CROZIER, A. 2004. Flavonoid metabolites in human plasma and urine after the consumption of red onions: analysis by liquid chromatography with photodiode array and full scan tandem mass spectrometric detection. *Journal of Chromatography A,* 1058**,** 163-168.

MULLEN, W., EDWARDS, C. A. & CROZIER, A. 2006. Absorption, excretion and metabolite profiling of methyl-, glucuronyl-, glucosyl- and sulpho-conjugates of quercetin in human plasma and urine after ingestion of onions. *British Journal of Nutrition,* 96**,** 107-116.

NARAYANA, K. R., REDDY, M. S., CHALUVADI, M. R. & KRISHNA, D. R. 2001. Bioflavonoids classification, pharmacological, biochemical effects and therapeutic potential. *Indian Journal of Pharmacology,* 33**,** 2-16.

NIELSEN, I. L. F., CHEE, W. S. S., POULSEN, L., OFFORD-CAVIN, E., RASMUSSEN, S. E., FREDERIKSEN, H., ENSLEN, M., BARRON, D., HORCAJADA, M. N. & WILLIAMSON, G. 2006. Bioavailability is improved by enzymatic modification of the citrus flavonoid hesperidin in humans: A randomized, double-blind, crossover trial. *Journal of Nutrition,* 136**,** 404-408.

O'LEARY, K. A., DAY, A. J., NEEDS, P. W., MELLON, F. A., O'BRIEN, N. M. & WILLIAMSON, G. 2003. Metabolism of quercetin-7-and quercetin-3-glucuronides by an in vitro hepatic model: the role of human β-glucuronidase, sulfotransferase, catechol-O-methyltransferase and multi-resistant protein 2 (MRP2) in flavonoid metabolism. *Biochemical pharmacology,* 65**,** 479-491.

OLIVEIRA, E. J., WATSON, D. G. & GRANT, M. H. 2002. Metabolism of quercetin and kaempferol by rat hepatocytes and the identification of flavonoid glycosides in human plasma. *Xenobiotica,* 32**,** 279-287.

OLTHOF, M. R., HOLLMAN, P. C., BUIJSMAN, M. N., VAN AMELSVOORT, J. M. & KATAN, M. B. 2003. Chlorogenic acid, quercetin-3-rutinoside and black tea phenols are extensively metabolized in humans. *The Journal of nutrition,* 133**,** 1806-1814.

OMAR, M. H. 2013. *Analysis of phytochemical in a Malaysian medicinal plant and the bioavailability of dietary hydroxycinnamates.* University of Glasgow.

OMAR, M. H., MULLEN, W., STALMACH, A., AUGER, C., ROUANET, J.-M., TEISSEDRE, P.-L., CALDWELL, S. T., HARTLEY, R. C. & CROZIER, A. 2012. Absorption, Disposition, Metabolism, and Excretion of [3-14C] Caffeic Acid in Rats. *Journal of agricultural and food chemistry,* 60**,** 5205-5214.

OSMAN, A. & MAKRIS, D. P. 2010. Comparison of fisetin and quercetin oxidation with a cell-free extract of onion trimmings and peel, plant waste, containing peroxidase enzyme: a further insight into flavonol degradation mechanism. *International journal of food science & technology,* 45**,** 2265-2271.

OU, J., HUANG, J., WANG, M. & OU, S. 2017. Effect of rosmarinic acid and carnosic acid on AGEs formation in vitro. *Food Chemistry,* 221**,** 1057-1061.

OU, S. & KWOK, K. C. 2004. Ferulic acid: pharmaceutical functions, preparation and applications in foods. *Journal of the Science of Food and Agriculture,* 84**,** 1261-1269.

PETERSON, J. & DWYER, J. 1998. Flavonoids: Dietary occurrence and biochemical activity. *Nutrition Research,* 18**,** 1995-2018.

RAGU RAMANATHAN, S. N. Ç., AND W. GRIFFITH HUMPHREYS 2010. 5-Metabolite identification strategies and procedures. *In:* WALTER, A. K. (ed.) *Using mass spectrometry for drug metabolism studies.* New York: Boca Raton, FL : CRC Press.

RAMANATHAN, D. M. & LELACHEUR, R. M. 2008. Evolving Role of Mass Spectrometry in Drug Discovery and Development. *Mass Spectrometry in Drug Metabolism and Pharmacokinetics.* John Wiley & Sons, Inc.

RAMEŠOVÁ, Š., SOKOLOVÁ, R., DEGANO, I., BULÍČKOVÁ, J., ŽABKA, J. & GÁL, M. 2012. On the stability of the bioactive flavonoids quercetin and luteolin under oxygen-free conditions. *Analytical and bioanalytical chemistry,* 402**,** 975-982.

RECHNER, A. R. 2003. Absorption and Metabolism of Hydrocinnamates. *In:* CATHERINE, A. R.-E., ENRIQUE, C. & LESTER, P. (eds.) *Flavonoids in Health and Disease, Second Edition.* New York, Basel: Routledge.

RENTON, K. W. 1987. 4 - Cytochrome P-450-Dependent Monooxygenase Systems in Mouse Hepatocytes. *In:* PADILLA, E. J. R. M. (ed.) *The Isolated Hepatocyte.* Academic Press.

SATO, M. 1966. METABOLISM OF PHENOLIC SUBSTANES BY CHLOROPLASTS .2. CONVERSION BY ISOLATED CHLOROPLASTS OF P-COUMARIC ACID TO CAFFEIC ACID. *Phytochemistry,* 5**,** 385-&.

SCHMIDT, T. J., AK, M. & MROWIETZ, U. 2007. Reactivity of dimethyl fumarate and methylhydrogen fumarate towards glutathione and N-acetyl-l-cysteine—Preparation of S-substituted thiosuccinic acid esters. *Bioorganic & medicinal chemistry,* 15**,** 333-342.

SCHONBORN, J. L. & GWINNUTT, C. 2010. THE ROLE OF THE LIVER IN DRUG METABOLISM ANAESTHESIA TUTORIAL OF THE WEEK 179 17th MAY 2010.

SEGLEN, P. O. & GORDON, P. B. 1982. 3-Methyladenine: specific inhibitor of autophagic/lysosomal protein degradation in isolated rat hepatocytes. *Proceedings of the National Academy of Sciences,* 79**,** 1889-1892.

SERRA, A., MACIÀ, A., ROMERO, M.-P., REGUANT, J., ORTEGA, N. & MOTILVA, M.-J. 2012. Metabolic pathways of the colonic metabolism of flavonoids (flavonols, flavones and flavanones) and phenolic acids. *Food chemistry,* 130**,** 383-393.

SHEN, L., HILLEBRAND, A., WANG, D. Q. H. & LIU, M. 2012. Isolation and Primary Culture of Rat Hepatic Cells. *Jove-Journal of Visualized Experiments*.

SILVERMAN, R. B. 2004. *The organic chemistry of drug design and drug action,* Amsterdam ; Boston : Elsevier Academic Press.

SILVERMAN, R. B. & HOLLADAY, M. W. 2014. Chapter 8 - Drug Metabolism. *The Organic Chemistry of Drug Design and Drug Action (Third Edition).* Boston: Academic Press.

SKETT, G. G. G. A. P. 1986. Pathways of drug metabolism. *In:* SKETT, G. G. G. A. P. (ed.) *Introduction to Dtug Metabolism.* First Edition ed. London: Chapman & Hall.

SPENCER, J. P. E., EL MOHSEN, M. M. A. & RICE-EVANS, C. 2004. Cellular uptake and metabolism of flavonoids and their metabolites: implications for their bioactivity. *Archives of Biochemistry and Biophysics,* 423**,** 148-161.

SRIVASTAVA, N. & BEZWADA, R. 2015. Flavonoids: The Health Boosters. White Paper. Hillsborough, NJ: Indofine Chemical Company.

STALMACH, A., MULLEN, W., BARRON, D., UCHIDA, K., YOKOTA, T., CAVIN, C., STEILING, H., WILLIAMSON, G. & CROZIER, A. 2009. Metabolite profiling of hydroxycinnamate derivatives in plasma and urine after the ingestion of coffee by humans: identification of biomarkers of coffee consumption. *Drug Metabolism and Disposition,* 37**,** 1749-1758.

SUH, Y., AFAQ, F., KHAN, N., JOHNSON, J. J., KHUSRO, F. H. & MUKHTAR, H. 2010. Fisetin induces autophagic cell death through suppression of mTOR signaling pathway in prostate cancer cells. *Carcinogenesis,* 31**,** 1424-1433.

TAXAK, N. & BHARATAM, P. V. 2014. Drug metabolism. *Resonance,* 19**,** 259-282.

TEIXEIRA, J., GASPAR, A., GARRIDO, E. M., GARRIDO, J. & BORGES, F. 2013. Hydroxycinnamic acid antioxidants: an electrochemical overview. *BioMed research international,* 2013**,** 251754-251754.

THOMSON, T. N. J. A. A. H. 2008. Pharmacokinetics of drugs in liver disease. *In:* PENNY, N.-L. (ed.) *Drugs and the liver : a guide to drug handling in liver dysfunction* London ; Chicago : Pharmaceutical Press.

TRIPOLI, E., LA GUARDIA, M., GIAMMANCO, S., DI MAJO, D. & GIAMMANCO, M. 2007. Citrus flavonoids: Molecular structure, biological activity and nutritional properties: A review. *Food Chemistry,* 104**,** 466-479.

TYSON, C. A. & GREEN, C. E. 1987. 6 - Cytotoxicity Measures: Choices and Methods. *In:* PADILLA, E. J. R. M. (ed.) *The Isolated Hepatocyte.* Academic Press.

VAGBJIANI, S. T. 2008. Functions of the liver. *In:* PENNY, N.-L. (ed.) *Drugs and the liver : a guide to drug handling in liver dysfunction* London ; Chicago : Pharmaceutical Press.

VAGHJIANI, S. T. 2008. Functions of the liver. *In:* NORTH-LEWIS, P. (ed.) *Drugs and the Liver.* Royal Pharmaceutical Society of Great Britain: Pharmaceutical Press.

VAN ACKER, S., VAN BALEN, G. P., VAN DEN BERG, D. J., BAST, A. & VAN DER VIJGH, W. J. F. 1998. Influence of iron chelation on the antioxidant activity of flavonoids. *Biochemical Pharmacology,* 56**,** 935-943.

VAN ACKER, S. A. B. E., VAN DEN BERG, D.-J., TROMP, M. N. J. L., GRIFFIOEN, D. H., VAN BENNEKOM, W. P., VAN DER VIJGH, W. J. F. & BAST, A. 1996. Structural aspects of antioxidant activity of flavonoids. *Free Radical Biology and Medicine,* 20**,** 331-342.

VAN DER WOUDE, H., BOERSMA, M. G., VERVOORT, J. & RIETJENS, I. M. 2004. Identification of 14 quercetin phase II mono-and mixed conjugates and their formation by rat and human phase II in vitro model systems. *Chemical research in toxicology,* 17**,** 1520-1530.

VESSAL, M., HEMMATI, M. & VASEI, M. 2003. Antidiabetic effects of quercetin in streptozocin-induced diabetic rats. *Comparative Biochemistry and Physiology Part C: Toxicology & Pharmacology,* 135**,** 357-364.

VICKERS, A. E. M. 1996. 5 - Experimental In Vitro Models to Evaluate Hepatotoxicity. *In:* CASTELL, J. V. & GÓMEZ-LECHÓN, M. J. (eds.) *In Vitro Methods in Pharmaceutical Research.* San Diego: Academic Press.

VIRGILI, F., PAGANA, G., BOURNE, L., RIMBACH, G., NATELLA, F., RICE-EVANS, C. & PACKER, L. 2000. Ferulic acid excretion as a marker of consumption of a French maritime pine (Pinus maritima) bark extract. *Free Radical Biology and Medicine,* 28**,** 1249-1256.

WATSON, D. G. 2010. The potential of mass spectrometry for the global profiling of parasite metabolomes. *Parasitology,* 137**,** 1409-1423.

WATSON, D. G. 2012. *Pharmaceutical Analysis, A Textbook for Pharmacy Students and Pharmaceutical Chemists, 3: Pharmaceutical Analysis,* Elsevier Health Sciences.

WEN, B. & NELSON, S. D. 2011. Common Biotransformation Reactions. *Mass Spectrometry in Drug Metabolism and Disposition.* John Wiley & Sons, Inc.

WILLIAMS, R. 1972. Hepatic metabolism of drugs. *Gut,* 13**,** 579-585.

WILMSEN, P. K., SPADA, D. S. & SALVADOR, M. 2005. Antioxidant activity of the flavonoid hesperidin in chemical and biological systems. *Journal of Agricultural and Food Chemistry,* 53**,** 4757-4761.

WONG, C. C., MEINL, W., GLATT, H.-R., BARRON, D., STALMACH, A., STEILING, H., CROZIER, A. & WILLIAMSON, G. 2010. In vitro and in vivo conjugation of dietary hydroxycinnamic acids by UDP-glucuronosyltransferases and sulfotransferases in humans. *The Journal of nutritional biochemistry,* 21**,** 1060-1068.

XING, J., XIE, C. F. & LOU, H. X. 2007. Recent applications of liquid chromatography-mass spectrometry in natural products bioanalysis. *Journal of Pharmaceutical and Biomedical Analysis,* 44**,** 368-378.

YANG, C. Y., TSAI, S. Y., CHAO, P. D. L., YEN, H. F., CHIEN, T. M. & HSIU, S. L. 2002. Determination of hesperetin and its conjugate metabolites in serum and urine (vol 10, pg 143, 2002). *Journal of Food and Drug Analysis,* 10**,** 284-284.

YOON, S.-A., KANG, S.-I., SHIN, H.-S., KANG, S.-W., KIM, J.-H., KO, H.-C. & KIM, S.-J. 2013. p-Coumaric acid modulates glucose and lipid metabolism via AMP-activated protein kinase in L6 skeletal muscle cells. *Biochemical and Biophysical Research Communications,* 432**,** 553-557.

ZANG, L. Y., COSMA, G., GARDNER, H., SHI, X. L., CASTRANOVA, V. & VALLYATHAN, V. 2000. Effect of antioxidant protection by p-coumaric acid on low-density lipoprotein cholesterol oxidation. *American Journal of Physiology-Cell Physiology,* 279**,** C954-C960.

ZHANG, H., ZHANG, D., RAY, K. & ZHU, M. 2009. Mass defect filter technique and its applications to drug metabolite identification by high-resolution mass spectrometry. *Journal of Mass Spectrometry,* 44**,** 999-1016.

ZHANG, J.-L., ZHANG, G.-D. & ZHOU, T.-H. 2005. Metabolism of ferulic acid in rats. *Journal of Asian natural products research,* 7**,** 49-58.

ZHANG, R., WATSON, D. G., WANG, L., WESTROP, G. D., COOMBS, G. H. & ZHANG, T. 2014. Evaluation of mobile phase characteristics on three zwitterionic columns in hydrophilic interaction liquid chromatography mode for liquid chromatography-high resolution mass spectrometry based untargeted metabolite profiling of Leishmania parasites. *Journal of Chromatography A,* 1362**,** 168-179.

ZHAO, Z., EGASHIRA, Y. & SANADA, H. 2004. Ferulic acid is quickly absorbed from rat stomach as the free form and then conjugated mainly in liver. *The Journal of nutrition,* 134**,** 3083-3088.

ZHAO, Z. & MOGHADASIAN, M. H. 2008. Chemistry, natural sources, dietary intake and pharmacokinetic properties of ferulic acid: A review. *Food Chemistry,* 109**,** 691-702.

ZHOU, A., KIKANDI, S. & SADIK, O. A. 2007. Electrochemical degradation of quercetin: Isolation and structural elucidation of the degradation products. *Electrochemistry Communications,* 9**,** 2246-2255.

ZHOU, S.-S., DA LI, W.-P. S., GUO, M., LUN, Y.-Z., ZHOU, Y.-M., XIAO, F.-C., JING, L.-X., SUN, S.-X., ZHANG, L.-B. & LUO, N. 2009. Nicotinamide overload may play a role in the development of type 2 diabetes. *World Journal of Gastroenterology: WJG,* 15**,** 5674.

Appendices

Appendix A: Proposed structures and spectrums derived from the fragmentation of the hesperidin metabolites formed in incubations with rat hepatocytes.

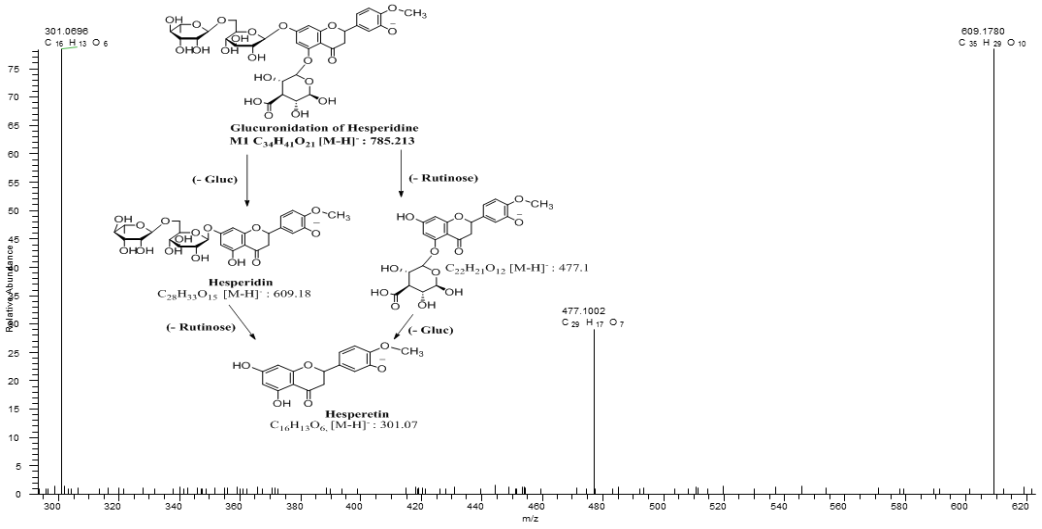

Figure A1 MS^2 spectrum (35eV) of the glucuronidation of hesperidin.

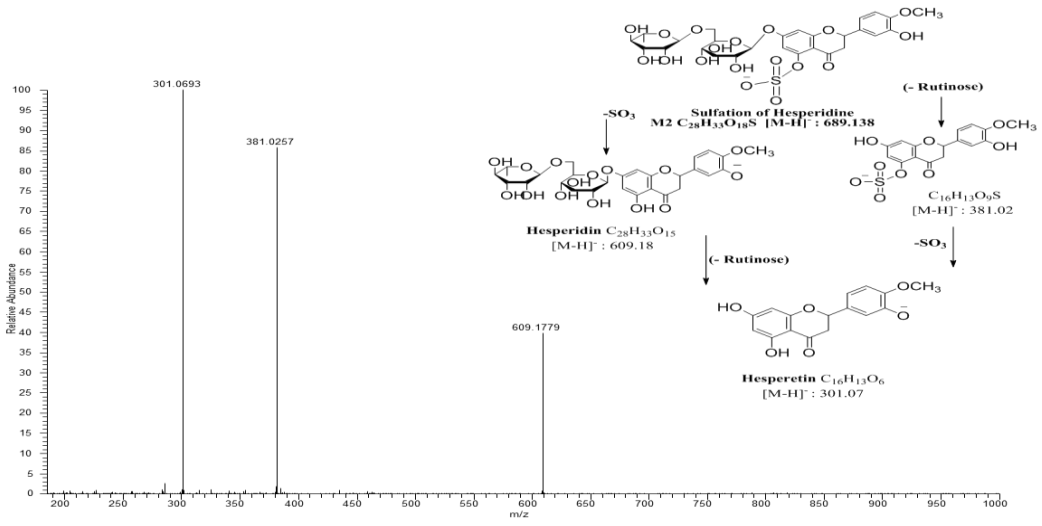

Figure A2 MS^2 spectrum (35eV) of the sulfation of hesperidin.

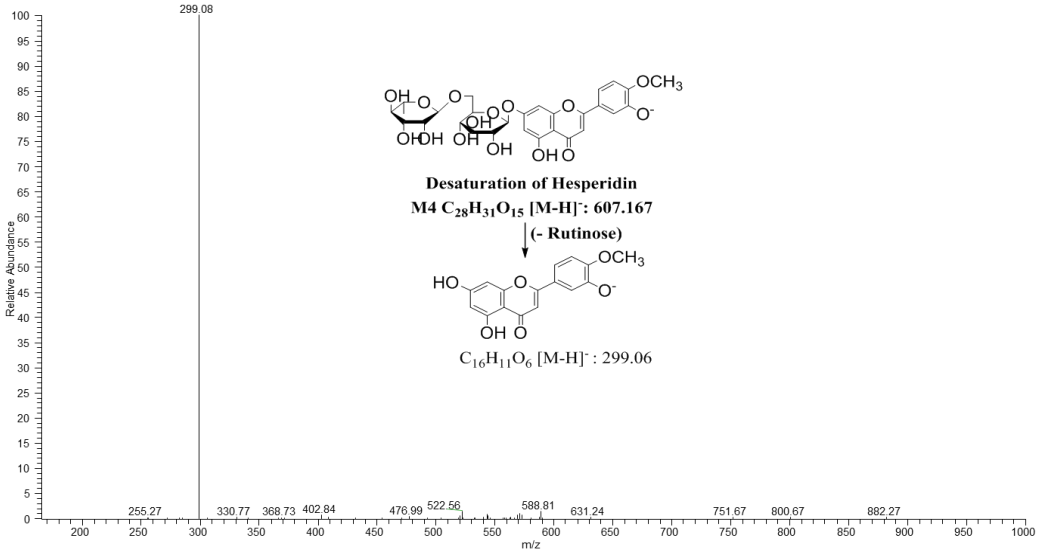

Figure A3 MS^2 spectrum (35eV) of desaturation of hesperidin.

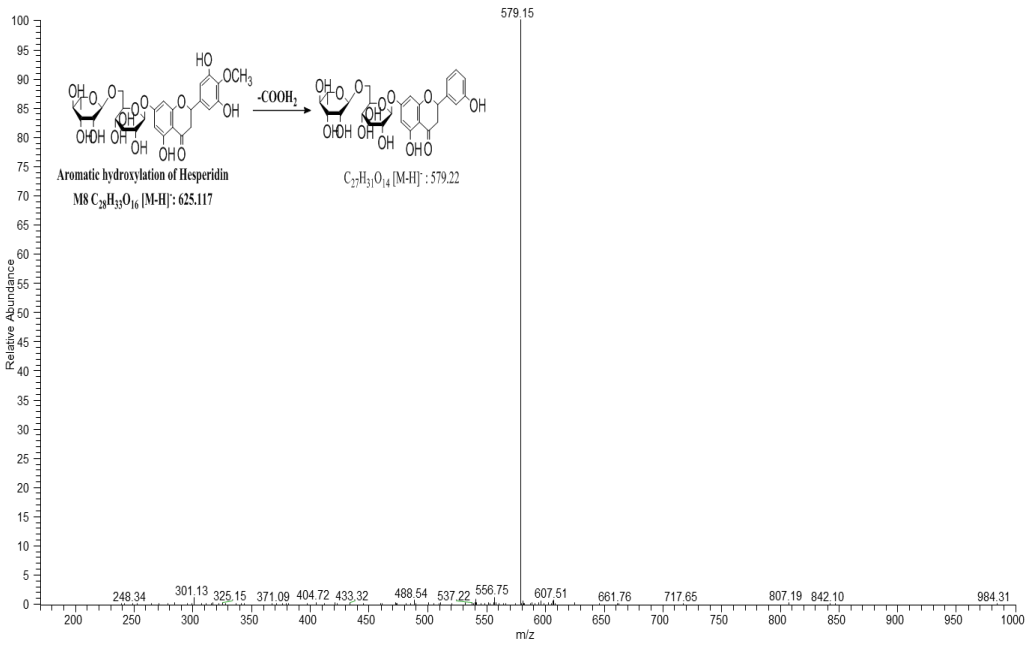

Figure A4 MS^2 spectrum (35eV) of aromatic hydroxylation of hesperidin.

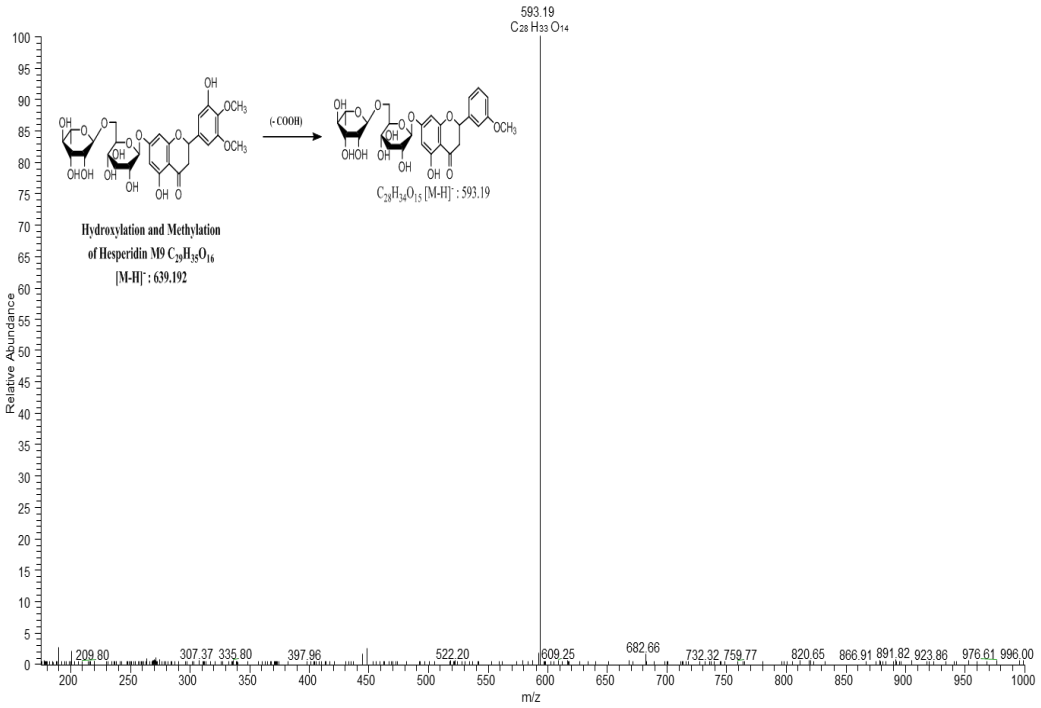

Figure A5 MS^2 spectrum (35eV) of hydroxylation and methylation of hesperidin.

Appendix B: Proposed structures and spectrums of derived from the fragmentation of the *p*-coumaric acid metabolites formed in incubations with rat hepatocytes.

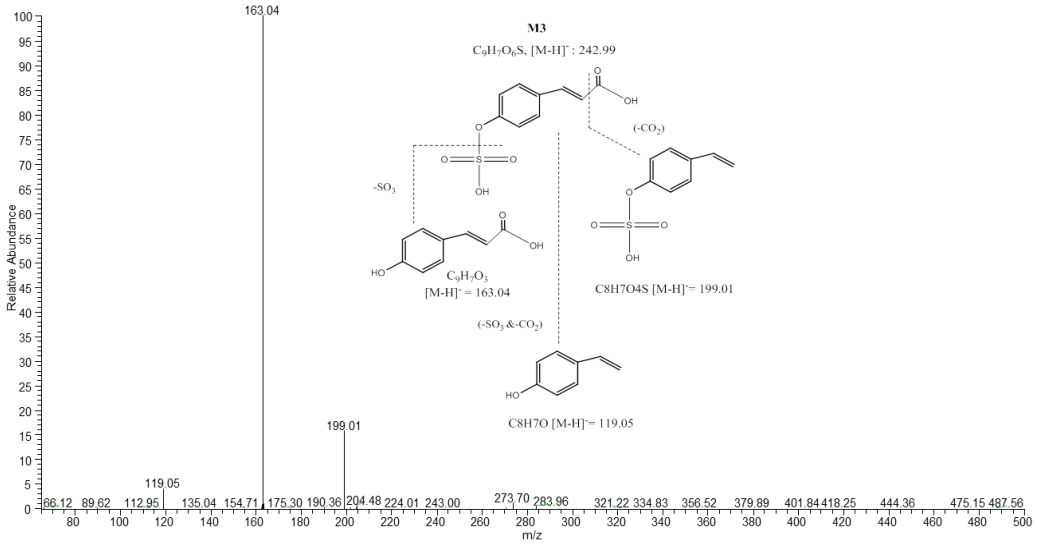

Figure B1 MS^2 spectrum (35eV) of the sulfation of *p*-coumaric acid.

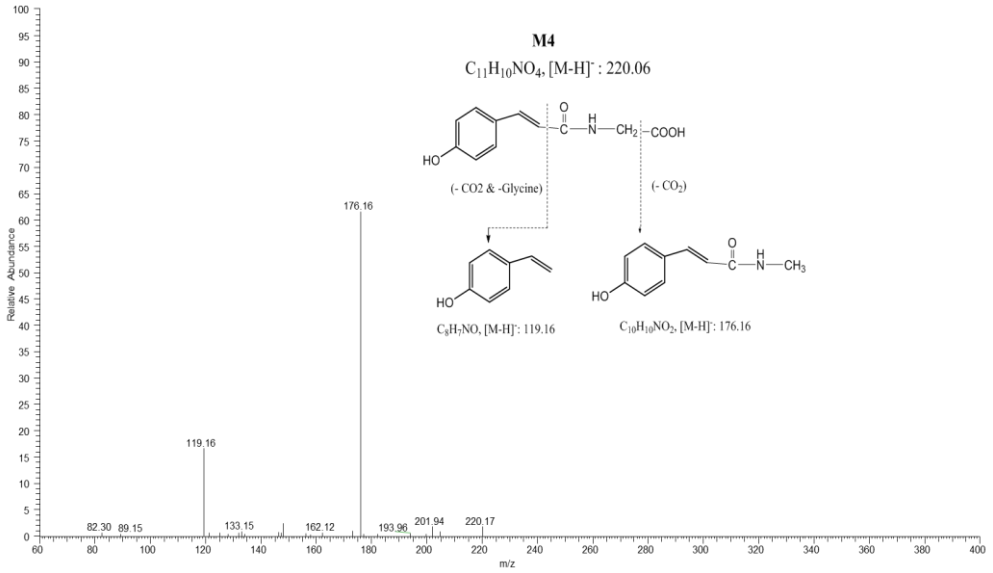

Figure B2 MS^2 spectrum (35eV) of glycination of *p*-coumaric acid.

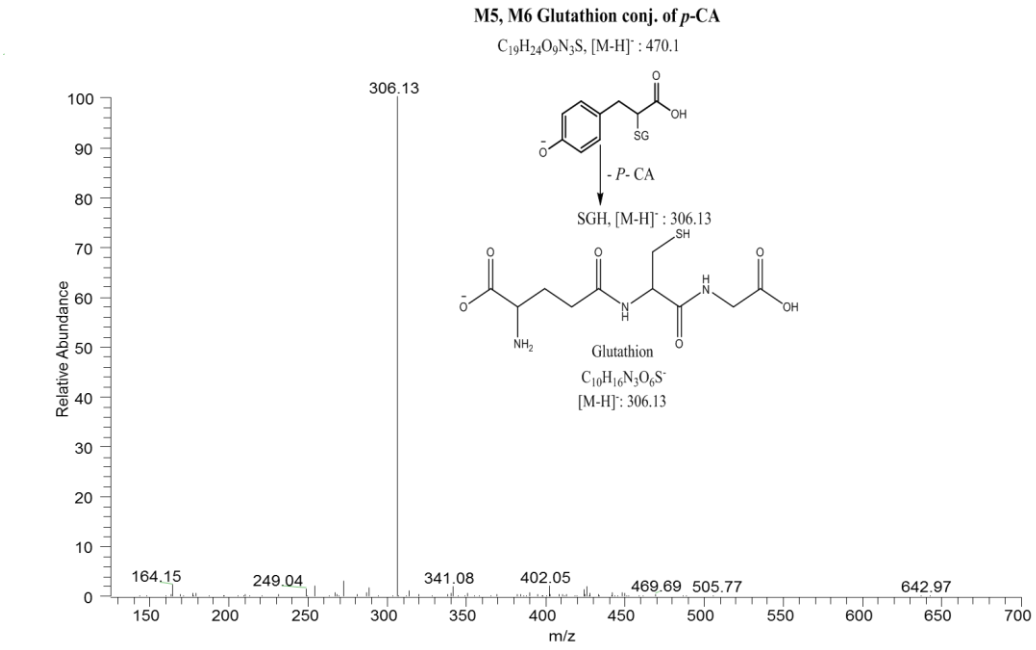

Figure B3 MS^2 spectrum (35eV) of glutathione conjugation of *p*-coumaric acid.

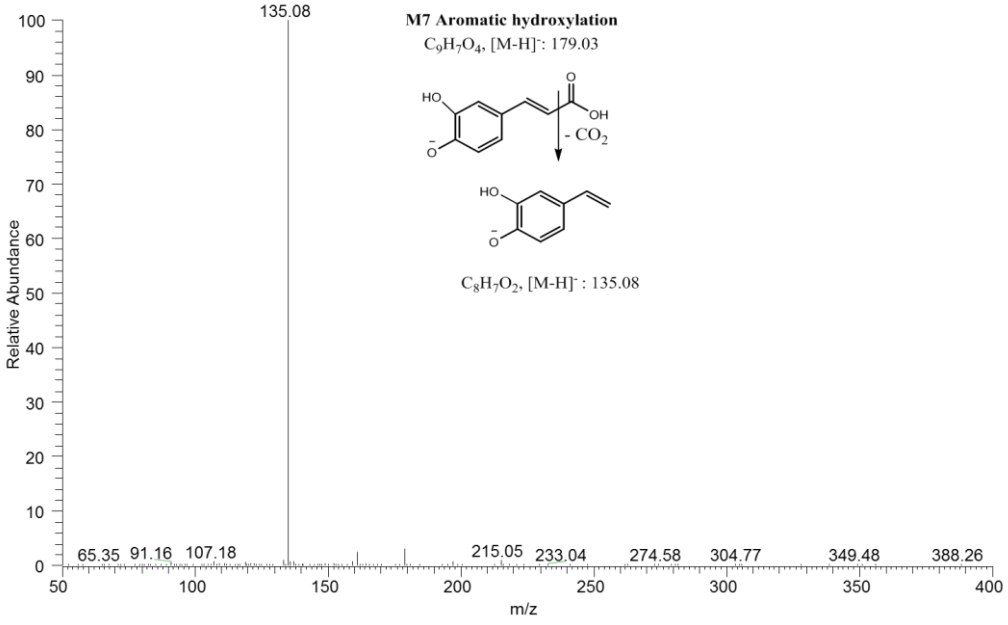

Figure B4 MS^2 spectrum (35eV) of aromatic hydroxylation of *p*-coumaric acid.

Appendix C: Effects of quercetin, *p*-coumaric acid and ferulic acid on the metabolome of hepatocytes.

Table C1 Effect of quercitin on the metabolome of hepatocytes

MASS	t_R (min)	Putative metabolite	P value 180 min	Ratio 180 min	P value 120 min	Ratio 120 min	P value 30 min	Ratio 30 min
132.03	15.2	L-Aspartate	0.000	2.549	0.001	4.638	0.024	2.590
103.04	9.6	(R)-3-Hydroxybutanoate	0.000	1.991	0.005	4.224	0.013	1.587
179.04	8.1	3-(4-Hydroxyphenyl)pyruvate	0.000	0.000	0.000	0.001	0.014	0.001
194.05	9.9	Dopaquinone	0.000	0.373	0.054	0.615	0.247	0.576
191.02	17.9	Citrate	0.000	0.000	0.000	0.000	0.000	0.000
254.98	18.7	Ascorbate 2-sulfate	0.000	1.948	0.024	2.400	0.005	2.029
163.04	8.5	Phenylpyruvate	0.001	1.391	0.007	1.929	0.288	1.299
145.01	15.9	2-Oxoglutarate	0.001	0.039	0.000	0.001	0.001	0.001
87.009	8.6	Pyruvate	0.001	0.410	0.001	0.455	0.325	1.193
193.06	7.6	4-Aminohippuricacid	0.003	0.295	0.000	0.307	0.018	0.498
179.04	10.3	3-(4-Hydroxyphenyl)pyruvate	0.004	0.598	0.004	0.367	0.245	1.496
188.04	6.7	Kynurenate	0.007	0.019	0.001	0.005	0.010	0.045
266.09	8.9	Adenosine	0.008	0.596	0.001	0.575	0.745	0.950
283.07	12.8	Xanthosine	0.010	0.702	0.099	1.289	0.865	1.041
180.03	7.6	DL-Methionine sulfone	0.018	0.454	0.009	0.780	0.129	0.724
117.06	8.0	5-Hydroxypentanoate	0.022	1.747	0.130	1.588	0.826	1.086
200.99	4.6	4-Sulfobenzoate	0.022	1.328	0.001	1.877	0.218	2.034
157.04	14.0	Allantoin	0.023	0.004	0.005	0.003	0.153	0.008
267.07	15.2	inosine	0.024	0.771	0.946	1.003	0.987	1.001
464.30	5.1	Glycocholate	0.039	2.267	0.074	2.211	0.063	2.748
121.04	7.1	Nicotinamide	0.041	0.785	0.272	1.135	0.860	0.981

168.99	15.5	DL-Glyceraldehyde 3-phosphate	0.054	0.787	0.125	0.758	0.740	1.043
115.00	16.3	Fumarate	0.061	1.391	0.004	1.470	0.409	1.040
163.03	13.6	2-Dehydro-D-xylonate	0.064	1.335	0.003	1.598	0.001	1.804
503.16	16.7	glycogen 3 units	0.065	2.122	0.137	1.568	0.113	5.289
465.09	15.7	N-Adenylylanthranilate	0.073	1.432	0.035	1.196	0.006	1.350
151.03	11.9	Xanthine	0.074	4.062	0.169	5.245	0.172	10.038
96.96	18.1	Sulfate	0.076	0.606	0.195	0.410	0.160	0.779
154.06	14.5	L-Histidine	0.078	1.107	0.031	1.245	0.796	1.024
118.05	24.1	L-Threonine	0.079	0.810	0.201	1.167	0.431	0.911
425.08	16.9	S-glutathionyl-L-cysteine	0.080	0.472	0.706	1.332	0.519	2.781
111.02	9.8	Uracil	0.098	1.123	0.438	1.057	0.653	1.249
219.08	10.3	5-Hydroxy-L-tryptophan	0.099	0.850	0.569	1.070	0.643	0.962
163.04	22.2	Phenylpyruvate	0.104	1.671	0.118	0.521	0.328	1.934
113.04	27.1	5,6-Dihydrouracil	0.104	0.097	0.228	0.232	0.723	0.722
243.06	11.9	Uridine	0.106	0.602	0.370	0.152	0.960	0.979
505.99	16.6	ATP	0.107	0.807	0.053	1.109	0.522	1.207
180.07	12.9	L-Tyrosine	0.107	1.248	0.142	1.767	0.964	1.007
579.03	19.2	UDP-glucuronate	0.110	1.114	0.002	1.254	0.149	1.104
200.02	15.9	2-hydroxy-5-nitro-6-oxohepta-2,4-dienoate	0.116	1.208	0.040	1.793	0.137	1.249
665.22	17.3	Glycogen 4 units	0.135	1.918	0.169	1.670	0.024	2.388
565.05	16.5	UDP-glucose	0.137	1.293	0.007	1.319	0.111	1.183
346.06	13.9	AMP	0.148	1.296	0.197	1.407	0.754	1.038
827.27	17.8	Amylopectin	0.154	0.487	0.688	1.134	0.960	1.006
154.05	23.2	2-amino-5-methyl-muconate semialdehyde	0.157	1.399	0.004	1.404	0.106	1.214
203.08	11.5	L-Tryptophan	0.167	0.458	0.609	0.801	0.385	3.932
426.02	15.3	ADP	0.180	1.092	0.001	1.357	0.769	0.982

97.03	24.0	[FA (5:2)] 2,4-pentadienoic acid	0.187	1.372	0.166	2.509	0.593	0.925
245.08	10.0	5-6-Dihydrouridine	0.189	0.000	0.622	1.472	0.363	9.507
606.08	15.3	UDP-N-acetyl-D-glucosamine	0.195	1.509	0.282	1.343	0.377	1.539
191.02	14.3	Citrate	0.196	1.326	0.191	1.368	0.607	0.944
346.06	13.0	AMP	0.200	0.807	0.187	1.153	0.545	0.924
505.98	21.3	3'-Phosphoadenylyl sulfate	0.202	0.889	0.388	0.802	0.514	1.156
174.09	15.6	L-Citrulline	0.213	0.688	0.036	3.232	0.001	4.008
193.04	15.8	D-Glucuronate	0.218	1.142	0.784	0.960	0.001	0.412
113.072	28.7	L-proline amide	0.226	1.148	0.029	1.511	0.225	1.136
175.02	15.2	Ascorbate	0.227	0.245	0.568	0.743	0.396	9.336
784.15	11.8	FAD	0.232	0.101	0.717	1.167	0.406	0.374
156.07	26.6	Paramethadione	0.234	0.841	0.039	1.764	0.431	0.836
154.05	24.2	2-amino-5-methyl-muconate semialdehyde	0.257	0.623	0.369	0.300	0.069	0.410
202.07	26.8	N2-Acetyl-L-aminoadipate	0.272	0.511	0.443	0.666	0.353	6.113
171.01	15.1	sn-Glycerol 3-phosphate	0.276	0.245	0.332	0.254	0.790	1.161
383.108	11.8	Succinyladenosine	0.277	1.124	0.096	1.162	0.786	0.978
115.04	12.1	3-Methyl-2-oxobutanoic acid	0.282	1.540	0.836	0.911	0.609	0.631
145.01	14.0	2-Oxoglutarate	0.295	0.140	0.768	1.146	0.302	0.648
133.01	16.3	(S)-Malate	0.301	0.309	0.143	1.294	0.801	0.752
308.10	13.8	N-Acetylneuraminate	0.304	1.099	0.002	2.014	0.000	2.012
155.08	28.5	N-acetyl prolinamide or isomer	0.305	0.874	0.005	1.480	0.268	1.201
114.02	28.6	Maleamate	0.306	0.310	0.176	0.677	0.357	5.745
147.03	16.2	(R)-2-Hydroxyglutarate	0.312	0.645	0.514	1.803	0.769	0.745
96.97	14.7	Orthophosphate	0.327	0.802	0.652	1.085	0.121	0.721
766.11	13.5	CoA	0.327	0.536	0.019	1.429	0.080	1.286
103.04	18.9	(R)-3-Hydroxybutanoate	0.332	0.182	#DIV/0!	#DIV/0!	0.431	0.353

229.01	15.2	D-Ribose 5-phosphate	0.344	34.272	0.026	2.637	0.705	1.220
114.02	23.2	Maleamate	0.349	0.894	0.517	0.813	0.412	0.938
182.05	5.0	4-Pyridoxate	0.357	0.729	0.386	0.073	0.310	1.441
125.04	14.6	Thymine	0.362	0.932	0.015	1.180	0.812	1.045
154.05	21.0	2-amino-5-methyl-muconate semialdehyde	0.362	11.756	0.449	1.602	0.152	0.370
213.02	24.3	2-Deoxy-D-ribose 5-phosphate	0.364	0.076	0.123	3.134	0.135	2.307
180.99	13.9	3-methylphosphoenolpyruvate	0.366	0.178	0.589	2.584	0.391	0.000
146.046	14.9	L-Glutamate	0.375	0.277	0.007	0.000	0.975	0.963
117.02	14.5	Succinate	0.375	0.938	0.130	1.080	0.013	1.323
181.04	11.8	1-Methyluric acid	0.387	0.195	0.659	1.572	0.207	0.609
375.29	3.7	3alpha-Hydroxy-5beta-cholanate	0.387	0.527	#DIV/0!	#DIV/0!	0.601	0.557
115.04	16.3	3-Methyl-2-oxobutanoic acid	0.388	0.960	0.817	0.984	0.038	0.699
114.02	26.5	Maleamate	0.389	0.395	0.817	1.071	0.327	0.642
213.02	25.5	2-Deoxy-D-ribose 5-phosphate	0.399	0.051	0.403	0.166	0.101	0.538
118.05	25.8	L-Threonine	0.410	0.121	0.851	1.291	0.728	1.741
117.07	28.6	L-2,4-Diaminobutanoate	0.413	0.124	0.756	1.365	0.577	1.425
193.07	14.6	1-Phenanthrol	0.418	0.597	0.341	0.644	0.311	3.776
115.00	14.9	Fumarate	0.421	1.456	0.991	1.004	0.165	2.784
87.01	7.1	Pyruvate	0.421	0.608	0.502	1.652	0.206	0.177
174.02	14.9	Monodehydroascorbate	0.429	0.648	0.239	0.583	0.158	0.335
350.11	9.8	N-Acetyl-4-O-acetylneuraminate	0.437	0.365	#DIV/0!	#DIV/0!	0.478	0.430
226.08	10.4	Deoxycytidine	0.452	0.924	0.006	1.291	0.699	0.951
184.99	17.0	3-Phospho-D-glycerate	0.456	1.072	0.623	0.858	0.949	0.970
163.02	28.8	2-Dehydro-D-xylonate	0.464	1.243	0.038	2.012	0.917	1.006
426.01	17.2	Adenylyl sulfate	0.465	3.357	0.853	1.110	0.631	0.638
168.07	26.7	Pyridoxine	0.467	1.559	0.124	3.216	0.048	4.606

164.04	13.3	L-Methionine S-oxide	0.485	0.609	0.421	0.487	0.859	0.924
136.04	11.6	Anthranilate	0.490	1.067	0.195	1.247	0.170	1.672
124.01	15.0	Taurine	0.494	1.261	0.201	1.425	0.326	1.167
179.04	4.8	3-(4-Hydroxyphenyl)pyruvate	0.528	1.032	0.001	1.184	0.100	1.091
190.01	27.6	indole-5,6-quinone-2-carboxylate	0.529	0.807	0.021	0.070	0.332	0.068
114.02	22.2	Maleamate	0.529	0.499	0.434	3.549	0.375	0.006
166.98	17.6	Phosphoenolpyruvate	0.530	0.761	0.837	0.940	0.138	12.516
96.97	29.0	Orthophosphate	0.540	1.161	0.024	1.764	0.425	1.122
613.14	15.4	CMP-N-acetylneuraminate	0.545	0.733	0.698	1.401	0.415	1.846
282.08	12.5	Guanosine	0.551	1.159	0.045	1.437	0.560	0.909
118.05	28.2	L-Threonine	0.557	0.865	0.394	0.761	0.457	1.504
241.08	7.0	Thymidine	0.569	2.393	0.347	0.314	0.770	1.177
243.06	9.8	Uridine	0.571	1.099	0.028	0.596	0.774	1.052
540.05	14.2	Cyclic ADP-ribose	0.579	1.042	0.107	1.230	0.697	1.054
273.00	17.7	D-Glucuronate 1-phosphate	0.607	1.130	0.462	1.376	0.939	0.987
190.05	6.7	N-Acetylmethionine	0.626	1.156	0.019	1.787	0.906	0.973
373.28	3.7	3-Oxo-5beta-cholanate	0.628	1.057	0.860	1.011	0.474	0.945
193.07	10.0	1-O-Methyl-myo-inositol	0.631	1.025	0.566	0.970	0.024	0.764
383.12	13.2	S-Adenosyl-L-homocysteine	0.632	0.885	0.027	4.449	0.878	1.094
240.10	10.9	5-Methyl-2'-deoxycytidine	0.649	1.076	0.001	1.811	0.708	0.883
304.03	12.9	2',3'-Cyclic CMP	0.664	1.418	0.215	1.779	0.219	0.565
117.02	15.4	Succinate	0.664	0.930	0.020	0.671	0.196	1.532
558.07	17.1	Phosphoribosyl-AMP	0.711	0.818	0.027	1.491	0.010	1.297
195.05	14.1	D-Gluconic acid	0.730	0.974	0.017	1.279	0.848	0.982
111.02	8.6	Uracil	0.743	0.962	0.006	1.471	0.297	1.106
191.02	16.2	Citrate	0.748	0.915	0.566	0.964	0.901	1.017
168.00	15.1	L-Cysteate	0.763	1.027	0.359	1.204	0.906	1.030

369.07	17.5	Digalacturonate	0.786	1.059	0.026	1.303	0.278	1.244
193.04	14.9	D-Glucuronate	0.790	0.954	0.005	1.438	0.481	1.108
207.08	6.8	L-Kynurenine	0.791	0.919	0.045	1.513	0.412	2.662
514.29	4.8	Taurocholate	0.803	1.065	0.001	2.958	0.123	2.104
243.08	11.8	Biotin	0.804	0.980	0.002	1.327	0.071	1.108
742.07	16.7	NADP+	0.851	1.013	0.032	1.168	0.727	0.899
151.05	7.5	N1-Methyl-2-pyridone-5-carboxamide	0.857	1.038	0.061	1.455	0.075	0.841
156.07	28.7	Paramethadione	0.866	0.933	0.382	0.725	0.905	1.037
254.09	13.1	2-Amino-4-hydroxy-6-(D-erythro-1,2,3-trihydroxypropyl)-7,8-dihydropteridine	0.867	0.911	0.353	2.066	0.751	0.851
103.04	15.4	(R)-3-Hydroxybutanoate	0.873	1.045	0.316	1.435	0.082	7.077
245.04	13.2	Glycerophosphoglycerol	0.873	1.144	0.000	6.390	0.609	0.875
289.03	16.3	Sedoheptulose 7-phosphate	0.882	0.985	0.001	1.341	0.500	1.094
611.15	17.4	Glutathione disulfide	0.885	1.013	0.313	0.785	0.870	1.023
242.08	11.8	Cytidine	0.925	1.006	0.010	1.371	0.481	1.093
191.02	12.3	Citrate	0.928	0.994	0.110	1.129	0.155	1.170
132.03	26.5	L-Aspartate	0.998	1.000	0.055	1.179	0.442	1.115

Table C2 Effect of p-coumaric acid on the metabolome of hepatocytes metabolic changes differing from those produced by quercetin

MASS	t_R (min)	Putative metabolite	P value 180 min	Ratio 180 min	P value 120 min	Ratio 120 min	P value 30 min	Ratio 30 min
132.03	15.2	L-Aspartate	0.000	2.516	0.000	4.602	0.009	2.370
103.04	9.6	(R)-3-Hydroxybutanoate	0.000	2.308	0.000	4.036	0.015	1.562
179.04	8.1	3-(4-Hydroxyphenyl)pyruvate	0.000	0.371	0.089	0.632	0.261	0.615
194.05	9.9	Dopaquinone	0.000	0.000	0.000	0.000	0.000	0.000
191.02	17.9	Citrate	0.000	1.561	0.014	1.925	0.001	1.792
254.98	18.7	Ascorbate 2-sulfate	0.001	1.354	0.001	1.840	0.441	1.223
163.04	8.5	Phenylpyruvate	0.000	0.044	0.000	0.002	0.000	0.000
145.01	15.9	2-Oxoglutarate	0.000	0.409	0.000	0.451	0.341	1.160
87.009	8.6	Pyruvate	0.000	0.291	0.000	0.259	0.006	0.400
193.06	7.6	4-Aminohippuricacid	Nil	Nil	Nil	Nil	Nil	Nil
179.04	10.3	3-(4-Hydroxyphenyl)pyruvate	0.000	0.028	0.000	0.000	0.000	0.000
266.09	8.9	Adenosine	0.362	0.867	0.416	1.108	0.805	1.054
283.07	12.8	Xanthosine	0.006	0.506	0.199	0.901	0.136	0.832
180.03	7.6	DL-Methionine sulfone	0.010	1.376	0.000	1.687	0.385	1.228
117.06	8.0	5-Hydroxypentanoate	0.000	1.613	0.000	2.487	0.046	1.372
200.99	4.6	4-Sulfobenzoate	Nil	Nil	Nil	Nil	Nil	Nil
157.04	14.0	Allantoin	0.015	0.749	0.512	1.039	0.841	0.989
267.07	15.2	Inosine	Nil	Nil	Nil	Nil	Nil	Nil
464.30	5.1	Glycocholate	0.048	0.840	0.452	1.062	0.764	1.028
121.04	7.1	Nicotinamide	0.076	0.784	0.019	0.668	0.708	0.969
168.99	15.5	DL-Glyceraldehyde 3-phosphate	0.045	1.431	0.001	1.630	0.590	1.046
115.00	16.3	Fumarate	0.387	1.103	0.002	1.632	0.000	2.180
163.03	13.6	2-Dehydro-D-xylonate	0.050	2.158	0.131	1.415	0.070	5.054
503.16	16.7	glycogen 3 units	Nil	Nil	Nil	Nil	Nil	Nil

465.09	15.7	N-Adenylylanthranilate	Nil	Nil	Nil	Nil	Nil	Nil
151.03	11.9	Xanthine	0.105	0.645	0.163	0.445	0.123	0.753
96.96	18.1	Sulfate	Nil	Nil	Nil	Nil	Nil	Nil
154.06	14.5	L-Histidine	0.156	0.864	0.886	0.992	0.707	1.034
119.058	35.920	L-Threonine	0.786	1.453	0.080	0.382	0.352	22.665
425.08	16.9	S-glutathionyl-L-cysteine	0.442	1.065	0.823	1.014	0.675	1.205
111.02	9.8	Uracil	0.043	0.824	0.675	1.050	0.851	1.016
219.08	10.3	5-Hydroxy-L-tryptophan	Nil	Nil	Nil	Nil	Nil	Nil
164.04	15.267	Phenylpyruvate	0.000	0.003	0.000	0.004	0.000	0.007
113.04	27.1	5,6-Dihydrouracil	Nil	Nil	Nil	Nil	Nil	Nil
243.06	11.9	Uridine	0.253	0.855	0.016	1.161	0.822	0.976
505.99	16.6	ATP	0.354	1.109	0.198	1.533	0.994	1.001
180.07	12.9	L-Tyrosine	0.269	1.080	0.002	1.194	0.081	1.145
579.03	19.2	UDP-glucuronate	0.131	1.173	0.050	1.734	0.084	1.303
200.02	15.9	2-hydroxy-5-nitro-6-oxohepta-2,4-dienoate	Nil	Nil	Nil	Nil	Nil	Nil
665.22	17.3	Glycogen 4 units	0.050	1.347	0.002	1.321	0.054	1.189
565.05	16.5	UDP-glucose	0.178	1.180	0.163	1.415	0.628	1.066
346.06	13.9	AMP	0.252	0.900	0.329	0.753	0.443	1.171
827.27	17.8	Amylopectin	0.185	1.162	0.004	1.501	0.162	1.203
154.05	23.2	2-amino-5-methyl-muconate semialdehyde	Nil	Nil	Nil	Nil	Nil	Nil
203.08	11.5	L-Tryptophan	0.145	1.098	0.001	1.325	0.908	1.008
426.02	15.3	ADP	0.196	3.137	0.133	2.967	0.962	0.994
97.03	24.0	[FA (5:2)] 2,4-pentadienoic acid	Nil	Nil	Nil	Nil	Nil	Nil
245.08	10.0	5-6-Dihydrouridine	0.093	1.232	0.070	1.361	0.028	#DIV/0!
606.08	15.3	UDP-N-acetyl-D-glucosamine	0.248	1.174	0.243	1.289	0.375	0.898
191.02	14.3	Citrate	0.136	0.801	0.368	1.090	0.803	1.030

346.06	13.0	AMP	0.252	0.900	0.329	0.753	0.443	1.171
505.98	21.3	3'-Phosphoadenylyl sulfate	0.149	1.345	0.016	2.355	0.000	2.674
174.09	15.6	L-Citrulline	0.001	0.518	0.016	0.712	0.008	0.546
193.04	15.8	D-Glucuronate	0.066	1.239	0.001	1.872	0.005	1.547
113.07	28.7	L-proline amide	Nil	Nil	Nil	Nil	Nil	Nil
175.02	15.2	Ascorbate	0.190	0.098	0.314	1.138	0.340	0.323
784.15	11.8	FAD	0.191	0.833	0.018	1.734	0.298	0.815
156.07	26.6	Paramethadione	Nil	Nil	Nil	Nil	Nil	Nil
154.05	24.2	2-amino-5-methyl-muconate semialdehyde	Nil	Nil	Nil	Nil	Nil	Nil
203.079	9.490	N2-Acetyl-L-aminoadipate	0.451	0.959	0.000	1.494	0.193	1.421
203.079	14.916	N2-Acetyl-L-aminoadipate	0.650	1.043	0.373	1.101	0.967	0.995
171.01	15.1	sn-Glycerol 3-phosphate	0.420	1.073	0.059	1.173	0.946	1.005
383.108	14.656	Succinyladenosine	0.059	0.648	0.130	1.186	0.592	1.162
116.047	11.208	3-Methyl-2-oxobutanoic acid	0.730	1.022	0.155	1.171	0.310	1.126
145.01	14.0	2-Oxoglutarate	Nil	Nil	Nil	Nil	Nil	Nil
133.01	16.3	(S)-Malate	0.256	1.109	0.000	1.971	0.000	1.985
308.10	13.8	N-Acetylneuraminate	0.382	0.841	0.003	1.653	0.405	1.193
155.08	28.5	N-acetyl prolinamide or isomer	Nil	Nil	Nil	Nil	Nil	Nil
115.027	41.071	Maleamate	0.225	1.483	0.451	0.891	0.664	1.108
115.027	40.007	Maleamate	0.628	1.143	0.412	0.886	0.454	1.264
115.027	7.049	Maleamate	0.000	0.298	0.325	0.655	0.242	0.356
148.037	33.031	(R)-2-Hydroxyglutarate	0.327	0.540	0.130	2.722	0.715	1.579
148.037	28.439	(R)-2-Hydroxyglutarate	0.594	1.611	0.567	0.672	0.525	0.637
148.037	30.798	(R)-2-Hydroxyglutarate	0.411	0.623	0.404	0.742	0.480	2.632
97.977	18.333	Orthophosphate	0.459	0.593	0.277	1.395	0.876	0.928
766.11	13.5	CoA	Nil	Nil	Nil	Nil	Nil	Nil

103.04	18.9	(R)-3-Hydroxybutanoate	Nil	Nil	Nil	Nil	Nil	Nil
229.01	15.2	D-Ribose 5-phosphate	0.276	0.876	0.270	0.809	0.414	0.926
114.02	23.2	Maleamate	Nil	Nil	Nil	Nil	Nil	Nil
182.05	5.0	4-Pyridoxate	0.050	1.136	0.048	1.276	0.849	0.974
125.04	14.6	Thymine	0.695	0.870	0.637	0.940	0.329	0.843
154.05	21.0	2-amino-5-methyl-muconate semialdehyde	Nil	Nil	Nil	Nil	Nil	Nil
213.02	24.3	2-Deoxy-D-ribose 5-phosphate	Nil	Nil	Nil	Nil	Nil	Nil
180.99	13.9	3-methylphosphoenolpyruvate	Nil	Nil	Nil	Nil	Nil	Nil
146.045	14.9	L-Glutamate	0.517	0.950	0.178	1.080	0.007	1.335
118.027	36.968	Succinate	0.541	1.339	0.321	0.348	0.341	8.325
118.027	25.202	Succinate	0.497	1.606	0.904	1.062	0.943	0.976
118.027	28.759	Succinate	0.748	0.889	0.574	1.303	0.615	1.194
181.04	11.8	1-Methyluric acid	0.505	0.930	0.171	3.435	#DIV/0!	#DIV/0!
375.29	3.7	3alpha-Hydroxy-5beta-cholanate	0.374	0.962	0.357	1.070	0.025	0.824
116.047	28.245	3-Methyl-2-oxobutanoic acid	0.417	0.822	0.688	0.884	0.275	0.315
116.047	37.063	3-Methyl-2-oxobutanoic acid	0.260	1.640	0.426	0.698	0.646	1.218
114.02	26.5	Maleamate	Nil	Nil	Nil	Nil	Nil	Nil
213.02	25.5	2-Deoxy-D-ribose 5-phosphate	Nil	Nil	Nil	Nil	Nil	Nil
118.05	25.8	L-Threonine	Nil	Nil	Nil	Nil	Nil	Nil
117.07	28.6	L-2,4-Diaminobutanoate	Nil	Nil	Nil	Nil	Nil	Nil
193.07	14.6	1-Phenanthrol	Nil	Nil	Nil	Nil	Nil	Nil
115.00	14.9	Fumarate	Nil	Nil	Nil	Nil	Nil	Nil
88.016	14.874	Pyruvate	0.029	0.745	0.009	0.721	0.018	0.600
88.016	26.541	Pyruvate	0.403	0.209	0.422	0.569	0.046	0.218
88.016	28.516	Pyruvate	0.260	0.571	0.558	0.764	0.201	0.219
88.016	17.956	Pyruvate	0.093	0.824	0.832	1.019	0.856	1.039

174.02	14.9	Monodehydroascorbate	Nil	Nil	Nil	Nil	Nil	Nil
350.11	9.8	N-Acetyl-4-O-acetylneuraminate	0.466	0.930	0.011	1.264	0.470	0.902
226.08	10.4	Deoxycytidine	Nil	Nil	Nil	Nil	Nil	Nil
184.99	17.0	3-Phospho-D-glycerate	0.795	1.039	0.021	1.452	0.820	1.017
163.02	28.8	2-Dehydro-D-xylonate	Nil	Nil	Nil	Nil	Nil	Nil
426.01	17.2	Adenylyl sulfate	Nil	Nil	Nil	Nil	Nil	Nil
168.07	26.7	Pyridoxine	Nil	Nil	Nil	Nil	Nil	Nil
164.04	13.3	L-Methionine S-oxide	0.589	1.090	0.129	1.424	0.035	2.136
136.04	11.6	Anthranilate	Nil	Nil	Nil	Nil	Nil	Nil
124.01	15.0	Taurine	0.761	0.986	0.005	1.182	0.138	1.100
179.04	4.8	3-(4-Hydroxyphenyl)pyruvate	0.066	0.655	0.025	0.176	0.332	0.164
190.01	27.6	indole-5,6-quinone-2-carboxylate	Nil	Nil	Nil	Nil	Nil	Nil
114.02	22.2	Maleamate	Nil	Nil	Nil	Nil	Nil	Nil
166.98	17.6	Phosphoenolpyruvate	0.702	0.958	0.060	1.559	0.546	1.084
96.97	29.0	Orthophosphate	Nil	Nil	Nil	Nil	Nil	Nil
613.14	15.4	CMP-N-acetylneuraminate	0.979	0.997	0.004	1.242	0.640	0.953
282.08	12.5	Guanosine	0.497	0.852	0.312	0.727	0.416	1.542
118.05	28.2	L-Threonine	Nil	Nil	Nil	Nil	Nil	Nil
241.08	7.0	Thymidine	0.745	1.062	0.010	0.562	0.908	0.974
243.06	9.8	Uridine	0.452	0.945	0.247	1.134	0.586	1.071
540.05	14.2	Cyclic ADP-ribose	0.259	1.292	0.186	1.651	0.261	1.178
273.00	17.7	D-Glucuronate 1-phosphate	0.999	1.000	0.041	1.348	0.790	1.038
190.05	6.7	N-Acetylmethionine	0.974	1.004	0.524	0.946	0.558	1.092
373.28	3.7	3-Oxo-5beta-cholanate	0.374	0.962	0.357	1.070	0.025	0.824
193.07	10.0	1-O-Methyl-myo-inositol	Nil	Nil	Nil	Nil	Nil	Nil
383.12	13.2	S-Adenosyl-L-homocysteine	0.722	1.077	0.020	1.583	0.623	0.931
240.10	10.9	5-Methyl-2'-deoxycytidine	Nil	Nil	Nil	Nil	Nil	Nil

304.03	12.9	2',3'-Cyclic CMP	0.672	0.927	0.013	0.747	0.430	1.229
117.02	15.4	Succinate	0.135	1.201	0.122	1.544	0.001	2.324
558.07	17.1	Phosphoribosyl-AMP	0.792	0.976	0.013	1.250	0.942	0.992
195.05	14.1	D-Gluconic acid	0.559	0.931	0.007	1.507	0.600	1.061
111.02	8.6	Uracil	0.022	0.792	0.044	0.845	0.533	0.926
191.02	16.2	Citrate	0.810	1.015	0.265	1.239	0.847	1.041
168.00	15.1	L-Cysteate	0.040	0.863	0.082	1.300	0.924	0.983
369.07	17.5	Digalacturonate	0.381	0.887	0.004	1.508	0.720	0.963
193.04	14.9	D-Glucuronate	Nil	Nil	Nil	Nil	Nil	Nil
207.08	6.8	L-Kynurenine	0.338	0.917	0.000	1.555	0.008	2.282
514.29	4.8	Taurocholate	0.921	0.993	0.001	1.336	0.084	1.099
243.08	11.8	Biotin 244.0887	0.121	1.105	0.084	1.117	0.389	1.109
742.07	16.7	NADP+	0.757	0.960	0.073	1.478	0.145	0.857
152.059	14.406	N1-Methyl-2-pyridone-5-carboxamide	0.738	1.095	0.077	1.388	0.624	1.067
156.07	28.7	Paramethadione	0.340	0.888	0.748	1.039	0.136	1.110
254.09	13.1	2-Amino-4-hydroxy-6-(D-erythro-1,2,3-trihydroxypropyl)-7,8-dihydropteridine	0.333	1.249	0.192	1.588	0.146	2.519
103.04	15.4	(R)-3-Hydroxybutanoate	Nil	Nil	Nil	Nil	Nil	Nil
245.04	13.2	Glycerophosphoglycerol	0.946	0.993	0.000	1.314	0.538	1.079
289.03	16.3	Sedoheptulose 7-phosphate	0.918	0.991	0.261	0.790	0.624	1.074
611.15	17.4	Glutathione disulphide	0.884	0.991	0.008	1.373	0.400	1.110
242.08	11.8	Cytidine	0.258	1.071	0.057	1.097	0.251	1.137
191.02	12.3	Citrate	0.783	1.031	0.016	1.172	0.391	1.124
132.03	26.5	L-Aspartate	Nil	Nil	Nil	Nil	Nil	Nil

Table C3 Effect of ferulic acid on the metabolome of hepatocytes

MS	t_R (min)	Putative metabolite	P value 180 min	Ratio 180 min	P value 120 min	Ratio 120 min	P value 30 min	Ratio 30 min
132.03	15.2	L-Aspartate	0.126	1.129	0.001	1.102	0.000	1.575
103.04	9.6	(R)-3-Hydroxybutanoate	0.258	1.069	0.136	1.060	0.000	1.280
179.04	8.1	3-(4-Hydroxyphenyl)pyruvate	0.002	0.291	0.004	0.520	0.065	0.884
194.05	9.9	Dopaquinone	Nil	Nil	Nil	Nil	Nil	Nil
191.02	17.9	Citrate	0.028	1.132	0.153	1.153	0.062	1.521
254.98	18.7	Ascorbate 2-sulfate	0.832	1.011	0.001	1.260	0.000	1.514
163.04	8.5	Phenylpyruvate	0.001	0.653	0.002	0.725	0.001	0.763
145.01	15.9	2-Oxoglutarate	0.000	0.506	0.000	0.518	0.497	1.032
87.01	8.6	Pyruvate	0.142	0.882	0.023	0.852	0.047	0.919
193.06	7.6	4-Aminohippuricacid	Nil	Nil	Nil	Nil	Nil	Nil
179.04	10.3	3-(4-Hydroxyphenyl)pyruvate	0.009	0.780	0.290	0.929	0.374	1.146
266.09	8.9	Adenosine	0.708	0.932	0.529	0.924	0.028	0.777
283.07	12.8	Xanthosine	0.083	0.789	0.000	0.759	0.410	1.055
180.03	7.6	DL-Methionine sulfone	Nil	Nil	Nil	Nil	Nil	Nil
117.06	8.0	5-Hydroxypentanoate	0.238	1.127	0.076	1.415	0.009	1.310
200.99	4.6	4-Sulfobenzoate	Nil	Nil	Nil	Nil	Nil	Nil
157.04	14.0	Allantoin	0.386	1.027	0.815	0.990	0.089	1.101
267.07	15.2	Inosine	Nil	Nil	Nil	Nil	Nil	Nil
464.30	5.1	Glycocholate	Nil	Nil	Nil	Nil	Nil	Nil
121.04	7.1	Nicotinamide	0.711	1.021	0.057	0.932	0.601	0.976
170.00	15.53	D-Glyceraldehyde 3-phosphate	0.952	1.010	0.379	1.099	0.023	1.441
115.01	16.3	Fumarate	0.063	0.796	0.069	0.903	0.000	1.425
163.03	13.6	2-Dehydro-D-xylonate	0.002	4.594	0.000	3.118	0.035	3.663
503.16	16.7	glycogen 3 units	Nil	Nil	Nil	Nil	Nil	Nil

465.09	15.7	N-Adenylylanthranilate	Nil	Nil	Nil	Nil	Nil	Nil
151.03	11.9	Xanthine	0.004	0.632	0.035	0.806	0.913	1.010
96.96	18.1	Sulfate	Nil	Nil	Nil	Nil	Nil	Nil
154.06	14.5	L-Histidine	0.001	0.614	0.000	0.699	0.037	1.287
118.05	24.1	L-Threonine	Nil	Nil	Nil	Nil	Nil	Nil
425.08	16.9	S-glutathionyl-L-cysteine	0.030	1.371	0.720	0.970	0.005	1.313
111.02	9.8	Uracil	0.187	0.898	0.170	0.960	0.878	1.004
219.08	10.3	5-Hydroxy-L-tryptophan	0.012	3.041	0.004	1.993	0.136	#DIV/0!
163.04	22.2	Phenylpyruvate	Nil	Nil	Nil	Nil	Nil	Nil
114.04	39.01	5,6-Dihydrouracil	0.799	1.131	0.349	1.131	0.595	0.910
114.04	40.92	5,6-Dihydrouracil	0.068	1.577	0.203	1.304	0.844	0.973
243.06	11.9	Uridine	0.076	0.899	0.089	1.043	0.004	1.118
505.99	16.6	ATP	0.599	1.059	0.828	0.976	0.011	1.420
180.07	12.9	L-Tyrosine	0.091	0.942	0.003	0.880	0.370	1.023
579.03	19.2	UDP-glucuronate	0.723	0.951	0.004	0.826	0.000	1.481
200.02	15.9	2-hydroxy-5-nitro-6-oxohepta-2,4-dienoate	Nil	Nil	Nil	Nil	Nil	Nil
665.22	17.3	Glycogen 4 units	0.735	1.023	0.025	1.081	0.011	1.142
565.05	16.5	UDP-glucose	0.157	1.156	0.378	0.958	0.002	1.298
346.06	13.9	AMP	0.015	0.713	0.052	0.843	0.029	1.175
827.27	17.8	Amylopectin	Nil	Nil	Nil	Nil	Nil	Nil
154.05	23.2	2-amino-5-methyl-muconate semialdehyde	Nil	Nil	Nil	Nil	Nil	Nil
203.08	11.5	L-Tryptophan	0.001	0.757	0.021	0.903	0.259	0.944
426.02	15.3	ADP	0.242	0.844	0.180	0.909	0.684	1.048
97.03	24.0	[FA (5:2)] 2,4-pentadienoic acid	Nil	Nil	Nil	Nil	Nil	Nil
245.08	10.0	5-6-Dihydrouridine	0.378	0.918	0.470	1.100	0.144	3.749
606.08	15.3	UDP-N-acetyl-D-glucosamine	0.766	0.972	0.004	0.846	0.362	1.049

191.02	14.3	Citrate	0.901	1.013	0.715	0.979	0.461	1.064
346.06	13.0	AMP	0.015	0.713	0.052	0.843	0.029	1.175
505.98	21.3	3'-Phosphoadenylyl sulfate	0.222	1.225	0.691	1.046	0.000	1.876
174.09	15.6	L-Citrulline	0.469	0.968	0.533	0.960	0.572	0.957
193.04	15.8	D-Glucuronate	0.481	0.943	0.015	0.869	0.000	1.369
114.08	7.53	L-proline amide	0.368	1.584	0.006	1.430	0.390	0.918
114.08	9.84	L-proline amide	0.141	0.800	0.818	1.025	0.765	0.956
175.02	15.2	Ascorbate	0.017	0.026	0.000	0.114	0.034	0.312
784.15	11.8	FAD	0.023	0.772	0.056	0.917	0.232	1.095
156.07	26.6	Paramethadione	Nil	Nil	Nil	Nil	Nil	Nil
154.05	24.2	2-amino-5-methyl-muconate semialdehyde	Nil	Nil	Nil	Nil	Nil	Nil
203.08	14.92	N2-Acetyl-L-aminoadipate	0.357	0.862	0.692	0.927	0.571	0.925
203.08	9.56	N2-Acetyl-L-aminoadipate	0.358	0.855	0.151	0.798	0.378	1.109
171.01	15.1	sn-Glycerol 3-phosphate	0.020	1.223	0.004	1.244	0.003	1.225
383.11	11.8	Succinyladenosine	0.073	0.554	0.000	0.477	0.527	0.927
115.04	12.1	3-Methyl-2-oxobutanoic acid	0.495	1.054	0.863	1.015	0.822	1.020
145.01	14.0	2-Oxoglutarate	Nil	Nil	Nil	Nil	Nil	Nil
133.01	16.3	(S)-Malate	0.016	0.812	0.000	0.855	0.000	1.438
308.10	13.8	N-Acetylneuraminate	0.641	0.900	0.159	0.831	0.031	1.789
155.08	28.5	N-acetyl prolinamide or isomer	Nil	Nil	Nil	Nil	Nil	Nil
114.02	28.6	Maleamate	0.007	0.101	0.004	0.286	0.024	0.708
148.04	11.27	(R)-2-Hydroxyglutarate	0.371	1.490	0.032	1.311	0.178	1.112
148.04	15.44	(R)-2-Hydroxyglutarate	0.002	0.665	0.000	0.720	0.006	1.470
96.97	14.7	Orthophosphate	0.001	1.196	0.025	1.136	0.000	1.174
766.11	13.5	CoA	0.040	0.000	0.043	0.000	0.181	1.379
103.04	18.9	(R)-3-Hydroxybutanoate	Nil	Nil	Nil	Nil	Nil	Nil

229.01	15.2	D-Ribose 5-phosphate	0.210	0.918	0.183	1.120	0.007	1.290
114.02	23.2	Maleamate	Nil	Nil	Nil	Nil	Nil	Nil
182.05	5.0	4-Pyridoxate	0.279	0.890	0.033	1.222	0.077	1.298
126.04	40.68	Thymine	0.077	2.067	0.061	1.285	0.961	0.993
126.04	12.11	Thymine	0.494	1.194	0.724	0.967	0.904	1.008
126.04	7.05	Thymine	0.226	1.159	0.255	0.892	0.139	1.296
154.05	21.0	2-amino-5-methyl-muconate semialdehyde	0.327	0.985	0.324	1.214	0.316	1.724
213.02	24.3	2-Deoxy-D-ribose 5-phosphate	Nil	Nil	Nil	Nil	Nil	Nil
180.99	13.9	3-methylphosphoenolpyruvate	0.327	0.984	0.325	1.217	0.321	1.769
146.05	14.9	L-Glutamate	0.000	1.392	0.000	1.415	0.000	1.993
117.02	14.5	Succinate	0.136	1.538	0.001	0.795	0.107	1.123
181.04	11.8	1-Methyluric acid	0.025	0.000	0.129	0.000	0.146	0.739
375.29	3.7	3alpha-Hydroxy-5beta-cholanate	Nil	Nil	Nil	Nil	Nil	Nil
115.04	16.3	3-Methyl-2-oxobutanoic acid	0.153	1.385	0.900	1.023	0.019	1.229
114.02	26.5	Maleamate	Nil	Nil	Nil	Nil	Nil	Nil
213.02	25.5	2-Deoxy-D-ribose 5-phosphate	Nil	Nil	Nil	Nil	Nil	Nil
118.05	25.8	L-Threonine	Nil	Nil	Nil	Nil	Nil	Nil
117.07	28.6	L-2,4-Diaminobutanoate	Nil	Nil	Nil	Nil	Nil	Nil
193.07	14.6	1-Phenanthrol	0.005	2.694	0.001	2.126	0.009	3.407
115.00	14.9	Fumarate	Nil	Nil	Nil	Nil	Nil	Nil
87.01	7.1	Pyruvate	Nil	Nil	Nil	Nil	Nil	Nil
174.02	14.9	Monodehydroascorbate	0.146	0.000	#DIV/0!	#DIV/0!	0.139	0.441
350.11	9.8	N-Acetyl-4-O-acetylneuraminate	0.594	0.966	0.354	0.961	0.019	1.115
226.08	10.4	Deoxycytidine	0.151	1.088	0.262	0.953	0.321	0.956
184.99	17.0	3-Phospho-D-glycerate	0.419	0.896	0.921	0.996	0.043	1.243
164.03	7.57	2-Dehydro-D-xylonate	0.086	1.632	0.552	1.074	0.140	0.846

164.03	10.44	2-Dehydro-D-xylonate	0.008	1.464	0.033	1.287	0.030	1.528
426.01	17.2	Adenylyl sulfate	0.110	1.273	0.241	1.143	0.000	1.990
168.07	26.7	Pyridoxine	Nil	Nil	Nil	Nil	Nil	Nil
164.04	13.3	L-Methionine S-oxide	0.965	1.005	0.546	1.061	0.043	1.103
136.04	11.6	Anthranilate	0.761	0.990	0.245	0.970	0.537	0.984
124.01	15.0	Taurine	0.062	1.322	0.000	1.419	0.000	1.285
179.04	4.8	3-(4-Hydroxyphenyl)pyruvate	Nil	Nil	Nil	Nil	Nil	Nil
190.01	27.6	indole-5,6-quinone-2-carboxylate	Nil	Nil	Nil	Nil	Nil	Nil
114.02	22.2	Maleamate	Nil	Nil	Nil	Nil	Nil	Nil
166.98	17.6	Phosphoenolpyruvate	0.260	0.864	0.275	0.858	0.006	1.296
97.98	21.16	Orthophosphate	0.000	1.729	0.028	1.287	0.014	1.164
97.98	18.26	Orthophosphate	0.019	1.571	0.124	1.199	0.067	1.167
97.98	14.71	Orthophosphate	0.001	1.196	0.025	1.136	0.000	1.174
97.98	15.73	Orthophosphate	0.029	1.336	0.124	1.096	0.001	1.256
613.14	15.4	CMP-N-acetylneuraminate	0.995	1.001	0.666	0.962	0.171	1.129
282.08	12.5	Guanosine	0.924	1.024	0.345	0.791	0.836	0.961
118.05	28.2	L-Threonine	Nil	Nil	Nil	Nil	Nil	Nil
241.08	7.0	Thymidine	0.320	1.117	0.415	0.905	0.625	1.096
243.06	9.8	Uridine	0.729	0.982	0.029	1.071	0.318	1.029
540.05	14.2	Cyclic ADP-ribose	Nil	Nil	Nil	Nil	Nil	Nil
273.00	17.7	D-Glucuronate 1-phosphate	0.071	0.734	0.053	0.825	0.044	1.073
190.05	6.7	N-Acetylmethionine	0.464	0.936	0.844	1.018	0.040	1.535
373.28	3.7	3-Oxo-5beta-cholanate	0.019	0.232	0.283	0.913	0.379	1.087
193.07	10.0	1-O-Methyl-myo-inositol	0.210	0.794	0.332	1.088	0.106	2.213
383.12	13.2	S-Adenosyl-L-homocysteine	0.099	0.609	0.019	0.689	0.134	1.134
240.10	10.9	5-Methyl-2'-deoxycytidine	0.222	1.126	0.136	1.209	0.143	1.130
304.03	12.9	2',3'-Cyclic CMP	0.267	2.324	0.941	1.014	0.342	1.453

117.02	15.4	Succinate	0.971	0.991	0.129	0.908	0.003	1.465
558.07	17.1	Phosphoribosyl-AMP	Nil	Nil	Nil	Nil	Nil	Nil
195.05	14.1	D-Gluconic acid	0.256	0.898	0.321	0.965	0.005	1.206
111.02	8.6	Uracil	0.064	1.179	0.006	1.151	0.003	1.092
191.02	16.2	Citrate	0.374	1.141	0.001	0.639	0.015	1.262
168.00	15.1	L-Cysteate	Nil	Nil	Nil	Nil	Nil	Nil
369.07	17.5	Digalacturonate	Nil	Nil	Nil	Nil	Nil	Nil
193.04	14.9	D-Glucuronate	Nil	Nil	Nil	Nil	Nil	Nil
207.08	6.8	L-Kynurenine	0.000	2.279	0.000	2.790	0.000	23.779
514.29	4.8	Taurocholate	0.489	1.035	0.039	1.079	0.002	1.098
243.08	11.8	Biotin	0.139	0.965	0.636	0.986	0.293	0.975
742.07	16.7	NADP+	0.642	0.945	0.015	0.826	0.993	1.000
151.05	7.5	N1-Methyl-2-pyridone-5-carboxamide	0.319	0.879	0.967	0.997	0.044	0.876
156.07	28.7	Paramethadione	Nil	Nil	Nil	Nil	Nil	Nil
254.09	13.1	2-Amino-4-hydroxy-6-(D-erythro-1,2,3-trihydroxypropyl)-7,8-dihydropteridine	0.095	1.548	0.013	1.380	0.001	1.688
103.04	15.4	(R)-3-Hydroxybutanoate	Nil	Nil	Nil	Nil	Nil	Nil
245.04	13.2	Glycerophosphoglycerol	0.489	0.948	0.881	1.005	0.010	1.202
289.03	16.3	Sedoheptulose 7-phosphate	0.401	1.058	0.355	1.054	0.038	1.169
611.15	17.4	Glutathione disulphide	0.826	0.980	0.000	0.880	0.011	1.262
242.08	11.8	Cytidine	0.754	1.008	0.469	0.980	0.089	0.975
191.02	12.3	Citrate	0.034	1.152	0.044	1.152	0.003	1.167
132.03	26.5	L-Aspartate	Nil	Nil	Nil	Nil	Nil	Nil